From summer growth to winter decline: brain size, captive effect, and cognitive outcomes in the common shrew during Dehnel's phenomenon

Doctoral thesis for obtaining the academic degree

Doctor of Natural Sciences

(Dr. rer. nat.)

submitted by

Cecilia Baldoni

at the

Faculty of Sciences

Department of Biology

Konstanz, 2024

From summer growth to winter decline: brain size, captive effect, and cognitive outcomes in the common shrew during Dehnel's phenomenon

Doctoral thesis for obtaining the academic degree

Doctor of Natural Sciences

(Dr. rer. nat.)

submitted by

Cecilia Baldoni

at the

Faculty of Sciences

Department of Biology

Konstanz, 2024

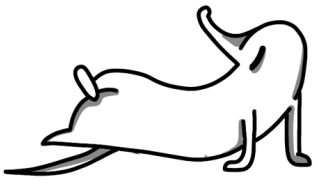

Date of oral examination: November 4th, 2024
Chair: Prof. Dr. Martin Wikelski
1. Reviewer: PD. Dr. Dina Dechmann
2. Reviewer: Prof. Dr. Dominik von Elverfeldt

Yesterday I talked to god, we had a conversation

I asked them why this life is a crazy combination

Of numbers, numbers, numbers we can't read.

I said that the things that I've been trying end up in frustration

Life ain't what it seems in any situation

Then (s)he said, (s)he said, (s)he said the strangest thing.

(S)he said: "*How does it feel to be human?*

Do some of the best plans you make get ruined?

Do people curse you and flowers ain't blooming?

How does it feel?"

(S)he said: "*How does it feel to be human?*

If I could for one day I just might do it

Dance till the sun comes up to my music,

How does it feel?

How's it feel?"

Human - OneRepublic

“Avere un’epifania è solo un modo elaborato per dire che sei un idiota.”

Cit.

Table of Contents

Summary

The vertebrate brain is a marvel of biological complexity and sophistication, responsible for coordinating sensory experiences, motor functions, and cognitive processes. Evolutionary studies have demonstrated that while brain size generally correlates with body size, there is significant variation among species. Larger brains relative to body size are often linked to enhanced cognitive abilities, as seen in both birds and mammals, suggesting that such adaptations are responses to complex environmental challenges. However, the size of the brain is constrained by its high metabolic costs, necessitating efficient neural mechanisms to optimize cognitive functions.

Brain plasticity, or neuroplasticity, enables the brain to adapt to new situations and challenges by reorganizing neural connections. This adaptability is particularly crucial for species living in temperate climates, where seasonal variations impact physiology and behavior. The common shrew, *Sorex araneus*, exemplifies this adaptability through Dehnel's phenomenon, a seasonal cycle in which brain and body size decrease during winter, with regrowth occurring in warmer months—an adaptation likely aimed at reducing metabolic demands when food resources are scarce. Studying these cyclical changes in the common shrew can reveal the relationship between brain structure and cognitive function, showing how brain plasticity enables organisms to cope with environmental fluctuations.

In my PhD research, I explored the dynamics of brain plasticity in the common shrew through advanced imaging techniques and behavioral analysis.

In the first chapter, I present the development of the first high-resolution brain atlases for the common shrew, representing an advancement in our ability to study neurological structures across different developmental stages and environmental conditions. These atlases, derived from both histological sections and Magnetic Resonance Imaging (MRI), serve as essential tools for both fundamental and applied neuroscience research. Creating these atlases will facilitate identifying changes in brain structures as they undergo significant seasonal size fluctuations, providing a framework to correlate these structural changes with functional outcomes.

In the second chapter, I used diffusion-weighted MRI (DW-MRI) imaging to investigate the microstructural changes in the shrew's brain during seasonal size changes. I found that brain size reduction in common shrews is marked by significant microstructural changes from summer to winter. These results reveal a notable decrease in intracellular

water volume fraction from summer to winter and an increase in extracellular water volume across most brain regions. Importantly, our cell population analyses indicate no reduction in the number of cells, suggesting that the observed changes result from a decrease in cell size. This adaptation likely leads to reduced energy requirements for cellular processes: smaller cells typically exhibit lower metabolic demands, which becomes essential in winter, when resources are limited and efficient metabolism is necessary for survival.

In the third chapter, I examined the impact of captivity on brain morphology, cognitive functions, and activity patterns of shrews from summer to winter, comparing wild-caught shrews with those kept in semi-natural captivity. In tasks involving associative learning with visual and olfactory cues, performance was better in summer shrews, especially in early trials. The slowdown of cognitive processes in winter suggests a potential trade-off: maintaining broader cognitive functions might come at the cost of reduced processing speed under resource-limited conditions.

In the fourth chapter, I assessed the associative and spatial learning abilities of shrews in relation to their seasonal brain size changes. Despite an overall reduction in brain volume during winter, cognitive testing indicates that common shrews maintain a certain level of functionality, particularly in tasks involving spatial navigation. However, the operational speed of these cognitive functions is compromised. This chapter connects structural brain changes with cognitive functions, demonstrating the importance of cognitive flexibility in adapting to environmental fluctuations. The differential prioritization of cognitive abilities could stem from their varied ecological functions. Spatial learning may be prioritized during winter despite reductions in hippocampal volume, possibly because navigating the environment remains important when resources are scarce.

Overall, my dissertation advances the understanding of brain plasticity, environmental adaptability, and cognitive functionality, emphasizing the seasonal impact on brain structure and behavior in the common shrew.

Zusammenfassung

In meiner Doktorarbeit konnte ich mit Hilfe von fortschrittlichen Bildgebungsverfahren und Verhaltensanalysen die Dynamik der Gehirnplastizität von Spitzmäusen untersuchen..

Im ersten Kapitel stelle ich die Entwicklung der ersten hochauflösenden Gehirnatlanten für die Spitzmaus vor. Diese stellen einen Fortschritt dar, mit welchen Möglichkeiten neurologische Strukturen über verschiedene Entwicklungsstadien und Umweltbedingungen hinweg untersucht werden können. Die Atlanten wurden sowohl basierend auf histologischen Schnitten als auch mit Hilfe von Magnetresonanztomographie (MRT) entstanden. Sie dienen als wichtige Instrumente für die Grundlagenforschung und die angewandte neurowissenschaftliche Forschung. Die erstellten Atlanten erleichtern die Identifizierung von Veränderungen in den Gehirnstrukturen, die erheblichen saisonalen Größenschwankungen unterliegen, und bieten einen Rahmen, um die strukturellen Veränderungen mit funktionellen Ergebnissen zu korrelieren.

Im zweiten Kapitel untersuche ich mit Hilfe diffusionsgewichteter MRT-Bildgebung (DW-MRI) mikrostrukturelle Veränderungen im Gehirn der Spitzmaus bei saisonalen Größenveränderungen. Meine Ergebnisse zeigen, dass die Verringerung der Hirngröße bei Spitzmäusen durch signifikante mikrostrukturelle Veränderungen zwischen Sommer und Winter gekennzeichnet ist. Außerdem stelle ich zwischen Sommer und Winter eine bemerkenswerte Abnahme des intrazellulären Wasservolumenanteils und eine Zunahme des extrazellulären Wasservolumens in den meisten Hirnregionen fest. Parallele Analysen der Zellpopulationen zeigten jedoch keine Verringerung der Anzahl der Zellen, was darauf hindeutet, dass die beobachteten Veränderungen auf eine Verringerung der Zellgröße zurückzuführen sind. Es lässt sich annehmen, dass diese Anpassung zu einem geringeren Energiebedarf für zelluläre Prozesse führt: Kleinere Zellen haben in der Regel einen geringeren Stoffwechselbedarf, was im Winter, wenn die Stoffwechseleffizienz aufgrund begrenzter Ressourcen an erster Stelle steht, eine entscheidende Anpassung darstellt.

In dem dritten Kapitel untersuche ich die Auswirkungen der Gefangenschaft auf die Gehirnmorphologie, die kognitiven Funktionen und die Aktivitätsmuster von Spitzmäusen zwischen Sommer und Winter, wobei ich wild gefangene Spitzmäuse mit solchen verglichen habe, die in naturnaher Gefangenschaft gehalten wurden. Bei Aufgaben, die assoziatives Lernen mit visuellen und olfaktorischen Reizen beinhalten, war die Leistung der Sommerspitzmäuse besser, insbesondere bei den ersten

Versuchen. Die Verlangsamung der kognitiven Prozesse im Winter deutet auf einen möglichen Ausgleich hin: Die Aufrechterhaltung breiterer kognitiver Funktionen scheint unter ressourcenbeschränkten Bedingungen auf Kosten einer geringeren Verarbeitungsgeschwindigkeit zu gehen.

Im vierten Kapitel untersuche ich die assoziativen und räumlichen Lernfähigkeiten von Spitzmäusen in Abhängigkeit von den jahreszeitlichen Veränderungen der Gehirngröße. Trotz einer allgemeinen Verringerung des Gehirnvolumens im Winter zeigen kognitive Tests, dass Spitzmäuse ein gewisses Maß an Funktionalität beibehalten, insbesondere bei Aufgaben, die die räumliche Navigation betreffen. Die Untersuchung zeigte jedoch, dass die Geschwindigkeit, mit der diese kognitiven Funktionen ausgeführt werden, beeinträchtigt ist. Dieses Kapitel stellt eine Verbindung zwischen strukturellen Gehirnveränderungen und kognitiven Funktionen her und zeigt, wie wichtig die kognitive Flexibilität für die Anpassung an Umweltschwankungen ist. Die unterschiedliche Priorisierung der kognitiven Fähigkeiten könnte auf ihre unterschiedlichen ökologischen Funktionen zurückzuführen sein. Im Winter wird das räumliche Lernen möglicherweise trotz der Verringerung des Hippocampus-Volumens priorisiert, weil das Navigieren in der Umwelt eine überlebenswichtige Fähigkeit bleibt, wenn Ressourcen knapp sind.

Insgesamt trägt meine Dissertation zu einem besseren Verständnis der Plastizität des Gehirns, der Anpassungsfähigkeit an die Umwelt und der kognitiven Funktionen bei. Im Vordergrund stehen dabei die jahreszeitlichen Auswirkungen auf die Gehirnstruktur und das Verhalten der Spitzmaus.

General Introduction

The vertebrate brain is a marvel of biological complexity and sophistication, responsible for coordinating an organism's sensory experiences, motor functions, and cognitive processes. Its study has long fascinated scientists because the brain's intricate mechanisms of processing and responding to external stimuli are central to understanding how organisms interact with their environment (Kandel et al., 2013). In mammals, the complexity of the brain is facilitated by its highly organized structure. One of the key features that distinguish mammals from other vertebrates is the presence of a neocortex with a unique neuronal organization, composition, and connectivity, which provides a platform for both parallel and serial processing of information (Wu et al., 2011).

Research on mammalian brain evolution has traditionally focused on how variations in brain size and structure connect to cognitive abilities and adaptive behaviors, offering a perspective on the evolutionary pressures that shape brain development (Jerison, 1974). Generally, brain size is highly conserved and positively correlated with body size, adhering to a negative allometric rule with an exponent of 0.6-0.8 (Smaers et al., 2021). This scaling implies that as body size increases, brain size grows in absolute terms but decreases in relative terms. For example, while the human brain constitutes about 2% of total body mass, the brain of a shrew—one of the smallest mammals—can account for as much as 10% of body mass (Van Dongen, 1998).

Across species, brain size is closely linked to brain organization, including the size of the neocortex, hippocampus, and other neural structures, as well as increased neuronal specialization and greater white matter volume (Barton, 2007; Bullmore & Sporns, 2012; Zhang & Sejnowski, 2000). Due to these correlations, it has often been proposed that larger brains (relative to body size) or larger association areas may facilitate more complex cognitive abilities (reviewed in Healy & Rowe, 2007). For instance, studies carried out in birds show that increased brain size is linked to innovation rate (Lefebvre et al., 2004) and learning (Garamszegi et al., 2005; Sol et al., 2005). Similar patterns have been observed in mammals, suggesting a convergent evolutionary process where increases in whole brain size correlate with better cognitive abilities. These include motor functions (Changizi, 2003), rates of innovation (Reader & Laland, 2002), problem-solving abilities (Benson-Amram et al., 2016), and sensory specialization (Barton, 1998).

Despite the potential cognitive benefits that larger brains might offer, the size of the brain is constrained by metabolic costs. The brain is one of the most energy-intensive organs, and its growth, function, and design are limited by available metabolic energy (Laughlin, 2001). For example, in humans, the brain accounts for 20% of resting oxygen consumption (Raichle et al., 2001), and studies on cerebral blood flow regulation suggest that energy supply limits neural function (Zhou et al., 2022).

To optimize the use of available resources and enhance cognitive functions, brains must rely on efficient neural mechanisms. A key component of this efficiency is brain plasticity or neuroplasticity, the brain's ability to adapt to new situations and challenges by reorganizing and forming new neural connections (Anderson, 2016). In neuroscience, brain plasticity is recognized as a fundamental property that enables the brain to adapt to new experiences, environments, and injuries (Kolb & Gibb, 2014). This capacity for targeted reorganization allows for significant cognitive advancements and adaptability without the metabolic burden of a uniformly larger brain. For instance, studies have shown that musicians exhibit increased gray matter volume in brain regions associated with auditory processing and motor control, reflecting structural changes due to extensive practice (Gaser & Schlaug, 2003). Similarly, London taxi drivers have larger hippocampi, a brain region involved in spatial navigation, compared to non-taxi drivers (Maguire et al., 2000). Both examples showcase how specific experiences can shape particular brain regions while leaving the overall brain size unchanged, demonstrating the brain’s ability to efficiently allocate resources and enhance function in a targeted manner.

A plastic nervous system allows organisms to adapt to and learn from their environment. This adaptability is crucial for species living in temperate climates, where seasonal variations influence the phenology of plants and animals due to distinct changes in temperature and precipitation throughout the year (Oberman & Pascual-Leone 2013). To adapt to these environmental variations, most mammalian species exhibit seasonal cycles in their physiology and behavior. For example, the neuroendocrine pathways involving melatonin and thyroid hormones are essential in linking seasonal factors to reproductive processes (Yoshimura, 2010). In golden hamsters, altering the photoperiod can lead to cell proliferation in several brain areas, including the hypothalamus (Huang et al., 1998).

The most extreme example of seasonal adaptation is known as Dehnel's phenomenon (Dehnel, 1949), which involves a significant reduction in brain size during the winter months, followed by regrowth in the spring and summer. This seasonal plasticity has been observed in small mammal species with high metabolisms and year-round

activity in cold climates, and it is likely an adaptation to winter as the shrinkage starts in autumn before the onset of winter (Lázaro et al., 2021). The common shrew, *Sorex araneus*, has one of the most dramatic size changes found to date, thus, I used it as a model species throughout my PhD research. Its cyclical change in brain size is accompanied by size changes of different organs, such as the liver, heart, kidneys, and spleen (Pucek, 1963), as well as a shortening of the spine that leads to a decrease of the total body length (Hyvarinen, 1969). This results in a 25-45% reduction of the whole body in the winter (Churchfield, 1981; Hyvarinen, 1969; Pucek, 1963). These changes are thought to be an energy-saving adaptation, reducing metabolic demands when food resources are scarce and environmental conditions are harsh. Therefore, it is hypothesized that Dehnel's phenomenon is an adaptive strategy for overwintering in terms of energetics and resource availability (Mezhzherin, 1964; Pucek, 1970). To further support this theory, the intensity of the phenomenon differs along a latitudinal and longitudinal gradient: in southern Germany, the winter decline is 5.1% less pronounced than in north Poland (Pucek, 1965) and 10.2% less than in Russia (Yaskin, 1994). Geographical areas with more severe winters might have driven a more pronounced decrease in body size to drastically reduce energetic demands. Finally, common shrews maintain, oxygen consumption between seasons, despite the high variation in temperature, confirming that size reduction decreases absolute energy consumption and overall energy costs (Schaeffer et al., 2020). However, this hypothesis does not explain all the morphological changes across seasons, particularly in the brain. Different brain regions change differently along the year: some of them – especially the neocortex and the hippocampus - experience large and reversible size transformation, whereas others such as the cerebellum or the olfactory bulbs either remain stable or change size in one direction (Yaskin, 1994).

This unique phenomenon makes the common shrew an excellent model to directly bridge the gap between neurological structures and cognitive outcomes and ultimately to understand if reduced brain size causes cognitive impairment within the same individuals. Very few studies have considered the cognitive consequences this species may encounter during each phase of Dehnel's Phenomenon. Page and collaborators (2012) showed that shrews in summer, at the peak of brain size, performed poorly in an associative learning task. However, it has not yet been investigated whether summer and winter shrews behave differently in the same task. Interestingly, a study carried out in my lab indicated a spatial learning impairment in winter shrews, which has been linked to a decrease in brain size, particularly in the hippocampus (Lázaro, Hertel, et al., 2017). This suggests that the large seasonal changes in brain size and structure could indeed affect brain functionality, potentially altering cognitive capabilities in phases of reduced brain size.

Considering that the reduction in brain size from summer to winter occurs unevenly across different brain regions, it suggests that this is not merely a passive isotropic process but involves an active, targeted reorganization of brain structure. However, the mechanisms behind these drastic transformations remain unknown. Previous research initially focused on the decreases in cell numbers, dendritic tree complexity, and white matter volume as potential explanations for seasonal brain size fluctuations because reductions in any of these areas could lead to a direct decrease in total brain volume. Bartkowska et al. (2008) have shown that changes in cell numbers do not significantly contribute to the observed seasonal brain size fluctuations. Moreover, Pucek (1965) observed that water and fat content influence this process, hinting at a possible seasonal reduction in white matter, but the reduction does not account fully to the size difference. Further studies by Lázaro (2017) revealed a decline in neuronal soma size within specific areas such as the caudoputamen and the somatosensory and anterior cingulate cortices, along with a reduction in basal dendritic volume in the anterior cingulate cortex during winter. However, these changes alone do not fully explain the total winter volumetric decline, indicating that additional, yet unidentified, mechanisms must also be contributing.

Exploring the unidentified mechanisms behind the seasonal brain size fluctuations during Dehnel phenomenon remains a significant challenge. Challenges stem in particular from the complex interplay of cellular, molecular, and physiological events that underlie these processes. Advanced neuroimaging techniques, particularly Magnetic Resonance Imaging (MRI), allow us to visualize brain structure and activity in ever-increasing detail under various conditions. MRI works by using strong magnetic fields to alter the states of hydrogen atoms in a tissue. The single proton in the nucleus of each hydrogen atom acts like a compass needle and aligns with the magnetic field. MRI scans can provide extremely detailed three-dimensional images of an individual's brain, from which a wide range of measurements can be extracted. The most obvious are the volume, thickness, or surface area of various brain regions and the volume of specific white matter tracts. MRI data can also be used to examine brain organization, specifically how different parts are connected. A technique called diffusion-weighted imaging (DWI) tracks the direction of water molecule diffusion inside the brain and can detect the orientation of bundles of nerve fibers. Using these signals, it is possible to measure the extent of nerve fiber connectivity between different areas and even to extract information on the overall brain network.

In my PhD research, I focused on elucidating the complex dynamics of brain plasticity and structural changes in the common shrew, *Sorex araneus*, exploring both the microstructural adaptations to seasonal changes and the cognitive implications of

these fluctuations. This comprehensive study combined advanced imaging techniques and behavioral analysis to bridge the gap between neurological structures and cognitive outcomes.

In Chapter 1, I present two brain atlases for the common shrew, *Sorex araneus*, compiled using histological sections and MRI, along with a region-specific gene expression profile. Brain atlases are crucial for providing detailed species-specific information on brain anatomy and cytological features, which are essential resources for neuroscience research (Hess et al., 2018). Histological sections offer high-resolution, bi-dimensional data crucial for understanding detailed brain anatomy, while MRI provides three-dimensional representations that are necessary for accurate anatomical mapping without tissue distortion (Ullmann et al., 2015). This chapter provides the first detailed, region-specific brain atlas of the common shrew. Additionally, it profiles gene expression across different brain regions to understand molecular underpinnings. This allows for a deeper understanding of how brain regions are differentially affected by seasonal changes, potentially uncovering mechanisms of brain plasticity that could inform broader neurological studies.

In Chapter 2, I investigate the microstructural changes in the common shrew's brain using Diffusion Microstructure Imaging (DMI) during their natural seasonal brain size changes. Understanding the microstructural basis of seasonal brain plasticity reveals how environmental pressures drive reversible brain adaptations. DMI is particularly suited for this study as it allows a non-invasive quantification of tissue architecture and structure through the use of metabolic water, enabling detailed osservation of cellular and microstructural changes (Kellner et al., 2022). The specific objectives of this chapter are to quantify seasonal variations in brain diffusion metrics and to determine the structural reorganization processes underlying brain size changes, including potential changes in cell counts. These findings can bridge the gap between observable anatomical changes and their underlying biological processes, potentially informing similar research in other species and contributing to a broader understanding of brain plasticity.

In Chapter 3, I explore the impact of captivity on the brain morphology, cognitive functions, and activity patterns of common shrews from summer to winter, comparing wild-caught shrews with those kept in semi-natural captivity. It is important to understand the effects of captivity on animal research, as captivity can induce significant physiological and behavioral changes. Captivity often leads to chronic stressors such as confinement, diet changes, and reduced sensory stimuli, (Fischer et al., 2018) which can alter hormone balances, immune responses, and gene expression,

ultimately affecting brain structure and function (Seeber et al., 2020). Understanding the effects of a captive environment on wild animals can inform guidelines for minimizing the impact of captivity on research outcomes and enhance the validity of experimental findings.

In Chapter 4, I examine the associative and spatial learning abilities of common shrews in relation to their seasonal brain size changes. Learning is crucial for optimizing resource use and responding to environmental variability. Associative learning helps animals form mental links between stimuli and behaviors, facilitating rapid adaptation to changing environments. Spatial learning enables them to map and navigate their surroundings effectively, securing necessary resources and avoiding threats. The objectives of this chapter are twofold. First, to assess how seasonal changes in brain size affect shrews' learning speeds in associative and spatial tasks; and second, to evaluate the impact of captivity on their overall performance. Through this, we explore how structural brain changes shape cognitive functions and learning strategies, emphasizing the role of cognitive flexibility in adapting to environmental changes. This chapter demonstrates how changes in brain structure support cognitive abilities and adaptive strategies, showing how brain plasticity enables animals to navigate fluctuating environments. My aim is to demonstrate how structural adaptations connect with functional outcomes, emphasizing the role of cognitive flexibility in ecological success.

Overall, my dissertation advances our understanding of the dynamic relationship between brain plasticity, environmental adaptability, and cognitive functionality, highlighting the profound impact of seasonal changes on brain structure and behavior in the common shrew, *Sorex araneus*.

Chapter 1

Histological and MRI brain atlas of the common shrew, *Sorex araneus*, with brain region-specific gene expression profiles

Published in *Frontiers in Neuroanatomy*,
https://doi.org/10.3389/fnana.2023.1168523

Cecilia Baldoni, William R. Thomas, Dominik von Elverfeldt, Marco Reisert, Javier Làzaro, Marion Muturi, Liliana M. Dávalos, John D. Nieland and Dina K. N. Dechmann

Abstract

The common shrew, *Sorex araneus*, is a small mammal of growing interest in neuroscience research, as it exhibits dramatic and reversible seasonal changes in individual brain size and organization (a process known as Dehnel's phenomenon). Despite decades of studies on this system, the mechanisms behind the structural changes during Dehnel's phenomenon are not yet understood. To resolve these questions and foster research on this unique species, we present the first combined histological, magnetic resonance imaging (MRI), and transcriptomic atlas of the common shrew brain. Our integrated morphometric brain atlas provides easily obtainable and comparable anatomic structures, while transcriptomic mapping identified distinct expression profiles across most brain regions. These results suggest that high-resolution morphological and genetic research is pivotal for elucidating the mechanisms underlying Dehnel's phenomenon while providing a communal resource for continued research on a model of natural mammalian regeneration. Morphometric and NCBI Sequencing Read Archive are available at https://doi.org/10.17617/3.HVW8ZN.

Introduction

The vertebrate brain is one of the most functionally important and biologically complex structures of the body, making research on this organ of extreme interest yet difficult to study without supporting resources. By providing species-specific information on the location and spatial relationships between anatomical and cytological features, brain atlases are an essential resource for neuroscience research (Arnatkevičiūtė et al., 2019; Hess et al., 2018). Many brain atlases have been created and applied to rodents (La Manno et al., 2021; Ortiz et al., 2020; Radtke-Schuller et al., 2016; Yamamoto et al., 2001) and primates (Agaronyan et al., 2022; Moirano et al., 2019; Newman et al., 2009; Sunkin et al., 2013) to better understand neurological processes ranging from circadian rhythms to neurodegenerative disease. However, a direct focus on these few mammalian lineages misses many of the naturally occurring phenotypes unique to other species that may prove pivotal for understanding brain function and evolution. For example, brain atlases created for the mustached bat (Washington et al., 2018), mole-rat (Dollas et al., 2019), and cavefish (Jaggard et al., 2020) have helped elucidate the adaptive mechanisms of sensory systems in darker environments.

Continued curation of brain atlases across divergent species with extraordinary phenotypes will help to further broaden our understanding of brain function, architecture, and evolution.

A unique yet understudied brain phenotype is the drastic seasonal and reversible brain size change known as Dehnel's phenomenon (Dehnel, 1949) that occurs in a handful of small mammals with exceptionally high metabolic rates and year-round activity (LaPoint et al., 2013; Nováková et al., 2022). The common shrew, *Sorex araneus*, has one of the most dramatic size changes found to date, thus, it is currently being used as model species for Dehnel's phenomenon (Dehnel, 1949; Lázaro & Dechmann, 2021). Young common shrews reach their first maximum brain size soon after birth in summer, followed by a progressive reduction in brain size, reaching a minimum in winter. Partial regrowth of their brains occurs in spring as they sexually mature, followed by reproduction at approximately 13 months, after which most die prior to a second winter (Churchfield, 1979). In Southern Germany, the mean relative brain size of common shrews decreases by 16.1% from summer to winter and later regrows by 9.8% (for detailed data on brain mass see Lázaro et al., 2019). Notably, brain regions do not change uniformly, as each brain region shows different seasonal variation (Lázaro et al., 2019), and size changes are not driven by adult neurogenesis, apoptosis (Bartkowska et al., 2008) or changes in neuron size (Lázaro et al., 2018). Therefore, the curation of a brain atlas for S. araneus can further resolve region-specific shrinkage and regrowth at a finer resolution and help elucidate the molecular underpinnings of this rare phenotype.

Here we present two brain atlases as well as a region-specific gene expression profile to facilitate research on the common shrew. Our first atlas is a traditional histological atlas compiled from histological sections paired with schematic drawings in which the major brain regions and structures have been identified. Although histological atlases are useful resources for easy comparisons between taxa, they provide only bidimensional data and can cause tissue distortions or other artifacts that can slightly alter the shape of the brain structures (Ullmann et al., 2015). Thus, we also compiled a second, three-dimensional atlas using Magnetic Resonance Imaging (MRI), a powerful tool for obtaining detailed anatomical information at a finer resolution (Ullmann et al., 2015). Finally, we characterized the RNA expression profiles of 5 major brain regions; the cortex, hippocampus, hypothalamus, thalamus, and olfactory bulb. Measurements of gene abundance identified 1,444 genes of high regional specificity and large expression divergence between tissues. With these three datasets, we aim to create a resource for the scientific community to study this fascinating phenomenon with many potential applied questions.

Materials and methods

Histological sections

We prepared histological sections at the Max Planck Institute of Animal Behavior in Möggingen, Germany. We caught animals in the area near the institute between August 2013 and October 2015 (see Lázaro et al., 2018 for details of capture). Before brain extraction, animals were perfused transcardially with PBS followed by 4% formaldehyde solution in PBS under deep anesthesia (Isoflurane). We used the left hemisphere of 10 individuals (5 males and 5 females). Brain tissues were sectioned on a freezing sliding microtome (Reichert- Jung Hn-40) to obtain 30 µm-thick coronal sections, mounted every fifth section on slides, and stained them with 0.5% cresyl violet (see Lázaro et al., 2018 for details about sampling and preparation of sections). For the atlas, we then selected the best sections from the 10 individuals' left hemisphere. To outline all brain regions, we used an Olympus BX51 microscope under an Olympus UIS2 Plan N 2 × (NA = 0.02) dry objective, inter-faced with a Neurolucida software system (MBF Bioscience, Williston, VT, USA). We then identified brain regions based on the cytoarchitecture revealed by this stain and used the mouse brain atlas as reference (Allen Mouse Brain Atlas; Paxinos and Franklin, 2019). The full list of brain regions identified can be found in Appendix Table A1.1.

MRI data acquisition

For magnetic resonance imaging (MRI) reconstruction, we used one adult male common shrew. The individual was euthanized using deep isoflurane overdose and perfused through the open heart with phosphate-buffered saline (PBS) (see Lázaro et al., 2018 for details). The head was then removed and stored in PBS/0.1% sodium azide at 4◦C. We performed MRI data acquisition with the brain preserved inside the skull to avoid tissue distortion and damage (Ullmann et al., 2015). Imaging was performed at the Universitätsklinikum Freiburg, Germany, using a BioSpec70/20 system (Bruker Biospin, Ettlingen, Germany) equipped with a BGA12S gradient insert with a cryogenically cooled 2-channel Tx/Rx mouse head surface coil. After tuning and matching the two coil channels' standard adjustments and an oblique single-slice pilot scan, we performed a multi-slice pilot centered within the brain. Field homogeneity was optimized via mapshim defining the shim volume of an ellipsoid containing the complete brain. For morphological imaging, a T2-weighted three-dimensional Rapid Imaging with Refocused Echoes (RARE) sequence with a turbo factor of eight and an isotropic resolution of 100 µm was employed. With a TEeff of 40 ms and a TR of 3,000 ms, a matrix of 320 × 160 × 120 at a field of view of 16 mm × 16 mm × 12 mm was acquired within 2 h. To support the delineation of brain region boundaries a

segmented, spin echo, 3D Diffusion Tensor Imaging sequence with an acquisition time of 12 h and 4 min was used. It used 10 segments, a TE/TR of 44/1,000 ms, 40 diffusion directions, and achieved a resolution of 100 μm isotropic with a field of view of 28.8 mm × 14 mm × 10.6 mm and a data matrix of 288 × 140 × 106.

MRI data post-processing

We analyzed the RARE images with the Nora Medical Imaging Platform (Anastasopoulos et al., 2017), a software for medical image processing developed by Universitätsklinikum Freiburg. We manually segmented brain regions of interest. The brain regions analyzed were olfactory bulb, neocortex, caudoputamen, nucleus accumbens, amygdala, hippocampus, thalamus, hypothalamus, medulla, midbrain, pons, and cerebellum. We used the histological atlas of the common shrew as well as the mouse brain atlas to identify brain regions (Allen Mouse Brain Atlas; Paxinos and Franklin, 2019). When in doubt about the identity of a particular structure due to image quality, no identification was made. The diffusion-weighted images were first denoised by a postprocessing technique that uses random matrix theory (Veraart et al., 2016). This was followed by Gibbs artifact removal based on local sub-voxel shift (Kellner et al., 2016) and finally up-sampled to isotropic resolution by an edge-preserving interpolation approach (Kellner et al., 2016).

RNA extraction, library preparation, and sequencing

We extracted RNA from five individuals caught in November, 2019 from five different brain regions: neocortex, hippocampus, hypothalamus, thalamus, and olfactory bulb. A five individual sample size was chosen a priori to maximize the power of our differential expression analyses, while also not depleting our sampling population (Todd et al., 2016). We used a modified Qiagen Micro RNA easy protocol for RNA extractions that previous research in our lab (Yohe et al., 2020) has created specifically for small amounts of mammalian neuro-sensory tissue described below. We ground tissues using glass mortar and pestles on dry ice for 1–2 min to limit the degradation of RNA through temperature increases. Carrier RNA (5 ml of 4 ng/ml) and dithiothreitol (DTT, 7 ml at 2 M) is added to the 350 ml of lysate to improve lysing and binding. This mixture is added to each sample while in the glass mortar and ground for an additional minute. Following disruption with mortar and pestle, each reaction was further homogenized with QIAshredder columns. After homogenization, we followed the standard Qiagen Micro RNAeasy protocol, with a slight reduction in DNAse time (from a 15- to a 2-minute incubation), which we have found sufficient to reduce DNA contamination while minimizing RNA degradation. RNA extracted was sent to Azenta Life Sciences for quality control, library preparation, and sequencing. Azenta Life Sciences measured RNA quantity with a nanodrop and quality with RNA

ScreenTape. RNA quality is measured with RNA Integrity Numbers (RINs), which quantifies RNA degradation by calculating RNA fragmentation. Generally speaking, RINs between 8 and 10 are high-quality samples, while those ranging from 6 to 8 are partially fragmented. RNA libraries were prepared with standard PolyA selection and sequenced with attempted depth of 15–25 million reads per sample using 150 bp paired-end reads.

Differential gene expression analysis

Adapters were trimmed and reads filtered using fastp (S. Chen et al., 2018). Filtered reads were quantified by pseudoaligning to the S. araneus genome (sorAra2; GCF_000181275.1) using Kallisto (Bray et al., 2016). Read counts were then normalized using the median of ratios in DESeq2 (M. I. Love et al., 2014). This normalization accounts for the library size of each sample and gene content. We conducted principal component analysis (PCA) of our samples using the top 500 varying genes across all our samples and plotted the principal components that explained the most variance. Using the distance between samples on PC space, we then hierarchically clustered the gene expression profiles and visualized the clustering on a heatmap of z-scores of the count data. We tested for differential expression in all five brain regions using DESeq2 by comparing the expression of genes in each region against all other brain regions at the same time. This was done to avoid multiple pairwise comparisons of each region against all other regions individually, as well as to identify region-specific genes. P-values were corrected for multiple testing with the Benjamini and Hochberg (1995) procedure. Significant differentially expressed genes were then filtered for those with an 1.58 log-fold change (absolute threefold change), to identify differentially expressed genes of high effect in the data set. Thresholds higher than this threshold are exceedingly rare in the brain, with minimal improvement in power (Todd et al., 2016). Finally, as differential gene expression analyses were largely exploratory, no a priori hypotheses were defined.

Results

We displayed the brain atlas of the common shrew as a series of histological sections and MRI images. We visualized landmarks in a series of sections and compared their position between images to match the alignment of MRI images to the histology sections. We identified 24 landmarks in the cerebrum, 19 in the brain stem, six in the cerebral nuclei, and three in the retrohippocampal region (Appendix Table A1.1). The complete set of histological sections is available online at https://doi.org/10.17617/3.HVW8ZN.

We identified 15 of the histological sections using magnetic resonance imaging (Appendix Table A1.1). A three-dimensional reconstruction of the common shrew brain can help understand relationships that are lost in two-dimensional sections (see representative sections in Figure 1.1; 3D orthogonal reconstruction of the brain in Figure 1.2) thus, the three-dimensional brain atlas based on MRI data is made available online on https:// doi.org/10.17617/3.HVW8ZN. MRI data are provided in NIFTI format, which can be uploaded to the Nora Medical Imaging Platform. Users can browse and visualize the atlas as well as the delineations of brain regions using the open online interface (https://www.nora-imaging.org).

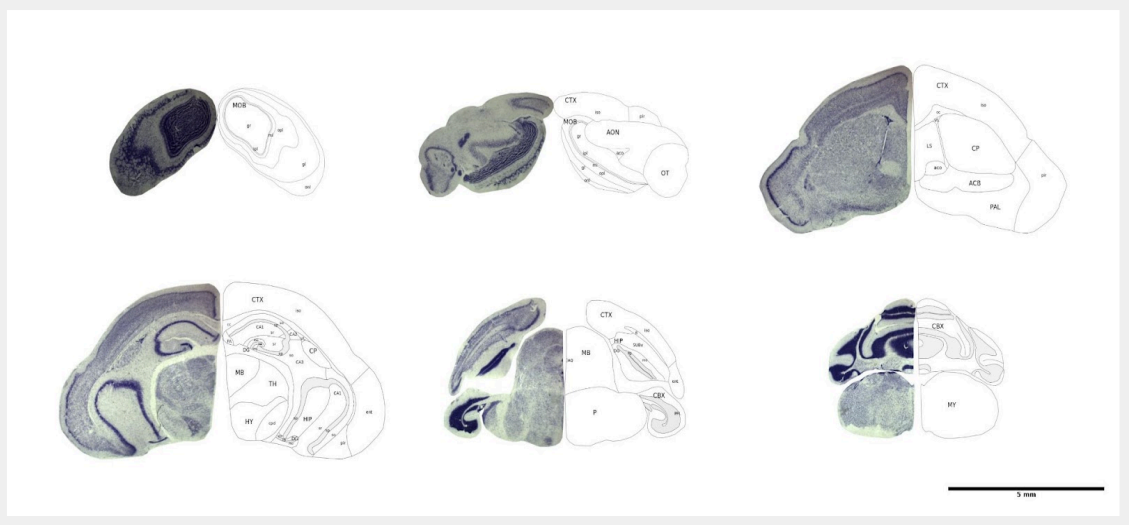

Figure 1.1. Representative histological brain sections with outlines of the brain regions. The image has been modified from Lázaro et al. (2018).

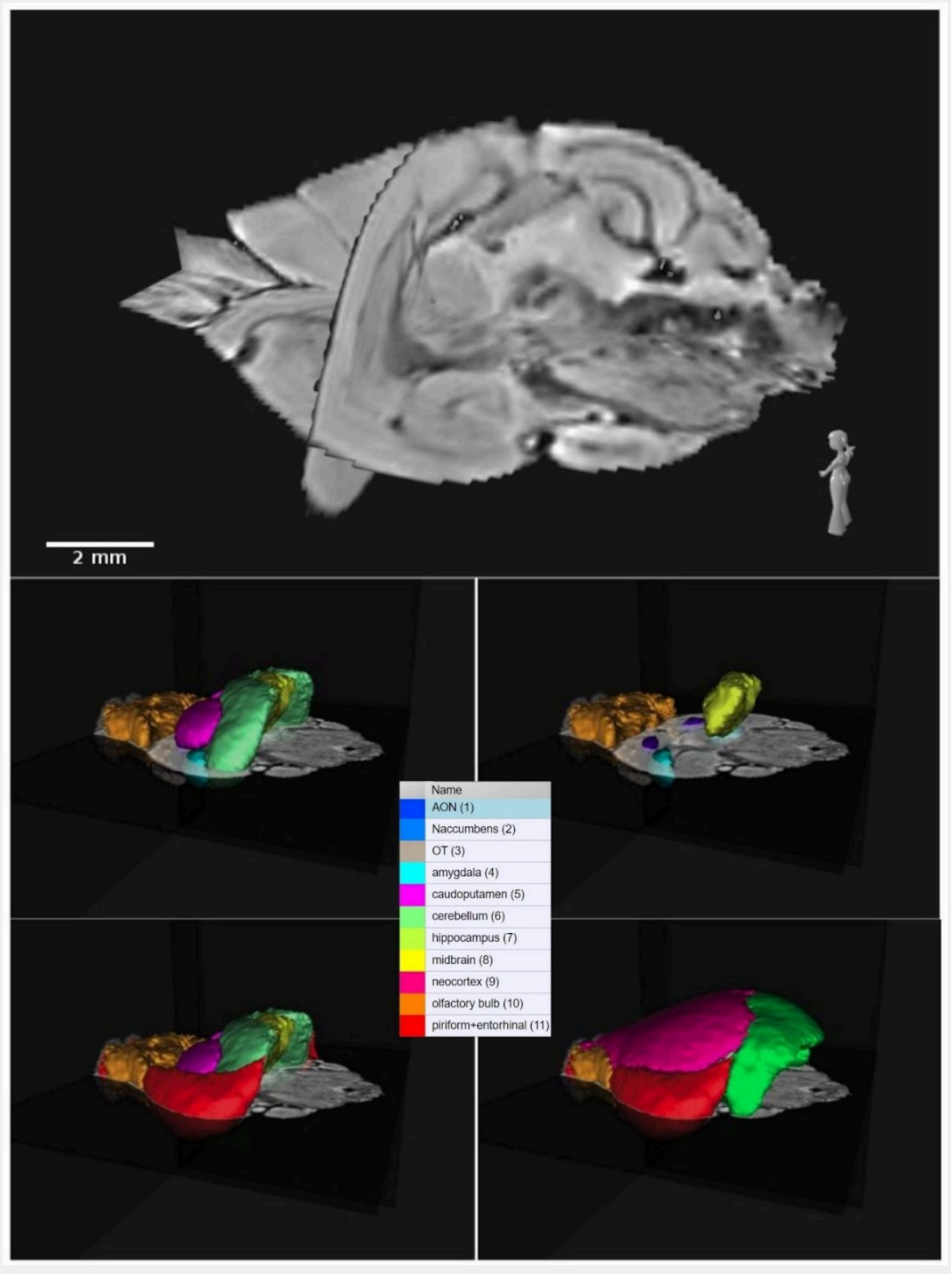

Figure 1.2. Three-dimensional orthogonal representation of the common shrew brain and related color-labeled brain regions. The acronyms correspond to: AON, anterior olfactory nuclei; OT, olfactory tubercle; Naccumbens, nucleus accumbens.

RNA sequencing

RNA was extracted from five individuals for five brain regions: neocortex, hippocampus, hypothalamus, thalamus, and olfactory bulb (Appendix Table A1.1). Extraction of a single individual hypothalamus produced no RNA, with no remaining tissue for further extraction, and this is not included in these results. Total sample reads ranged from approximately 15–27 million reads. RNA integrity Numbers (RIN) varied slightly between different brain regions; neocortex (6.4–8.6, mean 7.5), olfactory bulb (6.5–7.6, mean 7.1), hippocampus (7.0–8.6, mean 7.9), thalamus (5.6–7.8, mean 6.6), and hypothalamus (5.7–8.7, mean 7.1). We mapped reads to the reference transcriptome using Kallisto, with mapping rates ranging from 42.3–56.5%. This range excludes a hypothalamus sample with a mapping rate of 13.9%, however, we did not remove this sample from the experiment, as we normalized by library size prior to examining differential expression. The full list of samples with RIN and Accession Numbers can be found at https://doi.org/10.17617/3.HVW8ZN.

Transcriptomics

After normalizing using the median of ratios used in DESeq2, we transformed expression counts into log scale, and ran a principal component analysis (PCA) on the 750 genes in our data set with the most variance (Figure 1.3). The highest two principal components accounted for 35% (PC1) and 22% (PC2) of the variance found in the gene expression between regions. PC1 largely distinguished the olfactory bulb, hippocampus, and neocortex from the thalamus and hypothalamus, while PC2 accounted for the variance between the olfactory bulb and the rest of the brain regions. We then hierarchically clustered the samples using Euclidean distance between samples on principal component space (PC1 and PC2) (Figure 1.3). The neocortex, hippocampus, and olfactory bulb cluster into individual brain regions, while the hypothalamus and thalamus cluster together and could not be distinguished using these data.

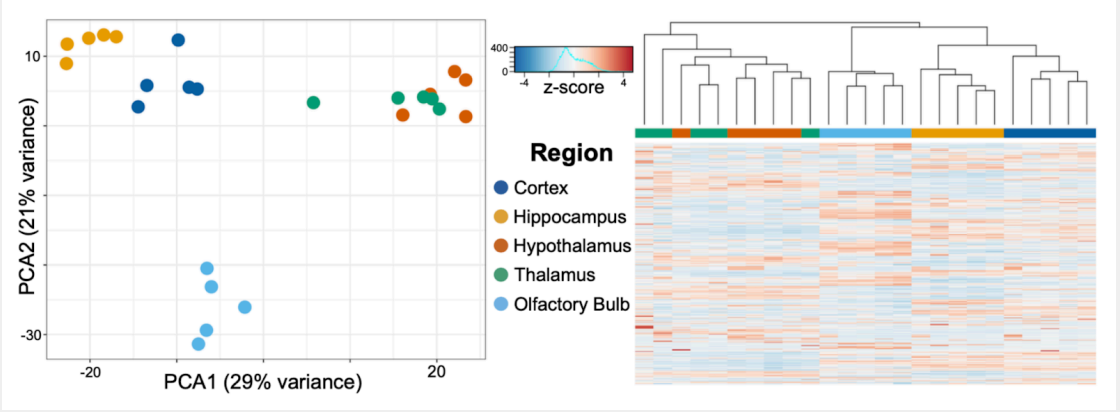

Figure 1.3. Principal component analysis (PCA) of the 750 most varying genes across brain regions characterized through RNA-seq. PC1 accounted for 35% and PC2 for 22% of the variance in gene expression. PC1 separated the olfactory bulb, hippocampus, and cortex from both the thalamus and hypothalamus. PC2 accounted for the variance from the olfactory bulb and the remaining brain regions. Hierarchical clustering of the samples confirms the unique expression profiles of the cortex, hippocampus, and olfactory bulb, while the hypothalamus and thalamus are largely indistinguishable from each other with these samples.

Next, we used DESeq2 to test for differential expression between brain regions and set a log-fold change threshold of 1.58 (absolute fold change = 3), to determine how many of the differentially expressed genes were of high effect (Figure 1.4). The neocortex had 4,619 differentially expressed genes (2,505 upregulated and 2,115 downregulated) in respect to the other brain regions. Of these, 436 were highly upregulated, and 245 highly downregulated. We found similar numbers of differentially expressed genes in the hippocampus, with 4,380 differentially expressed genes (2,220 upregulated and 2,160 downregulated), of which 455 had high upregulation and 390 had high downregulation. The olfactory bulb had more differentially expressed genes (5,100) than both the hippocampus and neocortex, which validates its divergence in PCA. Of these, 2,468 were upregulated in comparison to the other tissues, with 530 highly upregulated, while 2,632 were downregulated, with 507 highly downregulated. The hypothalamus had fewer differentially expressed genes compared to other tissues (3,450; 1,864 upregulated and 1,586 downregulated), as well as less highly differentially expressed genes (330 upregulated and 241 down regulated). This pattern continued into the thalamus, with 3,527 differentially expressed genes (1,739 upregulated and 1,788 downregulated), and a few differentially expressed genes at a high level, 372 upregulated and 242 downregulated. This pattern is caused by the highly similar expression profiles of the thalamus and hypothalamus and is evident from the shared significance in each tissue in ZFHX3 and SHOX2 genes (Figure 1.5). We identified which genes were significant and of high effect in multiple tissues (Figure 1.5) and found an overlap of 180 genes in both the hypothalamus and thalamus, found in no other pair of brain regions, further suggesting that even differentially expressed genes in these two regions have a very similar expression.

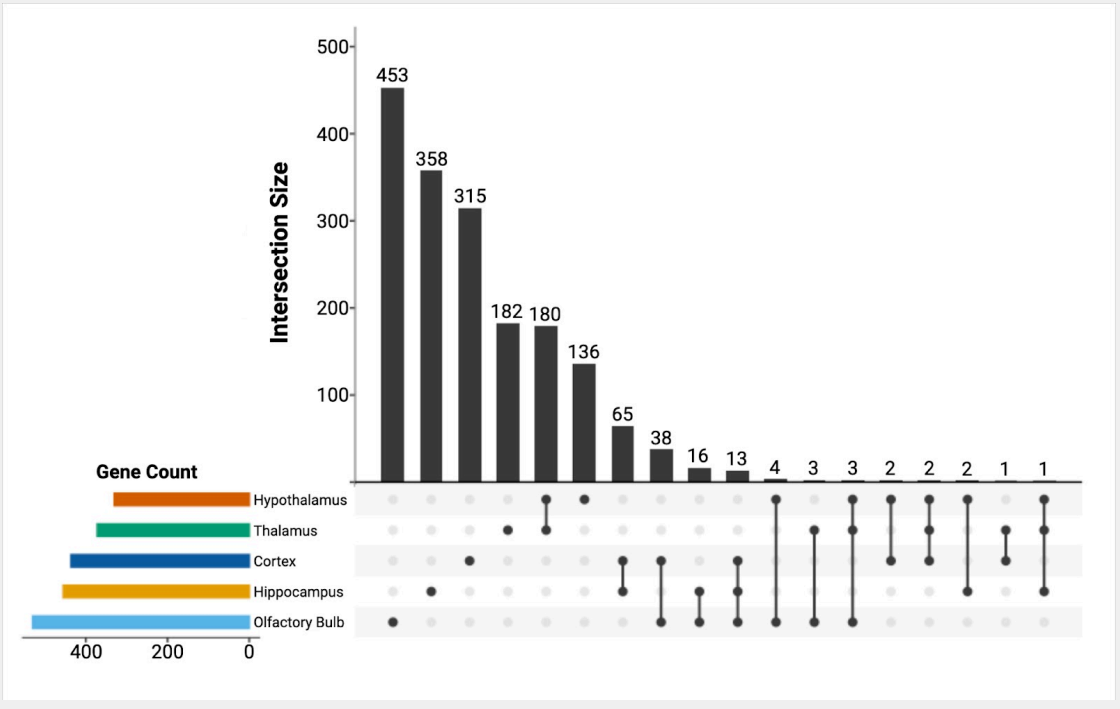

Figure 1.5. UPSET plot of the significantly differentially expressed genes for all the sampled brain regions. The set size measured the number of differentially expressed genes for each region, while the interaction size quantified the overlap between the below regions. A total of 1,444 differentially expressed genes do not have any overlap between brain regions. We also identified an overlap of 180 genes between the hypothalamus and thalamus, which further suggested the similarity of gene expression in these two regions.

Discussion

We created the first high-resolution brain atlas for the common shrew, *S. araneus* as a resource for neuroanatomical guidance of the common shrew brain. We developed two morphometric brain atlases using histological and MRI-based approaches to facilitate fundamental and applied research on the dramatic reversible brain size changes in individual common shrews. First, we generated a histological atlas from juvenile shrews. Here we identified a total of 52 brain structures throughout the cerebrum, brain stem, cerebral nuclei, and retrohippocampal region (Appendix Table A1.1). At this stage of shrew development, the brain is at its largest but beginning to decrease in size.

When looking at the brains of shrews from other ages researchers can expect brain regions to differ in size (see Lázaro et al., 2018 for details). Second, we visualized and identified regions of an old adult with MRI imaging (intermediate-sized brain compared to summer juveniles and winter subadults).

Of the 52 brain structures identified in our histological analysis, we validated 15 with MRI imaging. Incomplete overlap between the two atlases occurs as some structures are more difficult to delineate on the MRI images while others are only partially available in the histological sections. The combination of the two atlases will allow researchers with different infrastructure to access information about the common shrew's brain. While easily interpretable histological sections will be accessible to many collections, MRI data will allow researchers to visualize distinct neuroanatomical structures in three-dimensional space. Although MRI yields a reduction in the number of recognizable nuclei due to resolution limitations, the ability to locate brain structures using the accurate coordinate system is an advantage of this method. By combining traditional morphological (histology), advanced imaging (MRI), and RNA expression (transcriptomics), this new atlas can guide diverse future studies with a range of technologies.

We also produced and integrated transcriptomic data, further validating brain regions based on expression profiles. While each of our focal brain regions in this method (cortex, hippocampus, hypothalamus, thalamus, and olfactory bulb) had expression profiles consisting of thousands of differentially expressed genes (Figure 1.4), we identified 1,444 non-overlapping, highly differentially expressed genes across regions (Figure 1.5). Some of these genes include ZFHX3 (hypothalamus), SHOX2 (thalamus), SP7 (olfactory bulb), PLCD3 (cortex), and HOMER3 (hippocampus) (Figure 1.4). By comparing these genes to results to data found in the Human Protein Atlas,2 we found that while SHOX2 tissue specificity matches human, mouse, and pig thalamus specificity, the remaining genes are not brain-region-specific in humans but are in either pig or mouse. Although brain regions between species have similar expression profiles, differences in brain expression have been reported before (Pucek, 1963). Therefore, the divergence in region specificity between species found here is not uncharacteristic of mammalian brain expression. Our findings validate the need for our species-specific transcriptomic atlas for *S. araneus* to determine the molecular mechanisms of Dehnel's phenomenon, while also identifying a need for further characterization and analysis of evolutionary change in brain expression.

By focusing on the species that is most frequently studied for the brain size changes occurring during Dehnel's phenomenon, we intend to contribute to improved knowledge of the mammalian brain. Despite the long history of research on common shrew biology, the dramatic changes happening in the brain remain almost entirely unexplained. Variations in water and lipid content contribute significantly to the seasonal size fluctuations but do not explain them completely (Pucek, 1963), and the

proximal causes of the morphological changes at the cellular and molecular levels remain unknown(Bartkowska et al., 2008; Lázaro et al., 2018) .

This study focuses on generating a reference atlas of the common shrew brain, rather than quantifying the seasonal change in volume. As a result, we choose not to display the three age groups in the atlas and instead concentrate on developing a useful template using representative data. Moreover, although the changes can be quite significant based on the brain region, they have no impact on the structure of the brain as a whole. Thus, future research endeavors must tackle these unanswered questions through repeated in vivo MRI to study the different stages of brain size in the same individuals or using Diffusion Tensor Imaging (DTI) which would allow non-invasive tracking of brain white matter fibers, enabling researchers to determine how water travels differently across seasons. Furthermore, region-specific genes identified here can be used to validate regions as they are analyzed through shrew brain development. This atlas will both improve the common shrew as a model for future neuroscientific studies, and help understand the processes that contribute to brain regeneration in mammals, with potential implications for the biology of human neurodegenerative diseases.

Data availability statement

The data presented in this study are deposited in the Edmond repository, https://doi.org/10.17617/3.HVW8ZN.

Ethics statement

This animal study was reviewed and approved by the all experimental procedures were carried out according to guidelines for the care and use of animals approved by the Regierungspräsidium Freiburg, Baden-Württemberg (359185.81/G-11/21 and 35-9185.81/G-19/162).

Funding

This work was funded by the Human Frontiers Research Grant RGP0013/2019 to DD, LD, and JN, and the Max-Planck Poland Biodiversity Initiative to DD. LD was supported in part by NSF-IOS 2031906 and 2032063.

Chapter 2

Programmed seasonal brain shrinkage in the common shrew (*Sorex araneus*) alters tissue diffusion properties but does not lead to cell death

Manuscript in preparation

Cecilia Baldoni, Marco Reisert, Bethany Smith, Javier Lázaro, William R. Thomas, Liliana M. Dávalos, John Nieland, Dina K. N. Dechmann, Dominik von Elverfeldt

Abstract

Brain plasticity, the brain's inherent ability to adapt its structure and function, is crucial for responding to environmental challenges. This adaptability is strikingly exemplified by Dehnel's phenomenon, where small mammals experience seasonal reversible changes in brain size to meet the demands of their environments. This adaptive process conserves energy during resource-scarce winter months by reducing brain volume, thereby decreasing metabolic demands. Despite these volumetric changes being well-documented, the specific microstructural alterations that facilitate this adaptation remain poorly understood. Our study employed Diffusion Microstructure Imaging (DMI) to explore these changes in common shrews, revealing significant alterations in water diffusion properties, such as increased Mean Diffusivity and decreased Fractional Anisotropy, during winter. These findings confirm that brain size reduction correlates with a decrease in cell size, as our data indicate no reduction in cell numbers, showcasing a reorganization of brain tissue that supports survival without compromising brain function. This insight into brain plasticity extends our understanding of neuronal resilience and offers potential strategies for addressing neurodegenerative diseases.

Introduction

Brain plasticity is the remarkable ability to reorganize the structure, functions, and connections of the brain in response to environmental demands, learning, or recovery from injury. This adaptive capacity is essential for survival in fluctuating environments, as it enables the brain to maintain optimal function despite changes in external conditions (Kempermann, 2012; Rymer et al., 2013). These changes encompass structural and functional reorganization and metabolic shifts that help the brain cope with various stressors (Lambert et al., 2019). For example, recent evidence suggests that brain structure and properties can change seasonally, potentially influencing neurological disorders and cognitive processes (Kolb & Gibb, 2014; Mateos-Aparicio & Rodriguez-Moreno, 2019).

One extraordinary example of brain plasticity in response to changing environments is Dehnel's phenomenon. This phenomenon involves a considerable decrease in body and brain volume from summer to winter, followed by spring regrowth. This seasonal plasticity has been observed in small mammal species with high metabolisms and year-round activity in cold climates, and it is likely an adaptation to winter as the shrinkage starts in autumn before the onset of winter (Lázaro et al., 2021). By reducing overall size and especially the size of expensive organs such as the brain, the amount of food required for survival is reduced in winter, when food sources are scarce, more

sparsely spread, and slower to replenish (Schaeffer et al., 2020). With low-fat stores and a high metabolic rate, these animals must efficiently locate sufficient amounts of food without wasting energy searching in depleted areas (Keicher et al., 2017). To date, Dehnel's phenomenon has been observed in European moles (Nováková et al., 2022), stoats and weasels (LaPoint et al., 2016), subfamily of red-toothed shrews. Among this family, the common shrew is considered the model species for this unique form of brain plasticity (Dehnel, 1949; Lázaro & Dechmann, 2021) . In a population in Southern Germany, common shrews reach their minimum mass at the end of February, with brains 10-26% smaller compared to their summer size (Lázaro, et al., 2017). The brain begins to grow again in spring and a second, smaller, maximum is reached in summer adults in June (Lázaro, et al., 2017) shortly before reproduction, after which they rapidly senesce and die. This reversible change in brain size represents a natural response to environmental pressures and a possible adaptation for energy conservation and survival during harsh winters.

Extensive research has quantified the volumetric changes associated with Dehnel's phenomenon, noting a significant reduction in the brain weight and water content in the common shrew during winter compared to summer (Pucek, 1965). This reduction is accompanied by increased dry matter content, indicating that dehydration plays a significant role in these seasonal brain weight variations (Pucek, 1965). Additionally, the physiological basis of Dehnel's phenomenon change, with the lowest levels in juveniles during summer, an increase during winter and spring, and a subsequent decrease in adults during summer and autumn. Altered water and lipid content suggest that the brain undergoes significant structural changes to maintain function during harsh conditions, which likely contributes to the observed reduction in neuronal structures by Lázaro et al. (2018). A general decrease in soma size and total dendrite volume was found in the caudoputamen and anterior cingulate cortex, and it may partially explain the overall tissue shrinkage observed in winter.

Despite these findings, significant gaps remain in understanding the microstructural changes underlying these volumetric adaptations. Specifically, the precise quantification of water molecules and the fundamental mechanisms by which they move within the brain during this seasonal transition have yet to be fully explored. Thus, the physiological basis of Dehnel's phenomenon remains unknown. Brain diffusion properties describe the behavior of water molecules moving within brain tissue. This movement is measurable with advanced imaging techniques like diffusion-weighted MRI (DW-MRI), which allows for the non-invasive quantification of tissue architecture and structure through the use of endogenous water, making it a powerful tool in investigating local tissue microstructure (Lewis et al., 2014). Moreover, DW-MRI can distinguish between different water compartments within tissues, such as intracellular water, extracellular water, and water in the microvasculature (Trouard et al., 2008). Key

metrics derived from DW-MRI, such as Fractional Anisotropy (FA), Mean Diffusivity (MD), Axial Diffusivity (aD), and Radial Diffusivity (rD), help quantify these diffusion characteristics (for a more detailed description of these metrics, see box 1). In healthy brain tissue, diffusion is structured and restricted, indicative of intact microstructural integrity, better axonal coherence, density, and myelination (Reveley et al., 2022). Conversely, in neurodegenerative diseases, diffusion patterns become more random and less directional, resulting in lower FA and aD, and higher MD (Cercignani et al., 2001; Y. Zhang & Burock, 2020). These alterations in diffusion metrics are associated with loss of microstructural integrity and reduced tissue organization, reflecting breakdowns in neural pathways and myelin sheaths (Neukomm & Freeman, 2014; Wang et al., 2012).

In the context of Dehnel's phenomenon, seasonal changes in brain tissue properties, particularly variations in water content, might affect the overall cellular composition, potentially explaining the observed reduction in brain weight and increased dry matter content in winter, as documented by Pucek (1965). While Dehnel's phenomenon represents an adaptive, reversible modification of brain structure as a response to environmental stress, it contrasts strongly with the irreversible changes observed in human neurodegenerative diseases, such as Alzheimer's disease, which are characterized by chronic, progressive, and irreversible loss of neural integrity. Interestingly, both conditions share a decline in cognitive performance as a common symptom (Lázaro et al., 2017), suggesting that similar mechanisms related to disrupted water homeostasis might be involved. This similarity raises the question of whether the dysregulation of water diffusion could lead to cell dehydration and consequent cell death during Dehnel's phenomenon, mirroring the pathological processes observed in human neurodegeneration.

A previous study on cell death and recruitment during Dehnel's phenomenon concluded that neither significantly contributes to the seasonal oscillation in brain weight (Bartkowska et al., 2008). However, this result might have underestimated both processes due to methodological limitations. Dehnel's phenomenon may shift from year to year due to weather conditions, as temperature changes are a crucial signal for this phenomenon (Lázaro et al., 2019; Pucek, 1963).

Box 1. Diffusion metrics definitions.

Fractional Anisotropy (FA) measures the directional coherence of water diffusion. High FA values generally indicate well-structured, intact neural tracts where water movement is highly directional, suggesting healthy brain tissue.
Mean Diffusivity (MD) represents the average rate of water diffusion within the brain tissue. Lower MD values often signify denser tissue, while higher MD can indicate less restricted water movement, which might be seen in areas of tissue degradation.
Axial Diffusivity (aD) reflects water diffusion along the length of neural fibers, often used to assess axonal integrity. Reduced aD is typically associated with axonal injury.
Radial Diffusivity (rD) measures the extent of water diffusion perpendicular to the main axis of neural tracts and is sensitive to changes in myelin structure. Increases in rD can suggest myelin breakdown.

To address existing gaps in our understanding of seasonal brain adaptations, we employed Diffusion Microstructure Imaging (DMI) on common shrews in their natural summer and winter phenotypes, representing their maximum and minimum brain sizes, respectively. DMI is an efficient method in advanced diffusion-weighted MRI that decomposes and identifies the diffusion characteristics of brain tissue into intra-axonal, extra-axonal, and a free water compartment (Kellner et al., 2022). Additionally, we counted cell numbers in different brain regions of shrews freshly captured from the wild to quantify any differences in our own study population. Volume-corrected cell counts avoid potential problems, such as the effects of environmental conditions. First, we hypothesized that shrews will show seasonal variations in brain diffusion metrics, specifically increased MD and decreased FA. Second, we hypothesize that there will not be a significant reduction in cell population, contradicting the association between altered diffusion metrics and cell death. Last, we hypothesized that the nature of these brain adaptations in shrews is fundamentally different from the irreversible changes seen in human neurodegenerative diseases. This hypothesis rests on the premise that seasonal adaptations are beneficial and reversible responses to environmental stress, promoting survival without causing lasting cellular damage, typical of neurodegeneration. Understanding these distinctions could deepen our understanding of brain plasticity and resilience, potentially guiding approaches to mitigate neurodegenerative diseases in humans.

Methods

All handling and sampling methods were approved by the Regierungspräsidium Freiburg, Baden-Württemberg, Germany (35-9185.81/G-11/21, 35-9185.81/G-19/80 and 35-9185.81/G-22/082).

We caught common shrews in wet meadows and wet forest-edge areas in Möggingen, Germany (47°46'04.70''N, 8°59'47.11''E), near the Max Planck Institute of Animal Behavior. We caught shrews using live wooden traps (PPUH A. Marcinkiewicz, Rajgród, Poland). For the cell count, we captured five summer juveniles (males; maximum brain size) between June and September 2014 and five winter subadults (four males, one female; minimum brain size) between December 2013 and February 2014. The shrews were sacrificed on the day of capture by perfusion under anesthesia, to remove blood from the brain and other organs. Sex was determined during dissections by the presence of testes or ovaries. The extracted brains were weighed and placed into 4% formaldehyde for storage.

For the DMI study, we caught 19 summer juveniles in August 2021 and kept them in captivity for six months until February 2022. As is typical for this species, mortality occurred in autumn, and by February 2022, our captive group had been reduced to seven individuals. All shrews were housed individually in a double-cage system (see Lázaro et al., 2019 for details), in an outdoor aviary with natural light, temperature, and humidity.

MRI data acquisition and postprocessing

All MR imaging was performed at the Universitätsklinikum Freiburg, Germany using a dedicated small animal MRI system (BioSpec 70/20 | Bruker, Germany) using a cryogenically cooled, two-element transmit/receive surface mouse head coil. Animals were anesthetized in a knockdown box heated by a warming mat under the thorax to maintain body temperature and given 4.5 Vol% Sevoflurane in 1l/min O_2 gas flow. We then placed the animals into the animal bed, fixated them with sticky tape, applied ointment (Bepanthen®) to the eyes to prevent drying, and transferred into the MRI scanner. During pilot-, morphology- and diffusion weighted-scanning anesthesia was upheld with 2.5 Vol% Sevoflurane in a mixture of 0.8 l/min air and 0.4 l/min O_2. Morphology was depicted using a T2 weighted 2D TurboRARE pulse sequence covering the complete brain with 40 slices, 300 µm thick, a field of view of 16x12 mm, and a matrix size of 200x160 leading to an in-plane resolution of 80x80 µm. Acquisition parameters were TE/TR 40ms/5075ms, a RARE-factor of eight, two averages, and a bandwidth of 35 kHz leading to an acquisition time of approximately three minutes. To quantify brain volume, we followed the traditional approach of voxel-based morphology (Ashburner & Friston, 2000). Therefore, we first constructed a shrew brain template based on a group of animals. The template is then used as a reference to coregister individual animals in a deformable manner into template space, and the determinant of the Jacobian matrix of the warp is used to quantify the brain volume locally. A high-resolution post-mortem scan of a shrew served as a starting point for the template space (Baldoni et al., 2023).

Diffusion-weighted imaging was performed as 'high angular resolution diffusion imaging' (HARDI) with two different diffusion weighting values b_1= 1000 s/mm^2 and b_2=1600 s/mm^2, 30 diffusion encoding directions, and four A_0 images. For both scans a four segments, spin echo EPI pulse sequence covering the complete brain with 40 slices, 300 µm thick, a field of view of 15x8 mm, and a matrix size of 100x53 leading to an in-plane resolution of 150x151 µm was employed. A saturation slab ventral of the brain allowed for a smaller FOV in the sagittal direction. A TE/TR of 24ms/2200ms led to a total acquisition time of five minutes for each b-value.

Cell count and tissue histology

After the whole brain was extracted from the braincase, it was weighed, and the right hemisphere was weighed again after it was cut. The right hemisphere was then placed into increasing solutions of sucrose (10%, 20%, and 30%) until sinking occurred, to prevent damage when freezing. The hemisphere was then orientated with the olfactory bulb upwards, frozen into a small water block, and cut into 30µm thick sections with a sliding microtome. Sections were either stored in a freezing solution (3 ddH2O: 3 Glycerol: 3Ethylene glycol: 1PO4 Buffer) or PBSA with 10% Sodium Azide solution.

Nissl staining was performed on every 5th section as follows. The sections were soaked in ddH2O for one minute before progressing through increasing concentrations of ethanol (30%, 50%, 70%, 95%, and 100%) spending one minute in each solution. Ten minutes were then spent in a 50% chloroform/50% ethanol solution, with the solution changed over to a fresh solution halfway through. The sections were then rehydrated through decreasing ethanol solutions, in the same percentages as earlier but in reversed order, and soaked in ddH2O for another minute. Sections were then stained in Cresyl Violet solution for 8 minutes and rinsed in ddH2O for one minute twice, before ascending through the ethanol concentration once more, but with the 95% ethanol replaced with 95% ethanol with a small amount of acetic acid added. Finally, the Roti histology-clearing agent was used for 5 minutes. Slides were then mounted with DPX mountant.

After the sections were mounted they continued to shrink at a slow rate, and to counter this, it was necessary to count each brain series within a week of mounting. Thus brains were stained and mounted in randomly assorted groups of two or three. To prevent a counting bias the slide labels were covered and assigned a temporary identification letter so that the counter was unaware of which age group it came from.

We counted cells in the olfactory bulb, neocortex, nucleus accumbens, caudoputamen, amygdala, and hippocampus. Regions were traced with a 4x magnification, and counted at 64x magnification. Once we traced a region's outline, the Stereo Investigator 11.03 program would lay down a grid. The size of the grid's squares (step size) was determined for each region through the calculation below. Once a suggested step size

had been found for each region, a round number lower than this suggestion was selected for simplicity. A series of trial runs were performed in a single brain and the step size was altered where necessary. For example, it was calculated that a step size of 600µm was appropriate for the hippocampus, but after the trial run, this was reduced to 500µm due to the variation in cell density in this region. The frequency of sections to be counted was determined similarly: the neocortex, with its large number of sections and relatively homogenous distribution of cells, was counted in every tenth section, while the hippocampus, with its less homogenous distribution, was counted in every 5th section. In regions where the section frequency was reduced to every 10th section the step size was altered to compensate by halving the "total area" component of the formula.

The size of the counting frame, a 3D cuboid placed between the top focal layer and the bottom focal layer of the section, was selected to be large enough to contain 1-2 countable cells on average (Burke et al., 2002; West et al., 1991). This size was determined through a short trial run for each region. After the results of this trial the neocortex, caudoputamen, nucleus accumbens, amygdala, and hippocampus were all given the counting frame size of 15x15µm. Due to the higher density of cells found in the olfactory bulb, this region was given a smaller counting frame size of 7x7µm. As trial staining found that sections shrank from 30µm to ca 15µm in thickness, the guard regions were set to 2µm and the counting frame height to 10µm.

The counting frame was automatically placed in a random position within the squares of the grid at the start of a counting procedure by the Stereo Investigator program. The position of the counting frame within the grid square was different between counts but remained the same throughout that counting (West, 2001). The Stereo Investigator program and the microscope setup automatically moved one counting area to the next within the same region with great precision. Cells were determined to be either neurons or glia and were counted accordingly. Neurons were typically characterized by the presence of a single nucleolus and dendrites (Cotter et al., 2001). Neurons also tended to be larger than glia with irregular or triangular-shaped cytoplasm with pale staining. Microglia were small, dark, comma-shaped cells. Epithelial cells (dark, no nucleus, curved) were not counted. Oligodendrocytes were identified by their dark staining and smooth, round appearance (Cotter et al., 2001). Astrocytes were rare but appeared as large, irregularly shaped cells with pale staining. In the olfactory bulb and certain layers of the hippocampus, a large number of neurons are similar in appearance to oligodendrocytes – round and darkly stained. Thus, any cells found in these areas were counted as neurons. The Stereo Investigator program was then used to estimate the total cell number from the volume of the region and the number of cells counted. The final population estimate was weighted by the average section thickness and adjusted for the missing section fraction.

Statistical Analyses

We evaluated the effects of seasonal changes on various brain metrics using a Bayesian hierarchical modeling framework in R (v4.1.2; R Core Team, 2021). Initially, we created models to assess the direct effect of season on various brain metrics and their interactions with each brain region. This allowed us to investigate region-specific seasonal impacts on metrics such as intracellular and extracellular water volume fractions, mean diffusivity (MD), axial diffusivity (aD), radial diffusivity (rD), fractional anisotropy (FA), and cerebrospinal fluid (CSF) volume fraction. We modeled each metric separately to account for their potential different response to seasonal variation. The models were implemented using Stan through the rstan package in R (Stan Development Team, 2024). Next, we extended the analysis to examine how the correlation between metrics of interest varied between seasons. This analysis aimed to understand whether the relationship between these metrics differed significantly with seasonal variation, potentially indicating a seasonal modulation of brain physiology. To do this, we implemented a Bayesian hierarchical model to investigate the relationship between CSF, intracellular and extracellular water volume fraction, and the relationship between FA, aD and rD. Changes in FA are closely associated with alterations in aD and rD, indicative of myelin and axonal damage, respectively (Coppola et al., 2020). Additionally, we created a separate model using the absolute values, obtained by multiplying the relative metric proportions by the corresponding brain region volume. These metrics provide a measure of the actual volume occupied by each component within the brain region, offering a more direct quantification of changes in brain tissue. Lastly, we aimed to determine if changes in microstructural metrics correlated with the observed volume shrinkage from summer to winter. Regarding the cell count, we conducted a regression analysis to understand how the cell population changes across different regions between the summer and winter groups. Hypothesis testing was performed to compare the differences in cell counts for each region by calculating the posterior estimates, standard errors, and credible intervals between the summer and winter groups. For all models, we assessed model stability and convergence with standard diagnostic metrics: effective sample sizes (n_eff), the Gelman-Rubin convergence statistic (Rhat) and Pareto k diagnostics. We used posterior predictive check functions to visually assess model fit.

Results

Seasonal effects on brain metrics. Our results showed that seasonality significantly affected brain tissue microstructure (Figure 2.1), with region-specific differences (Table 2.1, estimates reported in log odds). Intracellular water volume fraction declined significantly from summer to winter, with a seasonal effect estimate of -0.184 (95% CI: -0.258, -0.110). At the same time, the extracellular water volume fraction increased

significantly with the season change (0.310, 95% CI: 0.187, 0.432). Radial Diffusivity (rD), Axial Diffusivity (aD), and Mean Diffusivity (MD) showed a comparable significant decrease between summer and winter. Cerebrospinal Fluid volume fraction (CSF) decreased slightly, though not significantly (-0.103, 95% CI: -0.218, 0.007) and the seasonal effects between brain regions were generally not significant, with minor exceptions not showing consistent patterns across other metrics. Interestingly, neocortex and cerebellum opposed the general trends in all metrics, although in the cerebellum the deviations were generally less pronounced than in the neocortex (see Appendix to Chapter 2, Table A2.1, for all brain regions table by metric).

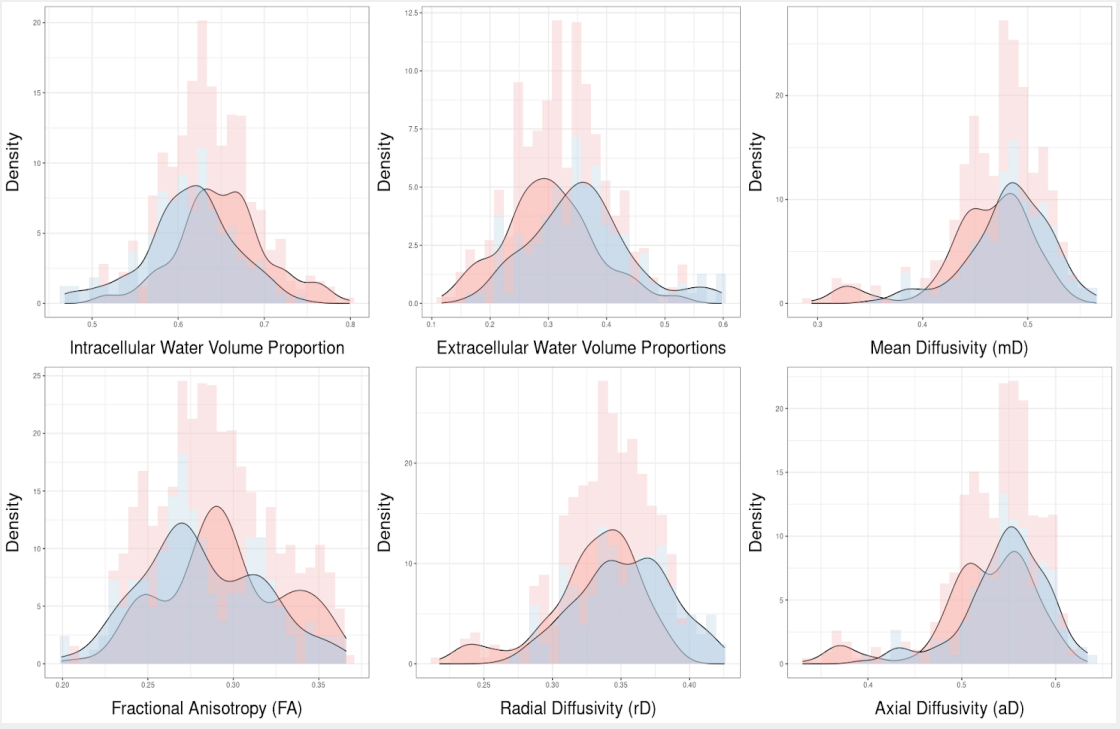

Figure 2.1. Density distributions of various water diffusion metrics and water volume proportions in the brain across summer (red) and winter (blue) seasons, derived from Bayesian models.

Correlation of metrics between seasons. The results from the relative values (water fraction) of intracellular and extracellular water volume and CSF by brain region showed that increases in extracellular volume significantly reduced the intracellular water by 2.92 in summer (-2.92, 95% CI: -3.13 to -2.71) and by 2.68 in winter (-2.68, 95% CI: -2.82 to -2.54). Additionally, CSF volume decreased the intracellular water fraction by 0.56 in summer (-0.56, 95% CI: -1.06 to -0.06) and by 0.62 in winter (-0.62, 95% CI: -1.02 to -0.22). This implies that changes in the surrounding fluid volumes - extracellular and CSF - tend to significantly decrease the probability of intracellular space being occupied from summer to winter. In the model assessing interactions between rD, aD, and FA as relative values, the analysis revealed significant season-dependent impacts. Specifically, increases in rD were associated with

substantial decreases in FA, with a larger decrease observed in summer (-8.28, 95% CI: -8.90 to -7.67) compared to winter (-7.40, 95% CI: -7.93 to -6.86). Conversely, increases in aD correlate with increases in FA, more pronounced in summer (5.04, 95% CI: 4.63 to 5.46) than in winter (4.71, 95% CI: 4.26 to 5.13). These results showed a more pronounced combined influence of radial and axial diffusivities on FA during summer, illustrating notable seasonal variations in brain tissue microstructure dynamics.

Table 2.1. Bayesian estimates of the seasonal differences between two-time points for brain tissue diffusion metrics (see also Box 1). Negative estimates indicate a decrease from Summer to Winter, while positive values denote an increase.

	Estimate	Est. Error	Lower CI	Upper CI
Intracellular water volume fraction	-0.184	0.037	-0.258	-0.11
Extracellular water volume fraction	0.31	0.062	0.187	0.432
Mean Diffusivity (MD)	0.097	0.033	0.032	0.164
Fractional Anisotropy (FA)	-0.072	0.023	-0.119	-0.025
Axial Diffusivity (aD)	0.092	0.035	0.022	0.161
Radial Diffusivity (rD)	0.113	0.03	0.053	0.173
Cerebrospinal fluid volume fraction (CSF)	-0.103	0.057	-0.218	0.007

Correlation between metric changes and volume shrinkage. None of the changes in microstructural metrics correlated with the observed volume shrinkage, either brain volume or brain region, from summer to winter. Results are summarised in the Appendix to Chapter 2 (Table A2.1).

Cell population. We observed a general trend of increased cell population (neurons and glia) from summer to winter across most brain regions. Only the caudoputamen showed a non-significant decrease in cell population from summer to winter. There was a significant increase in cell counts in the olfactory bulb, with winter showing higher counts compared to summer. The differences between summer and winter were not statistically significant for the other regions and the total brain.

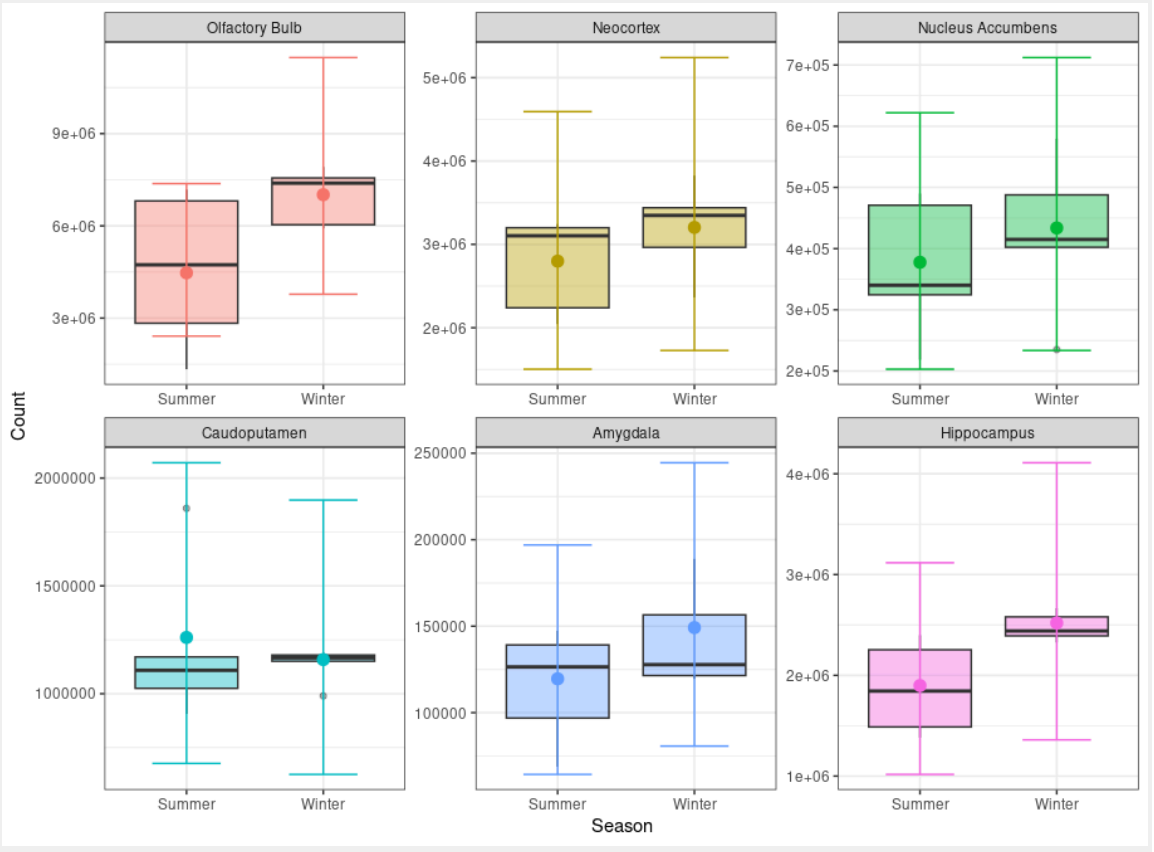

Figure 2.2. Estimated total cell population (neurons and glia) in six different brain regions, in the two seasons: summer and winter.

Discussion

Our study revealed significant changes in water diffusion properties that partially correlated with the changes in brain size. From summer to winter, we observed a 1.08-fold reduction in the intracellular water volume fraction across most brain regions. Our results indicated no decrease in cell population, therefore the decrease in brain volume is likely caused by a decrease in cell size rather than cell number. As cells lose water, they shrink and the space between them expands, which is only partly compensated by an increase in the extracellular water volume fraction. The expansion of extracellular water helps maintain structural integrity, despite the overall reduction in brain volume.

We observed increases from summer and winter in Mean Diffusivity (MD) and Radial Diffusivity (rD), indicating more unrestricted water movement within the brain's extracellular space. Concurrently, a decrease in Fractional Anisotropy (FA) suggests a loss of directional water movement, likely due to structural reorganizations within the brain (Chen & Schlaug, 2013; Panenka et al., 2015). These changes may help the brain maintain optimal function amidst varying seasonal conditions. The mixed changes in Axial Diffusivity (aD) across different regions suggest that some regions may experience

directional restructuring, while others do not. Additionally, Cerebrospinal Fluid volume fraction (CSF) showed overall decreases but regional increases in specific areas like the cerebellum and hippocampus, possibly reflecting compensatory mechanisms to maintain pressure and cushioning during brain shrinkage. Collectively, these changes point to a significant reconfiguration of brain tissue microstructure, likely involving changes in cellular density, cell size, and the composition of the extracellular matrix to cope with variations in environmental conditions and resource availability that accompany seasonal transitions (Zhou et al., 2021).

The reduction in the size is thought to be a shrew adaptation to a reduced resource landscape in winter. The cellular and molecular changes we found may facilitate additional energy conservation during winter. The decrease in intracellular volume may reflect a reduction in metabolic demand, while the increase in extracellular volume might help maintain ionic balance and neurotransmission under reduced energy consumption (Zhou et al., 2021). The shrew's survival strategy relies on these adaptations, which help it cope with limited resources during winter. A study by Lázaro (2018) observed significant seasonal changes in dendritic structures, with a reduction in dendrite complexity and spine density in the hippocampus during winter, partially regrowing in summer. This both supports our findings of reduced intracellular volume and suggests that dendritic retraction and regrowth may be part of the brain's strategy to reduce metabolic demands during winter.

Despite significant seasonal changes in individual metrics, the relationships between key microstructural components remained stable. When examining both relative metrics (proportions such as intracellular, extracellular, and cerebrospinal fluid fractions) and absolute metrics (volumes obtained by multiplying these proportions by the brain region's volume), we found consistent proportional contributions across seasons. This stability suggests a robust underlying organization that preserves interactions between these components, even as the brain adapts to environmental changes. Similarly, the relationships between FA, aD, and rD remained stable, indicating that the fundamental microstructural properties of the brain maintain their interactions despite significant seasonal changes (Assaf & Pasternak, 2008).

When examining whether these metric changes correlated with the observed volume shrinkage, we found no significant correlations. Specifically, variations in intracellular, extracellular, and cerebrospinal fluid (CSF) volumes did not significantly account for the overall reduction in brain volume. This suggests that other underlying mechanisms may drive the seasonal brain volume changes observed in shrews. The stability of these relationships amidst significant changes showcase the brain's structural resilience (Budde et al., 2007). Metabolic adjustments, such as those involving AQP4 and CPT1, may contribute to these stable relationships by optimizing water management and energy utilization without compromising structural integrity. AQP4, a water channel

protein primarily found in the brain, regulates water homeostasis and facilitates water transport across cell membranes. CPT1 is an enzyme located in the mitochondrial membrane that is essential for the transport of long-chain fatty acids into the mitochondria for beta-oxidation, a key process in fatty acid metabolism. These metabolic adaptations might explain why changes in individual metrics do not directly correlate with overall volume changes.

Metrics such as FA, rD, and aD, are often used in human studies to assess brain health. In neurodegenerative conditions like Alzheimer's disease and multiple sclerosis, changes in these metrics often indicate white matter degeneration and loss of structural integrity, typically showing both a decrease in FA and an increase in rD and aD, along with disrupted relationships between these metrics (Kenyon et al., 2024; Sun et al., 2006). A striking difference in our study is that while FA decreases, both rD and aD increase in the shrew brain from summer to winter, relationships between these metrics remain stable. This stability suggests a robust fundamental structure that adapts to environmental stressors without compromising the interactions between different brain components. In contrast, human neurodegenerative diseases show both changes in individual metrics and a breakdown in their relationships, reflecting a loss of structural and functional integrity (Rovaris et al., 2005).

One notable aspect of our findings is the variability in response across different brain regions. For example, while almost all regions showed changes in intracellular and extracellular water volume fractions consistent with overall brain shrinkage, regions like the neocortex and cerebellum often exhibited changes in the opposite direction. This regional variability suggests that different brain areas may employ distinct strategies to adapt to seasonal changes. The neocortex, involved in higher cognitive functions, and the cerebellum, essential for motor control, may prioritize maintaining certain structural and functional aspects over others. These differences could be attributed to the unique functional demands and connectivity patterns of these regions. For instance, the role of the neocortex in complex processing and integration of sensory information might require it to maintain a more stable microstructural environment to preserve cognitive function (Caroni et al., 2012; Holtmaat & Svoboda, 2009). Similarly, the involvement of the cerebellum in motor coordination and balance could necessitate maintaining specific structural integrity to ensure efficient motor performance (D'Angelo & Casali, 2013).

The varied responses of different brain regions to seasonal changes reveal the brain's adaptive mechanisms. A regional differential response shows the importance of considering regional differences in studies of brain structure and function. Our findings indicate that adaptation to seasonal demands is not uniformly distributed across the brain. Instead, it involves a complex balance between maintaining structural integrity, meeting functional demands, and managing metabolic needs. Such regional specificity suggests that certain brain areas may have evolved distinct strategies to optimize

survival during environmental changes.

Our observations also reveal that the changes in the volume of specific brain compartments do not correlate with overall brain shrinkage. This lack of correlation points to a sophisticated adaptive response, engaging a variety of physiological, molecular, and structural mechanisms. Although these findings enhance our understanding of brain plasticity, it is crucial to recognize the limitations inherent to the diffusion MRI techniques we employed. For example, factors such as FA can be affected by not only changes in cellular organization and water content but also by variations in brain temperature. Temperature fluctuations can alter the physical properties of cellular membranes and the viscosity of the intracellular environment, which in turn affects the diffusion behavior of water molecules measured by FA (Kuriyama et al., 2015). Such temperature-induced changes could potentially bias the results, leading to misinterpretations of the underlying microstructural integrity. To overcome these limitations and build a more comprehensive model of brain structural adaptations, future research should integrate additional imaging modalities, such as fMRI, and physiological measurements that can capture a broader spectrum of changes.

Funding

This work was funded by the Human Frontiers Research Grant RGP0013/2019 to DD, LMD, and JN. WRT was supported in part by a Stony Brook University Presidential Innovation and Excellence award to LMD.

Acknowledgments

We thank Marion Muturi, Ivan Lenzi, Marina Farantouri and Kostantinos Raptis for invaluable help in catching and bringing the shrews to Freiburg for MRI scans. The animal caretakers of the institute, and Drs. Inge Müller and Daniel Zuniga provided incredible help with shrew care. We wish to thank the core facility AMIR^{CF} (DFG-RIsources N° RI_00052) for support in MR imaging. Special thanks to Valerij Kiselev for feedback and help in interpreting the results.

Ethics statement

This animal study and all experimental procedures were carried out according to guidelines for the care and use of animals approved by the Regierungspräsidium Freiburg, Baden-Württemberg (35-9185.81/G-11/21, 35-9185.81/G-19/80 and 35-9185.81/G-22/082).

Competing interest

The authors declare no competing or financial interests.

Chapter 3

Captivity alters behavior but not seasonal brain size change in semi–naturally housed shrews

Accepted for publication in *Journal of Experimental Biology*

Cecilia Baldoni, Konstantinos Raptis, Marina Farantouri, Ivan Lenzi, Ka Sing Lim, Myles H. M. Menz, Marion Muturi, Marco Reisert, Maria Alejandra Bedoya Duque, William R. Thomas, Liliana M. Dávalos, John D. Nieland, Dominik von Elverfeldt, Dina K. N. Dechmann

Abstract

Captivity, frequently used in animal research, can profoundly alter brain size, cognitive abilities, and activity levels. Critically, persistent exposure to stressors in captive environments can lead to chronic stress, and subsequently to a range of health issues. However, the direct implications of captivity on research outcomes have not been thoroughly investigated. We examined the effects of captivity on the common shrew, *Sorex araneus*, a species that exhibits a profound seasonal reversible change in brain and body size. We compared wild shrews during summer and winter to assess seasonal changes in brain size and behavior and then contrasted these findings with shrews kept in captivity for six months. Using repeated *in vivo* MRI imaging, we determined that the extent of seasonal brain size change was not affected by the semi-natural captive conditions. However, captivity led to increased activity levels and reduced learning motivation in the shrews, indicative of chronic stress. These results suggest that even semi-natural conditions can significantly alter the outcome of studies and these effects need to be quantified before experimentation.

Introduction

Despite most animal research being conducted in captivity, the potential effects of the captive environment are rarely assessed. Captivity allows for controlled settings and standardized research approaches that are difficult to implement in complex natural environments. Yet, emerging evidence indicates captivity effects are profound and complex (Clubb & Mason, 2003; Marino et al., 2020; Schmidt et al., 2019), making it challenging to accurately study natural processes, such as behaviors (Rees 2015; but see (Cauchoix et al., 2017).

Captivity can lead to long– and short-term changes. Heritable changes can affect behavior (Crates et al., 2023), brain size (Lesch et al., 2022; Pohle et al., 2023), and genome (Araki et al., 2007; Larson & Burger, 2013) in animals bred for laboratory research, domestication, food, or fur production. These changes are often unintended byproducts of breeding in captivity, making many changes irreversible if animals return to the wild, resulting in lower survival (Frankham, 2008; Jule et al., 2008; Zeder, 2012 but see Pohle et al., 2023). In wild-caught animals, captivity can have short-term,

potentially reversible impacts, on many processes including behavioral and physiological adaptations. These changes stem directly from commonly used captive conditions, which expose the animals to chronic stressors such as intensive human interaction, confinement, diet, food-seeking behavior, or artificial lighting (Fischer et al., 2018; Morgan & Tromborg, 2006). Such chronic stress leads to changes in hormone balance, immune responses (Dickens et al., 2009; A. C. Love et al., 2017; Seeber et al., 2020), and gene expression (Bedoya Duque et al., 2023; DuRant et al., 2020; Morales & Sánchez, 1996), which can result in a variety of health issues, further affecting cognitive and physical abilities (Li et al., 2008). The cumulative impact of these factors can have additional behavioral effects such as altered activity levels in captive animals, ranging from lethargy to stereotypy (Resende et al., 2014). Interestingly, the negative cognitive effects of captivity can be mitigated to some extent, particularly by enriched environments (Salvanes et al., 2013; Zebunke et al., 2013), suggesting that strategic modifications can reduce the profound effects of captivity on animal well-being.

It is essential to recognize the differences between captive and wild animals not only in behavior but also in physiology and the underlying genetic mechanisms to understand the confounding effects of captivity on research (Calisi & Bentley, 2009). The common shrew (*Sorex araneus*) serves as an ideal model for such studies, particularly due to its unique seasonal physiological adaptation known as Dehnel's phenomenon (Dehnel, 1949). This adaptation involves significant morphological and behavioral changes throughout the shrew life cycle, characterized by a remarkable seasonal fluctuation in brain, skull, and body size (Lázaro & Dechmann, 2021). In a population in Southern Germany, brain mass decreases by 10-26% from summer to winter, which subsequently regrows by 9-16% in spring as they reach adulthood (Lázaro, et al., 2017). A practical approach for studying this cycle and its effects is to capture the shrews as newly independent juveniles in summer, and then maintain them in captivity throughout their lifespan, which averages 13 months in the wild. This allows for repeated measurements of brain size and behavioral tests. Thus, it is important to determine how captivity influences these changes. When kept in semi-natural conditions in outdoor aviaries, skull size, a proxy for brain size, showed the same pattern of change in captive shrews as in their wild counterparts (Lázaro et al., 2019). In contrast, when maintained indoors at a natural light cycle, but at a constant temperature, skull size steadily declined throughout their life. These two studies demonstrated that brain size changes in shrews are flexible and influenced by environmental factors.

Dehnel's phenomenon is increasingly recognized as an adaptation by high-metabolic species that remain active year-round, to endure winter conditions (LaPoint et al., 2013;

Nováková et al., 2022). Shrinking in overall size and reducing the mass of energetically expensive organs such as the brain reduces energy consumption and food requirements, yet this reduction in brain size compromises function. Shrews freshly caught from the wild perform less effectively in a spatial navigation task in winter, the period of reduced brain size (Lázaro et al., 2017). To work with captive shrews it is important to be able to distinguish the effects of Dehnel's phenomenon from those resulting from captivity. Previous work has identified significant changes in gene expression in this population after just two months of captivity, despite being kept in the semi-natural conditions described above (Bedoya Duque et al., 2023). These changes resemble those seen in depression, stress responses, and neurodegeneration, emphasizing the importance of accounting for the effects of captivity.

To explore the effects of captivity, we compared the cognition, brain morphology and activity of young shrews in summer with subadults in winter. Here we used two categories: shrews that had been in semi-natural captivity since summer and fresh caught ones from the wild. Summer to winter is when the greatest change in shrew brain size occurs, and we hypothesized that even semi-natural captive conditions will alter the shrews' behavioral and cognitive responses. First, we followed brain volume changes in shrews using in vivo Magnetic Resonance Imaging (MRI), anticipating that the semi-natural conditions would not influence the natural seasonal reduction in brain size (Lázaro et al., 2019). Then, we tested shrews in an associative learning task, considering how the cognitive impairment caused by Dehnel's phenomenon might be influenced by captivity, which imposes environmental constraints absent in the wild, such as limited foraging opportunities and reduced sensory stimuli, as well as being exposed to a different diet. If these constraints significantly affected shrews kept in captivity, we anticipated a noticeable decline in cognitive functions. Conversely, if the semi-natural conditions sufficiently mimicked the wild environment, then the expected cognitive decline might be less pronounced or absent. Lastly, building on the finding that all shrews immediately begin using running wheels in captivity (Schaeffer et al., 2020), we examined activity patterns between the three categories. Although wild shrews are less active in winter (Churchfield, 1982), we hypothesized that even semi-natural captive conditions would alter the shrews' behavioral and cognitive responses. This could manifest as increased activity levels, similar to the restlessness observed in captive migratory birds (Berthold & Querner, 1988), potentially indicative of chronic stress. Alternatively, if captivity does not significantly disrupt typical seasonal behaviors, we might observe activity patterns that resemble those of wild shrews, with reduced winter activity.

The impact of captivity is increasingly recognized as a factor that can significantly mask the effects of treatments or other experimental methods. Given the increasing interest in shrews for applied research, it is important to measure these effects at an early stage to establish protocols that account for the influence of captivity. These studies are crucial for understanding how captivity not only affects animal physiology and behavior but also influences the outcomes of experimental research.

Methods

All handling and sampling methods were approved by the Regierungspräsidium Freiburg, Baden-Württemberg, Germany (35-9185.81/G-19/80 and 35-9185.81/G-22/082). Common shrew individuals were caught from the wild in Möggingen, Germany (47°46'04.70''N, 8°59'47.11''E), near the Max Planck Institute of Animal Behavior. We caught 13 shrews with live wooden traps (PPUH A. Marcinkiewicz, Rajgród, Poland) in August 2021 when their brain size was at its maximum (from now on referred to as summer wild) and kept them in captivity until February 2022 (six months) when brain size was at a minimum (winter captive). As is typical for this species, mortality occurred in autumn, and by February 2022, our captive group had been reduced to seven individuals. Due to the rapid physiological changes inherent to Dehnel's phenomenon, it was not possible to conduct both behavioral and imaging experiments within the narrow time frame required to capture the peak of minimum brain size. Consequently, we caught eight additional shrews (winter wild) in February 2023, to be compared with our captive winter subadults. We did not determine the sex of the shrews in our experiments. Shrews typically reach sexual maturity in spring (April-May) but we tested them in summer and winter. Previous research indicated no significant differences between males and females regarding brain shrinkage and cognitive abilities (Lázaro et al., 2017) during the non-reproductive seasons. All shrews were housed individually in a double-cage system (see Lázaro et al., 2019 for details), in an outdoor aviary with natural light, temperature and humidity, which we consider to be semi-natural captive conditions. We carried out all MRI scans and cognitive tests and collected running wheel data within four weeks each season to coincide with brain size peaks - its maximum in summer and minimum in winter. This method helped to minimize the confounding effects of brain size fluctuations by capturing data at these narrow time peaks when changes are most pronounced.

Brain volumes

MRI scans of the brain were performed at the Universitätsklinikum Freiburg, Germany, using a BioSpec70/20 system (Bruker Biospin, Ettlingen, Germany) equipped with a BGA12S gradient insert, and with a cryogenically cooled 2-channel Tx/Rx mouse head

surface coil. We transported individual shrews to Freiburg inside their home cages and returned them to their holding facilities within 10 hours. We induced anesthesia in a knockout chamber utilizing 3.5-4% sevoflurane in O2 with a gas flow rate of 1.9 l/min. We then transferred them to an animal bed with a custom 3D-printed nose holder, ensuring a continuous supply of 2.5-3% sevoflurane (gas flow rate 1.2 l/min with ⅓ O2 and ⅔ Air). We maintained a constant body temperature with a warm water flow tube under the shrew and monitored the breathing rate with a respiratory pad beneath the shrew's abdomen. We recorded overall brain anatomy, which took 20 minutes or less. Following measurements, we returned the shrews to the knockout chamber, where they received pure oxygen until awakening, a process that typically takes only a few seconds. We then returned the shrews to their home cage with access to water and food and continuously observed them until the effects of anesthesia had completely worn off.

MRI data acquisition and validation

Following an oblique pilot scan, brain anatomy was recorded using a T_2 weighted Turbo RARE sequence with axial orientation, and the following parameters: TE/TR = 40ms / 5075ms, 2 averages, RARE-factor= 8, 40 slices, FOV= 16mm x 12mm, slice thickness of 0.3mm, matrix size 200x150, isotropic in-plane-resolution 80µm, bandwidth 35 kHz, and a total acquisition time of 3 minutes and 2 seconds. To quantify brain volume, we followed the traditional approach of voxel-based morphology (Ashburner & Friston, 2000). Therefore, we first constructed a shrew brain template based on a group of animals. The template is then used as a reference to coregister individual animals in a deformable manner into template space, and the determinant of the Jacobian matrix of the warp is used to quantify the brain volume locally. A high-resolution post-mortem scan of a shrew served as a starting point for the template space (Baldoni et al., 2023). Based on brain-masked and bias field-corrected T2w scans the ANTs toolbox was used for co-registration into the template space. After the coregistration of 50 animals, the mean T2w contrast in template space is computed, and the mean is again used as a reference contrast in template space to coregister the same 50 animals, which results in a final template image. The ANTs toolbox (Avants et al., 2011) was used for all registration steps and mutual information as a similarity measure.

Associative learning task

We evaluated the ability of shrews to associate an odor cue with a reward (associative learning task) in a Y-maze (graphic depiction in the Edmond repository, see Data Accessibility). For this, we selected five artificial food flavors as cues (“odors”, i.e. vanilla, lemon, orange, almond, sugar cane). Before running the experiment, we ensured that the five odors were neither strongly preferred nor actively avoided by running six

exposure trials (details in Appendix to Chapter 3). All five odors were randomly assigned as correct or incorrect cues for each individual, except orange and lemon, which we never presented simultaneously because their odors are isomers of the same molecule.

We conducted the main experiment on the day after the exposure trials as follows. We food-deprived the shrews for two hours, slightly longer than their natural feeding interval. We transported the shrews to the experimental room in their homecage, which was then connected to the Y-maze apparatus with a flexible tube. Shrews were then able to decide freely when to enter the Y-maze. Each arm of the Y-maze led to a box with a one-way door forcing the shrew to make an irreversible decision. These boxes contained one of two odor cues, applied to a sponge in a placeholder glued to the top of the box. Each box also contained either the scent of mealworms (unrewarded box) or a frozen mealworm (rewarded box), which was not visible from outside the box. As shrews do not exhibit high levels of food motivation in captivity, we additionally connected the rewarded box to the home cage allowing the shrew to return to the safety of the homecage as an additional incentive (adapted from Mazza et al., 2018). An equally long dead-end tube was connected to the unrewarded box. After each shrew returned to the homecage, whether after a correct choice or by the experimenter, we cleaned the Y-maze to remove scent marks, replaced the boxes, and positioned them on their designated sides for the next trial. Each shrew performed ten consecutive trials and was then returned to the aviary in the homecage.

Running wheel activity

We designed a running wheel system using a similar approach applied to construct computerized tethered flight mills for studying insect behavior, to investigate activity patterns in the shrews (Jones et al., 2015). We attached a black-and-white striped laminated paper ring (16 cm diameter, 1 cm height) to the outside rim of a commercially available mouse running wheel (16 cm diameter). A light sensor was fixed to an L-shaped wire arm attached to the wheel frame. The light sensor was positioned so that the black-and-white ring could pass through the sensor to detect rotations of the wheel, with the circumference of one rotation measuring 50 cm. The sensor was connected to a microcontroller board with eight channels, allowing up to eight running wheels to be operated simultaneously. Data was captured using custom software run on Microsoft Windows 11. Data recorded were distance moved (m), time spent running (s), and running speed (m/s). Data for each shrew were extracted via a MATLAB script (The MathWorks Inc. 2022). Shrews had constant access to the wheels and could choose when to run. All bouts of running were recorded in August-September 2021 for wild summer shrews and in February-March 2022 and 2023 for the wild and captive winter shrews. Data were collected in all three cases for four weeks. We collected a

total of 19,737 running bouts. To reduce the likelihood that recordings may have been due to movement from other influences such as the shrew brushing against the wheel, only bouts that were at least 0.3 m were included in the analyses. This corresponds to the wheel moving at least half a turn, or roughly four body-lengths of a shrew.

Statistical analyses

All analyses were performed in R version 4.3.1 (R Core Team, 2015). All models were developed using the brms package for Bayesian modeling (Bürkner 2021). All our models were stable with large effective sample sizes (Bulk ESS and Tail ESS over 1000 for all estimates) and R-hat values smaller than 1.01. Pareto k estimates were below 0.5 for all models. We used prior and posterior predictive check functions to visually assess priors and model fit. For all models, we included a random intercept for each individual (ID) to account for repeated measures of some individuals (between summer wild and winter captive). All models and data can be found in the Edmond repository (see Data Availability statement).

Brain volumes. We conducted a Bayesian mixed effect analysis to determine differences in brain volume between categories (summer wild, winter captive and winter wild). We compared the effect of categories on brain volume.

Associative Learning task. We compared the associative learning performance between wild summer juveniles, wild winter subadults and captive winter subadults. The model was based on a Bernoulli distribution for binary data (success = 1, failure = 0). We compared the effect of trial number in each category (summer wild- winter captive - winter wild) on success with generalized additive models (GAMs). We fit the model with mild regularising priors. To ensure the accurate interpretation of our findings regarding individual associative learning abilities, we conducted additional analyses to rule out alternative strategies, such as reinforcement learning, side preference, or random choice (see Appendix to Chapter 3 Material). Finally, we investigated the effect of category on latency (described as the time from the start of the experiment until the shrew entered the Y-maze) by implementing a hurdle model (negative binomial) to account for the large proportion of instances where latency was zero.

Running wheel activity. We used a Bayesian hierarchical model to analyze whether the logarithm of the distance run was influenced by a cyclic spline by hour of the day for each category (summer wild, winter wild, or winter captive) and average speed. Additionally, the model allowed the scale parameter (sigma) to vary by group. For the cyclic spline, “hour” was defined as a 24-hour period, capturing the cyclical nature of time throughout the day.

Results

Brain volumes

When we compared wild summer juveniles with wild and captive winter subadults, brain volume changed as predicted based on Dehnel's phenomenon. The brain volume in summer was 224.15 µl, which decreased to 210.2 µl in wild winter individuals and 207.25 µl in captive winter individuals (Table 3.1). This is a reduction of approximately 7.54% from summer to winter captive and approximately 6.22% from summer to winter wild (Figure 3.1). Similarly, there was no difference in the changes of individual brain regions (see Appendix to Chapter 3 for detailed models). To account for the smaller sample sizes in winter we additionally calculated contrasts between winter captive and winter wild brain sizes. The analysis revealed a mean difference in brain volume between the categories winter wild and winter captive of -2.94 units (95% credible interval: -13.22 to 7.22), indicating no statistically significant difference (Table 3.2). This suggests that captivity status does not significantly affect brain volume in our sample.

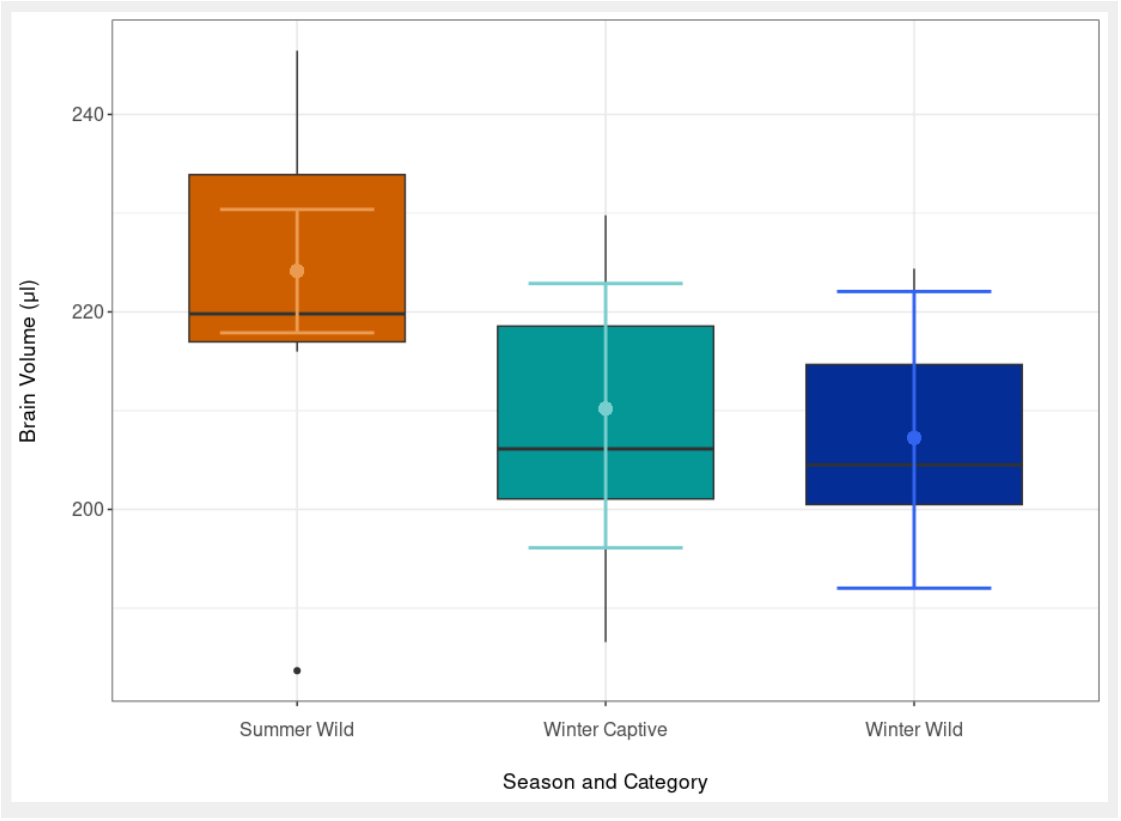

Figure 3.1. Brain volume comparison across the seasonal categories. The boxplots display brain volumes in microliters. Points with error bars represent the posterior means and 95% credible intervals (CIs) derived from the Bayesian model.

Associative Learning Task

The success rate between wild summer juveniles, wild winter subadults and captive winter subadults differed. In summer the estimated success rate increased by 0.48 on the log odds scale (95% CI: 0.08, 0.91), translating to 1.62 times higher success (95% CI: 1.08, 2.46). For winter wild, the log odds of success were estimated to be 0.12 (95% CI: -0.34, 0.57), translating to an odds ratio of 1.13 (95% CI: 0.71, 1.77). Conversely, winter captives showed a log odds of success of -0.29 (95% CI: -0.76, 0.18), with an odds ratio of 0.75 (95% CI: 0.47, 1.20). The seasonal trajectory of success rates over trial numbers also differed. In summer, the success rate increased from 0.504 in trial 1 to a peak of 0.894 in trial 6, then declined to 0.235 by the last trial. Winter wild individuals mirrored this pattern but peaked slightly later, in Trial 8 (estimate trial 1 = 0.376, estimate trial 8 = 0.725) (Figure 3.2, Appendix to Chapter 3: Table A3.2). Winter captives achieved their best performance during the first trial, and after that, performance declined with estimates 0.386 (95% CI = 0.230, 0.571) and 0.348 (95% CI = 0.136, 0.609) at trial 8 and 10 respectively.

There were non-linear relationships between trial number and latency to enter the arena for all categories (see Appendix to Chapter 3). Latency was higher in summer (estimate = 2.51, 95% CI = 1.99, 2.95), but the latency of captive winter animals was longer than that of wild winter shrews (estimate = -0.43, 95% CI = -1.00, 0.15). There were many instances where the latency was zero, meaning the shrew entered the arena within a minute. The patterns in these zero latencies reflected those found in overall latencies: 11% of the wild summer shrews had a latency of zero. In winter, this proportion increased to about 39%. This was because none of the wild winter shrews entered the arena within a minute. The random effect estimate for individual variation was 0.45. This suggests that individual variation was accounted for in the model.

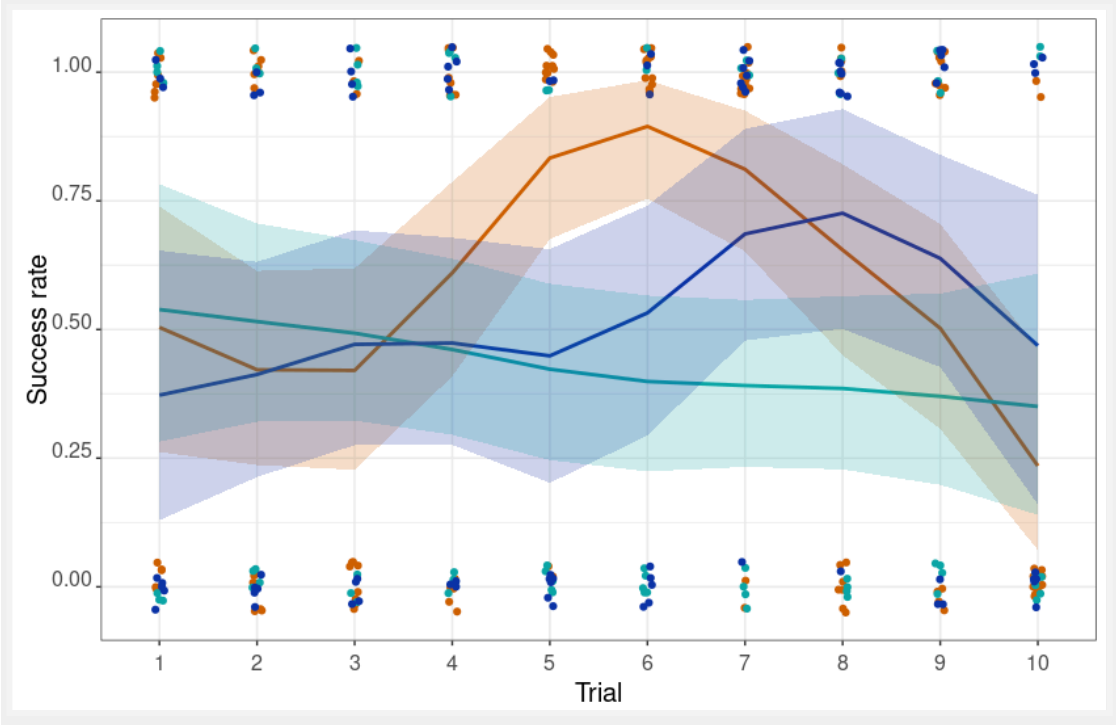

Figure 3.2. Success rate by category in the associative learning task. The solid lines show the estimated success rate across trials for three categories: Summer wild (orange), winter captive (light blue) and winter wild (dark blue). Shaded areas indicate the 95% credible intervals (CIs). Jittered points are the observed values recorded in each trial for the respective categories.

Running wheel activity

We estimated the running distances across different hours of the day between categories (Figure 3.3; table with estimates in Appendix to Chapter 3). Additionally, we estimated the average speed between categories (Table A3.1, data is presented on a log-log scale).

The analysis of run distance over different hours and categories revealed significant variations. We report all results log-transformed. In summer wild individuals, the

minimum run distance was observed at 11 AM with a value of -1.40 (95% CI: -1.58, -1.22), and the maximum was observed at 23 PM with a value of 3.18 (95% CI: 3.12, 3.24). For key hours corresponding to sunrise (6 AM) and sunset (20 PM), the estimate was 1.70 (95% CI: 1.61, 1.79) and 2.23 (95% CI: 2.15, 2.31), respectively. For the winter captive category, the minimum run distance was observed at 7 AM with a value of 1.87 (95% CI: 1.81, 1.93), and the maximum was observed at 3 AM with a value of 3.01 (95% CI: 2.96, 3.05). At sunrise (8 AM) and sunset (17 PM), the estimated run distance was 2.73 (95% CI: 2.67, 2.79) and 2.70 (95% CI: 2.65, 2.75), respectively. In the winter wild category, the minimum run distance was observed at 15 PM with a value of -0.899 (95% CI: -1.09, -0.726), and the maximum at 0 AM with a value of 0.592 (95% CI: 0.541, 0.645). At sunrise (8 AM) and sunset (17 PM), the estimated run distance was 0.182 (95% CI: 0.103, 0.265) and 0.587 (95% CI: 0.479, 0.691), respectively. The winter wild group exhibited the lowest run distances overall, with less pronounced fluctuations throughout the day compared to the other categories. For all categories, run distance for daytime was generally lower compared to nighttime.

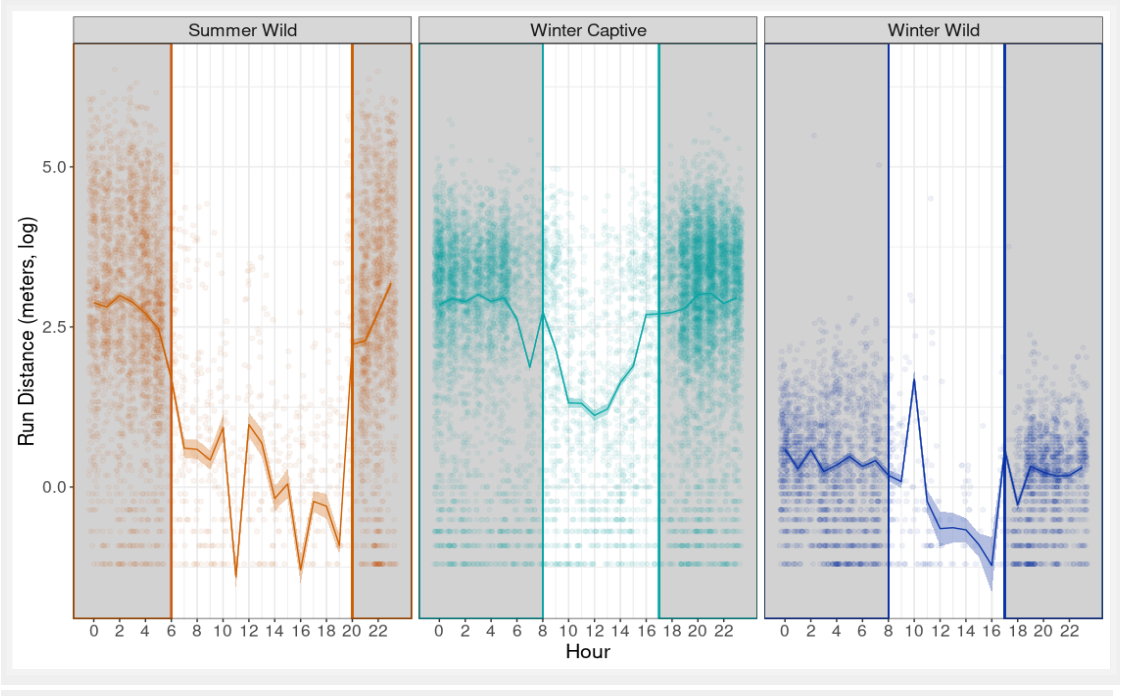

Figure 3.3. Running distances (meters, log-transformed) across the day for summer wild (orange line), winter captive (light-blue), and winter wild (dark-blue) shrews, with corresponding 95% credible intervals (CIs). Individual observations are shown as jittered points for each hour and category. Vertical grey lines separate day (white) from night (grey shaded) periods. In the summer wild category, sunrise and sunset occur at 6 AM and 8 PM, respectively, while in winter captive and winter wild, sunrise and sunset were at 8 AM and 5 PM, respectively.

Regarding average speed, summer wild individuals exhibited an average speed estimate of 1.39 (95% CI: 1.37, 1.41). In comparison, the winter wild category had a lower average speed estimate of 1.14 (95% CI: 1.10, 1.19). The winter captive category showed the highest average speed among the groups, with an estimate of 1.71 (95% CI: 1.69, 1.73).

Discussion

We assessed the effects of captivity on common shrews by comparing brain volume, cognitive abilities, and activity patterns between wild summer individuals and two different winter categories: freshly caught from the wild and after six months of captivity.

Despite the attenuated environment of captivity, there were no significant differences in overall brain volume in winter between wild common shrews and those held in semi-natural captive conditions for six months (Figure 3.1, Table 3.1). This aligns with skull measurements by Lazaro et al. (2019) suggesting that Dehnel's phenomenon remains unaffected under certain captive conditions. While the reduction is generally consistent across regions, there is a slight variance in the degree of the reduction among brain regions with the detailed neuroimaging presented here, (see Appendix to Chapter 3). Although these differences are not statistically significant, they suggest some brain regions respond differently to captivity. Overall brain volume reduction from summer to winter was approximately 5.63% in shrews caught in summer and kept until winter, and 6.78% between the same summer shrews and freshly caught individuals in winter. Size reduction was less pronounced than the 10-26% decrease in braincase height from the same population earlier (Lázaro, Dechmann, et al., 2017). While MRI directly measures the brain's soft tissue, X-ray and braincase height measurements are based on the external dimensions of the skull, likely explaining the much lower estimates of size plasticity noted here. Non-exclusively the increasingly warm winters could be affecting the changes, which are known to be flexible (Lázaro et al., 2019).

Summer wild shrews outperformed their wild winter counterparts in the associative learning task (Figure 3.2). This matches our expectations based on the reduced volume of the brain and specific brain regions associated with cognitive processing in winter. Lazaro (2019) reported a similar seasonal pattern in cognitive abilities in a spatial navigation task. However, the winter captive group performed even more poorly than the wild winter shrews. This could be due to additional cognitive impairment caused by captivity or lower motivation to participate in the task similar to

the loss of interest in reward and pleasure in chronically stressed mice (Vollmayr & Henn, 2003). Winter captives also took longer to enter the arena for the cognitive test (see Appendix to Chapter 3). Forty percent of the wild winter shrews entered the arena within a minute, but none of the winter captives did so. Poor performance and increased latency indicate that captivity affected the shrews' overall behavior, lowering their interest to participate in tasks they had previously engaged with. Various captivity-related factors, such as stress, altered environmental dynamics, or a lack of natural stimuli may explain the reduced motivation observed in the winter captive group. Differences between wild and captive winter shrews might be enhanced by cognitive impairment. Although even slight differences in specific brain regions may influence behavior, the consistent brain size change observed in wild and captive categories links behavioral differences observed here to captivity instead. In a dynamic environment teeming with challenges, despite similar brain volume, wild shrews may have developed stronger cognitive skills, while captive shrews lack this environmental stimulation resulting in altered behavior.

Continuous access to food in captivity may also diminish food-related motivation, which could explain the observed lower success rates and increased latencies in the behavioral test among winter captives. Conversely, while wild individuals might initially exhibit higher food motivation, the decline in correct choices in later trials could be attributed to the monotony of the same reward. Before the associative task with summer wild juveniles, we observed food preference, presenting them with two food items in different combinations (mealwork, earthworm, raw meat, low-sodium dog food). Shrews did not show a clear preference for any of the food types. Despite the inconclusive result from the food preference test, the consistent use of the same reward might have led to the observed decline in correct choices. Providing a different set of food rewards in later trials would account for this in the future (i.e. ‘variety effect’, Bouton et al., 2013; Webber et al., 2015).

If the stress of captivity and not impaired cognition caused cognitive test performance declines, changes in overall activity should also be evident. Supporting a captivity effect, the captive winter group increased running compared to their wild counterparts. To conserve energy and resources in the wild, common shrews naturally decrease their activity in winter when food is more scarce and conditions are harsh (Churchfield, 1982). This was also the pattern in both wild categories, with summer shrews running longer distances, mostly during the night, than winter shrews. In line with this result, winter captives also showed the highest average running speeds. The conditions of captivity resulted in higher running speeds compared to the wild conditions in both summer and winter. Several factors may contribute to this. Chronic

stress or anxiety in captive animals is often tied to their housing conditions (e.g., long-term confinement, limited space, and constant human presence; Morgan & Tromborg, 2006) which can disrupt the animals' normal behavior and physiological state. This matches the lack of motivation our captive shrews showed in the associative learning task. In some cases, anxiety or chronic stress can result in stereotypic activity, e.g., pacing, over-grooming, or, as in our shrews, excessive use of running wheels (Mallory et al., 2021). Hyperlocomotion has been identified as a confounding response in chronically stressed lab mice (Strekalova et al., 2005), and in captive wild animals this could be an attempt to cope with the psychological impact of confinement or to self-stimulate in an environment that lacks natural stimuli. Both heightened physical activity and a decrease in motivation for a reward can be adaptive responses to chronic stress caused by the artificial conditions of captivity.

Another non-exclusive explanation is the stress caused by the inability to perform natural foraging behavior. In their natural habitat, common shrews forage frequently because of an extremely high metabolism that requires them to eat every few hours to survive (Keicher et al., 2017; Ochocińska & Taylor, 2005). In captivity, food is delivered every 24 hours at the same time and location. As a result, the energy that wild shrews would typically expend on foraging may be redirected in captivity, leading to excessive running in winter.

The detailed mechanisms underlying the changes in activity and cognition we found remain unknown. However, our observations match recent findings from a parallel study comparing wild shrews with shrews kept in captivity for two months, which documented significant changes in gene expression related to the stress response (Bedoya Duque et al., 2023). Specifically, captive shrews show downregulation of FKBP5 across three brain regions (-1.44 LFC in the cortex, -1.34 LFC in the hippocampus, -1.68 in the olfactory bulb), whose encoded protein is found in a negative feedback loop with the glucocorticoid receptors which has been shown to induce changes in mood, behavior, and other downstream physiological stress responses. Human individuals with post-traumatic stress disorder consistently have decreased levels of FKBP5, which dampens the cortisol response (Levy-Gigi et al., 2013). Coupled with increased running and lower cognitive performance or motivation, the downregulation of FKBP5 in captive shrews suggests a complex adaptive response to the stress of captivity. Downregulation of FKBP5 might be an attempt to enhance stress resilience by improving glucocorticoid receptor sensitivity to cortisol (Zannas et al., 2016). This improved sensitivity allows the body to regulate the stress response, facilitating the shutdown of the stress pathway once the stressor is removed. While stress resilience may enhance the ability to cope with stress, it can

also lead to diminished cognitive performance and motivation due to the prioritization of coping mechanisms over other functions. In a chronically stressed state, the organism allocates resources toward survival and stress management, which can impair functions like learning, memory, and motivation (McNamara & Buchanan, 2005). This shift in resource allocation can result in a tradeoff, in which increased resilience to stress comes at the expense of cognitive capabilities and engagement in tasks requiring higher cognitive effort.

Investigating epigenetic and expression changes in genes in this and other pathways known to be involved in chronic stress, such as the serotonin or dopamine systems in the brain or regions of the brain will help us better understand observed differences between wild and captive shrews and interpret results, especially those gathered for applied research (Hamet & Tremblay, 2005; Lu et al., 2019; Wang et al., 2021).

In conclusion, semi-natural captive conditions did not significantly disrupt the natural pattern of seasonal brain size variation in common shrews over six months. Our study showed the effect of semi-natural captivity on common shrews, but it's important to use these findings carefully when applying them to other species. Shrews are characterized by their high metabolic rates and insectivorous diet, which necessitate continuous activity throughout the year as they do not hibernate or enter torpor. These traits may limit the applicability of our results to species with different ecological roles or environmental adaptations. Furthermore, the semi-natural conditions of our study, designed to replicate the shrews' natural daylight and temperature, may not directly compare with those used in conventional laboratory studies involving other species. Such differences in captive environments could influence the typical stress responses associated with captivity, potentially affecting the generalizability of our results. However, our research has shown the profound impact of captivity on the behavior and possibly cognition of common shrews that we attribute to the complex interplay between environmental stimulation and stress responses. There is surprisingly little information on such captive effects and how they have been dealt with in other species, but quantifying these behavioral changes is crucial for both the welfare of animals in captivity and to interpret the results of research studies that use captive animals, as these conditions can influence the results of experiments.

Moving forward, it would be valuable to conduct comparative studies involving species with varying ecological and physiological traits to gain a more comprehensive understanding of how captivity affects behavior across different taxa. By doing so, we can contribute to a broader understanding of the implications of captivity on animal

cognition and behavior while accounting for the diverse ecological and physiological factors that shape these responses.

Table 3.1. Result summary from Bayesian model estimates with lower and upper 95% Credible Interval on brain volume, associative learning performance, and running wheel activity in common shrews of three categories: Summer wild, Winter wild, and Winter captive.

Brain Volume	**Category**	**Volume Estimate (µl)**	**l-95% CI**	**u-95% CI**
	Summer Wild	224.15	217.88	230.38
	Winter wild	210.2	196.11	222.89
	Winter captive	207.25	192.06	222.07
Associative learning	**Category**	**Success Estimate**	**l-95% CI**	**u-95% CI**
	Summer Wild	0.48	0.08	0.90
	Winter wild	0.12	-0.34	0.57
	Winter captive	-0.29	-0.87	0.29
Running Wheel Speed	**Category**	**Estimate (log-log)**	**l-95% CI**	**u-95% CI**
	Summer Wild	1.39	1.37	1.41
	Winter wild	1.14	1.10	1.19
	Winter captive	1.71	1.69	1.73

Table 3.2. Contrast of brain volume between the categories winter wild and winter captive.

Contrast	**Category**	**Mean**	**l-95% CI**	**u-95% CI**
	Winter wild vs. winter captive	-2.94	-13.22	7.22

Data accessibility

All data and code for the analysis and plot of this paper can be found in the Edmond repository: https://doi.org/10.17617/3.XMQBQH

Funding

This work was funded by the Human Frontiers Research Grant RGP0013/2019 to DD, LMD, and JN. WRT was supported in part by a Stony Brook University Presidential Innovation and Excellence award to LMD.

Acknowledgments

We thank Pizza Ka Yee Chow, Shauhin Alavi and Urs Kalbitzer for their help with statistical analyses. Angela Litz and Milena Radtke helped with data collection and video analyses. The animal caretakers of the institute, and Drs. Inge Müller and Daniel Zuniga provided incredible help with shrew care. Furthermore, the authors wish to thank the core facility AMIR^{CF} (DFG-RIsources N° RI_00052) for support in MR imaging.

Ethics statement

This animal study and all experimental procedures were carried out according to guidelines for the care and use of animals approved by the Regierungspräsidium Freiburg, Baden-Württemberg (35-9185.81/G-19/80 and 35-9185.81/G-22/082).

Competing interest

The authors declare no competing or financial interests.

Chapter 4

Decreasing brain size has variable effects on learning abilities in common shrews (*Sorex araneus*) from summer to winter

Manuscript in preparation

Cecilia Baldoni, Marina Farantouri, Elham Nourani, Konstantinos Raptis, Dina K.N. Dechmann

Abstract

Learning is an adaptive mechanism that enables organisms to navigate complex and changing environments. In animals living in temperate climates, this capability is intricately linked to seasonal adaptations. The common shrew (*Sorex araneus*) offers the unique opportunity to test if and how seasonal differences in learning abilities may be linked to changing brain size within individuals. This species exhibits a remarkable overwintering adaptation, i.e. Dehnel's phenomenon, a reversible reduction in body and brain size to conserve energy during winter. This facilitates survival but impacts cognitive functions. Variation in the extent of size change between brain regions invites targeted testing to assess the compromise between this energetic adaptation and cognitive impairment. Using spatial and associative learning, we investigated the link between brain region shrinkage and cognitive performance in captive and wild shrews. Shrews performed consistently better in spatial learning than in associative learning and path integration tasks in both seasons. In winter, freshly caught shrews as well as 6-month captives showed a ~30% decrease in associative learning. Performance in the path integration task was generally low and more stable over trials. This study emphasizes the adaptive value of cognitive flexibility in responding to environmental challenges and the need to preserve ecological competence in captivity.

Introduction

Learning is a fundamental process that critically shapes animal behavior, cognition, and survival strategies. Through different learning strategies, animals adapt to dynamic environments and navigate challenges such as finding food, avoiding predators, and optimizing reproductive success (Shettleworth 2010). Learning is essential for optimizing resource use, allowing animals to respond to both short-term environmental fluctuations and long-term habitat changes (Rochais et al., 2021; Sih et al., 2004). Beyond these immediate survival benefits, the capacity for adaptive learning supports broader ecological adaptability, allowing species to thrive in a wide array of ecological niches.

Examining these processes across various species reveals that learning mechanisms such as associative and spatial learning play vital roles in ecological adaptability. Associative learning allows animals to form mental links between stimuli and behaviors, facilitating rapid adaptations to environmental changes (Pontes et al., 2020).

On the other hand, spatial learning enables animals to map and navigate their environments effectively, securing necessary resources and avoiding threats (Healy & Jozet-Alves 2010). The efficiency and application of these learning strategies are adapted to each species' particular ecological needs, depending on the challenges they face in their environment (Rochais et al. 2021).

In temperate zones, pronounced seasonal differences demand high levels of cognitive flexibility for survival because animals must adjust their behaviors to cope with rapid and often unpredictable environmental changes. These cognitive adaptations are crucial for managing the ecological challenges of winter, allowing species to effectively navigate and utilize their environments even when resources are scarce or conditions are severe. For example, food-caching mountain chickadees living at high elevations with longer and colder winters have better spatial memory and larger hippocampal sizes than those at lower elevations (Freas et al., 2013). In contrast, Siberian hamsters exhibit fluctuations in brain regions involved in memory and navigation, adjusting to changes in daylight length and corresponding ecological demands (Yaskin, 2011).

The common shrew (*Sorex araneus*) exhibits one of the most extreme responses to seasonal variability. Unable to hibernate or use torpor, shrews undergo what is known as Dehnel's phenomenon: significant reductions in body and brain size during winter, leading to reduced energy demands while still maintaining activity (Dehnel 1949, Lázaro & Dechmann 2021). This process leads to a trade-off between reducing brain size to save energy and maintaining sufficient cognitive function to manage the dynamic challenges of seasonality (Lázaro et al, 2017; Baldoni et al. in press). The capacity of shrews to adjust their learning strategies in response to these dual pressures may affect their cognitive flexibility and suggest a link between brain size and cognitive capacity.

The trade-offs between energy conservation and cognitive function in shrews present a unique opportunity to study the adaptability of learning under environmental change. Specifically, the reduction in brain size from summer to winter is not uniform; rather, different brain regions are affected disproportionately. For example, the neocortex and hippocampus experience the most profound winter decrease compared to other brain regions, while others remain stable in size or grow in the following spring (Yaskin 1994; Lázaro et al., 2018). The differential resizing in brain size raises questions about how cognitive functions are maintained or optimized under limited resources. Our previous study using olfactory cues has demonstrated that shrews in summer outperform their winter counterparts in forming associations quickly and effectively, suggesting that brain size and seasonal conditions significantly influence their learning efficiency (Baldoni et al., in press). Spatial learning is equally important for shrews, particularly because the reliability of landmarks in their temperate habitats can shift with the

seasons. These changes might challenge shrews to rely more heavily on spatial learning rather than fixed environmental cues to navigate effectively. Furthermore, as shrews establish and maintain territories, it might become essential for them to accurately remember the spatial layout of their environment. This ability helps them adapt to seasonal variations and maintain control over their territories, underscoring the importance of spatial learning in their survival strategy. A previous study investigating shrews' ability to locate food based on spatial landmarks noted higher performance in summer shrews compared to their winter counterparts (Lázaro et al., 2018). However, the high variation in performance, both between and within trials, suggests that landmarks alone may not provide sufficient stability for navigation across seasons, demonstrating that a well-developed spatial memory can compensate for these environmental variabilities. Despite reduced performance in winter, shrews can sustain high cognitive functions by reorganizing their brain microstructure, adapting to a physically altered neural structure.

Building upon previous knowledge about seasonal changes in associative and spatial learning along with overall brain size, this study investigates how common shrews manage these cognitive processes with the dual challenges of environmental pressures and reduced brain region size. We conducted two separate experiments about the use of visual cues and spatial learning as follows. For the associative learning task we built upon the previous study from Lázaro (2018) where a landmark was used to infer the location of food. In our experiment, we positioned the landmark directly next to the food, transforming it into a visual cue to enhance associative learning. This modification aims to test whether the proximity of the cue to the food improves the shrews' ability to form visual associations. In the same experimental setup, we explored the shrews' use of path integration from the food source back to the entrance. Path integration is a specific mechanism for spatial learning and navigation, enabling animals to keep track of their position and orientation relative to a reference point solely based on self-motion cues. This process allows organisms to maintain their location relative to a starting point or goal without external landmarks (Vorhees et al., 2008; Collett et al., 2023), supporting tasks such as returning to a nest, foraging, and enhancing spatial learning (Goldschmidt et al., 2017). We also assessed the shrews' ability to learn a path using a multiple T-maze, without direct visual cues (see Figure 4.1 for an overview of experiments).

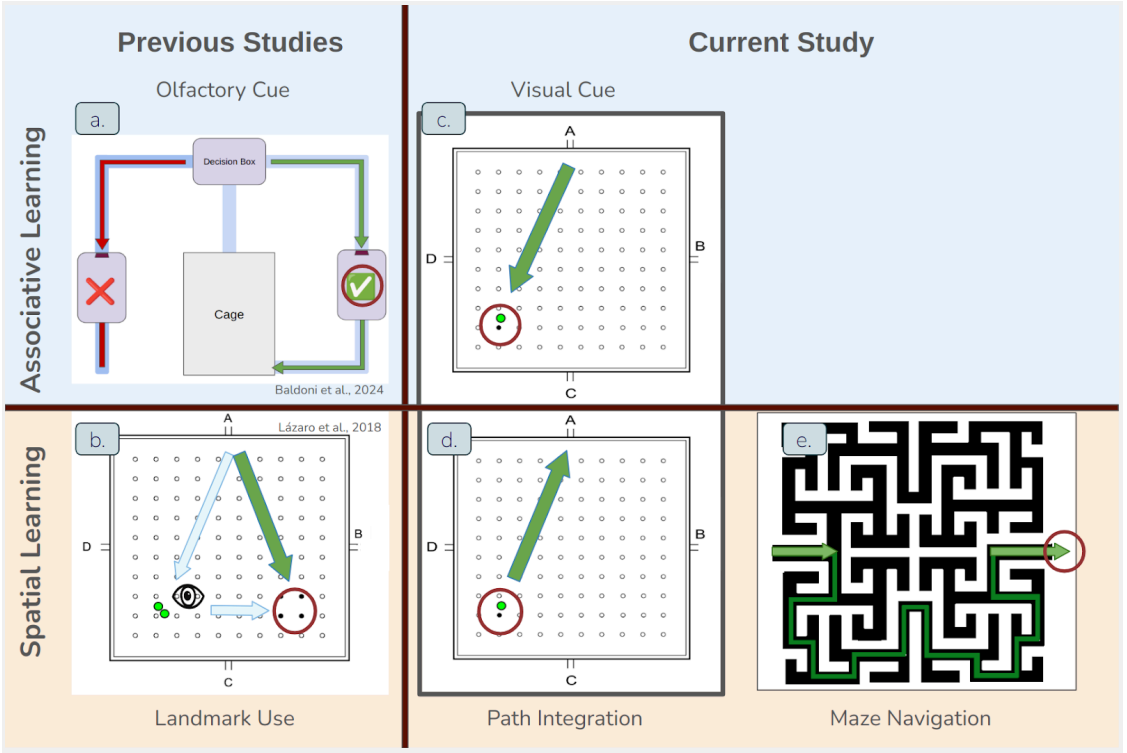

Figure 4.1. Overview of past experiments on common shrews (left side) and the experiments performed in this paper (right side). Associative learning: blue background; spatial learning: orange background. Green arrows: ideal correct path. Red circles: food location. A: associative learning task with an olfactory cue (see Baldoni et al., in press for details); B spatial navigation task with landmark use (see Lázaro et al., 2017 for details); C and D: the two parts of the open arena experiment: associative learning with visual cue (C) and path integration as the ability to find the arena entrance (D). E: the maze used in the spatial learning experiment.

First, we hypothesized that shrews should perform better in the spatial learning task than associative learning due to its direct implications for survival in seasonally changing food landscapes characterized by significant seasonal changes. The ability to update cognitive maps for effective navigation and resource location is deemed crucial for overcoming the challenges posed by changing landscapes (Fagan et al., 2013). Second, we hypothesized that the seasonal reduction in brain size would differentially affect the speed of learning in associative versus spatial tasks. We anticipated a more pronounced decrease in learning speed for associative tasks, which rely more heavily on complex visual cues, during winter when brain size is reduced. In contrast, spatial learning tasks, which depend on navigating and adapting to the environment, might demonstrate more resilience to these seasonal changes, maintaining a steadier learning speed across seasons. Last, we expected to confirm previously demonstrated effects of captivity on motivation on the shrews' performance, with captive shrews performing more poorly overall than freshly caught shrews from the wild. The fact that Dehnel's

phenomenon affects brain regions differently indicates that there is an adaptive compromise between energy-saving size reduction and cognitive abilities that are decreased, lost, or maintained.

Methods

All handling and sampling methods were approved by the Regierungspräsidium Freiburg, Baden-Württemberg, Germany (35-9185.81/G-19/80 and 35-9185.81/G-22/082).

For the arena task, shrews were trapped in June-August 2020 (large brained juveniles, “Summer Wild”, N=9), and February-March 2024 (small brained subadults, “Winter Wild”, N=11). Experiments took place within days of capture in wild individuals. Due to natural mortality, some juveniles died before winter, and additional individuals were caught in October 2020 (N = 12). In winter, captive subadults (the same individuals as caught in June-August and October) and wild subadults (caught in February-March) were tested within days of catching the wild individuals. For the maze experiment, we caught shrews during August-September 2021 (wild juveniles, N=16) and February-March 2024 (wild subadults, N=11). In summer 2021, ten individuals completed the test (Summer Wild). Out of these, six repeated the test during the winter (Winter Captive), along with another six freshly caught ones, who performed the test for the first time (Winter Wild). Before each behavioral test, we removed food from the cage two hours before testing. The test started between 7 AM and 9 AM when the shrews were usually fed in captivity and trials were recorded with an AXIS P3344 Network Camera.

Behavioural tests

Visual Cue and Path Integration. For these two tasks, a square arena (114×114 cm) was used. The wooden floor was covered with compressed sand, into which 100 wells (18 mm in diameter, 15 mm deep) were created using a convex template. Into the third well from one of the corners, always the same one to ensure consistency, a frozen mealworm and the visual cue (small yellow glow light. Brand: The Eurolite) were placed. To avoid possible odor cues caused by the mealworm, the sand in the arena was mixed with mealworm bedding. The arena was covered by a transparent acrylic glass plate ceiling, creating a 2.4 cm high space for the shrew to move in. Being the shrews mostly hunted in open spaces, the tight space created a more comfortable environment for them to move in (Wojcik et al.,, 2007). The sand was mixed between trials and completely replaced between individuals.

The arena had four entrances, one at the center of each side (A, B, C, and D, see Figure 4.1 panel ”C” and “D”). The home cage was attached to one of the entrances through a

connecting tube so the shrews could enter freely and perform the experiment without handling. The entrances not used in each trial were blocked. We generated a random sequence for the ten trials. For the first year of the experiment, the sequence was: A, C, A, B, D, C, B, D, B, C while for the wild individuals tested in 2024, the sequence was: A, C, A, B, D, C, B, D, C, A. The trial started the moment the shrew entered the arena and ended when the shrew returned to the home cage after finding the food.

Maze Navigation. We built a multiple T-maze (50×50 cm) using LEGO with 13 decision points for the spatial learning test. A transparent glass plate was placed on top of the maze to create a narrow space to move in. The maze was connected to the home cage through a tube allowing free access. The exit was also connected to the home cage, ensuring the shrew's return with zero handling. At the exit, we placed a single dead mealworm. We cleaned the maze with ethanol between trials to remove any odour cues. Each shrew performed ten consecutive trials.

Tracking

The videos were analyzed using two tools incorporated in TRex (version 1.1.9), a tracking software developed by Walter & Couzin (2021). TGrabs preprocesses the video, estimating the individual's position while TRex does the heavy processing and the tracking. Then frame-by-frame tracking parameters, such as xy coordinates, speed, acceleration and time, are exported. For the open arena (visual cue and path integration tasks), we tracked 319 out of 340 recorded videos spatial learning task 313, out of 320. Untracked videos were either corrupted or the quality was too low.

Data pre-processing

Visual Cue and Path Integration. Data pre-processing was performed with R, using the tidyverse packages for data cleaning (Wickham et al 2019) and the sf package for spatial data operations (Pebesma & Bivand, 2023). Each data frame, corresponding to the tracking data of each trial, was processed as follows. First, the datasets were cleansed of missing values by removing infinite values from the 'x' and 'y' coordinate columns. Buffers were created around the food and doors location to define the interaction space around targets of interest. This information was then used to detect when tracked positions intersected with defined buffers, categorizing segments of the track into behavioral sequences (journey sequence). The first frame when the track intersected with the food buffer was labeled as "arrival", while the following tracked position in the food buffer was labeled "at_food". "Departure" from the food location was the last frame within the food buffer. All the frames before arrival and after departure were labeled "trip_to" and "trip_back", respectively. Food and other door

revisits were then distinguished between a revisit during trip_back or exploration. Straightness was calculated using the package trajR (McLean 2018).

Maze Navigation. Data pre-processing for the maze navigation task was performed with Python. Data pre-processing for the maze navigation task was performed with Python (Van Rossum & Drake 2009). The AI language model ChatGPT was consulted during this phase for troubleshooting and debugging. ChatGPT provided explanations for error messages and offered solutions, which were then manually reviewed and implemented (OpenAI, 2024). Each trial had four associated files: the average image extracted from the video recording, a mask of the maze, a mask of the path, and a CSV file with the tracking information. The mask image was applied to the average image, ensuring that only the relevant parts of the maze were analyzed. From this processed image, coordinates representing the correct path were extracted from the correct path image, and subsequently cleaned to remove noise and irrelevant points.

Significant decision points along the path were identified by detecting locations with intersections within the maze. This was done by examining the angles between consecutive path segments: sharp changes in angle suggest decision points. Specific decision points where a sharp angle did not correspond to a decision were removed (see image in Appendix to Chapter 4). The individual's tracking data were then loaded and processed to replace infinite values and smooth out noise, then overlaid on the maze image, and the total path length was calculated by summing the Euclidean distances between consecutive points. The status of the path points was then marked to identify which points fall within the correct path buffer (1 cm on each side of the correct path coordinates). This process identified deviations from the path and associated with the closest decision point. A penalty-based path efficiency calculation was then performed to account for deviations more rigorously. If the initial adjusted path length is shorter than the correct path length, a fixed penalty (corner-cutting) was added. Then, a penalty proportional to the deviation length was applied for each deviation from the correct path. The deviation length was calculated as the cumulative distance the subject’s path strayed from the buffer zone around the correct path. The penalty was calculated as the product of the total deviation length and a specified penalty rate per unit length. The penalized path efficiency was then calculated as the ratio of the correct path length to the adjusted path length, including these penalties.

Statistical analyses

All analyses were performed in R version 4.3.1 (R Core Team, 2021). All models were developed using the brms package for Bayesian modeling (Bürkner 2021). All our models were stable with large effective sample sizes (Bulk ESS and Tail ESS over 1000

for all estimates) and R-hat values smaller than 1.01. Pareto k estimates were below 0.5 for all models. We used prior and posterior predictive check functions to visually assess priors and model fit. For all models, we included a random intercept for each individual (ID) to account for repeated measures of some individuals (between summer wild and winter captive).

For the arena, we employed two models to analyze path straightness during different phases: the approaching phase for associative learning (from the entrance to the food) and the departure phase for path integration (from the food back to the entrance). Both models were Bayesian hierarchical mixed-effects models using a beta distribution. For the few values at exact 1, we modified the data following Smithson and Verkuilen (2006). The response variables included trial number and interactions by category, and the interaction between category (Summer Wild, Winter Wild, or Winter Captive) and speed. To investigate whether the individual shrews revisited the door from the previous trial, we conducted a Bayesian logistic regression model based on the category or the journey sequence (during the trip back or exploration).

In the spatial learning task, we used a Bayesian hierarchical mixed-effects model with a beta distribution to investigate the effects of trial and category (Summer Wild, Winter Wild, or Winter Captive) on path efficiency. Within the same model, we evaluated whether the mean speed in each trial influenced path efficiency by category. Individual shrews (IDs) were modeled as random intercepts. We then employed a second Bayesian generalized linear model with a negative binomial distribution to examine whether the total number of deviations changed by trial and category.

Results

Visual Cue. The regression analysis revealed a significant effect of seasonal category on path efficiency in the approach phase (from the arena entrance to the food location). All regression coefficients are reported as changes in the log-odds of the expected path efficiency. Compared to the reference category Summer Wild (estimate: 0.29, 95% CI: -0.40, 0.96), both winter categories Winter Captive and Winter Wild decreased in path efficiency with an estimate of -0.82 (95% CI: -1.52, -0.12), and -0.74 (95% CI: -1.44, -0.02) respectively. Smoothing spline hyperparameters for trial effects showed that path efficiency trajectories varied notably between categories. Summer Wild individuals showed a progressive increase in path efficiency from the first trial (Estimate: 0.348, 95% CI: 0.180, 0.539) to a maximum in trial 7 (estimate: 0.57, 95% CI: 0.42, 0.73). Conversely, Winter Captive shrews started with lower efficiency at the first trial (Estimate: 0.315, 95% CI: 0.191, 0.453) and showed only modest improvements by the tenth trial (Estimate: 0.408, 95% CI: 0.263, 0.561). Interestingly, Winter Wild shrews

had initial efficiencies similar to Winter Captives but increased to a maximum in trial 5 (estimate: 0.523, 95% CI: 0.384, 0.664), and reached a higher level than Winter Captives by the tenth trial (estimate: 0.506, 95% CI: 0.346, 0.667, Figure 4.2). The impact of movement speed during the trip to the food also varied by category. Winter Wild shrews benefited more from increased speeds (interaction effect: 0.05, 95% CI: 0.01, 0.09) compared to Winter Captives (interaction effect: 0.02, 95% CI: -0.02, 0.07).

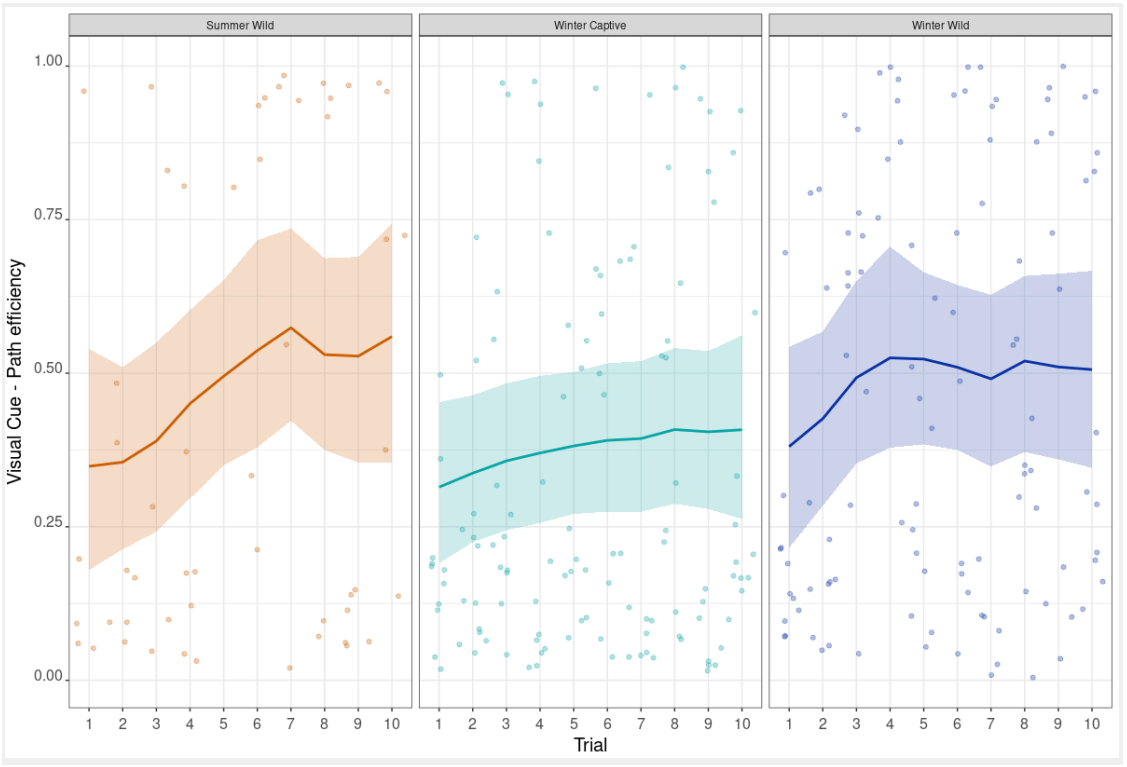

Figure 4.2. Visual cue path efficiency (Tracked Path Length / Shortest Possible Path) by category. The solid lines show the estimated success rate across trials for three categories: Summer wild (orange), winter captive (light blue) and winter wild (dark blue). Shaded areas indicate the 95% credible intervals (CIs). Jittered points are the observed values recorded in each trial for the respective categories.

Path Integration. The regression analysis on path efficiency in the departure phase (from the food location to the arena entrance) revealed again significant effects of category and speed on path efficiency with all categories decreasing. Winter Captive shrews decreased more strongly in path efficiency than Summer Wild, with an estimate of -1.03 (95% CI: -1.71, -0.34). Winter Wild shrews also had lower efficiency, though less strongly than Winter captives, with an estimate of -0.67 (95% CI: -1.34, 0.01). The speed during the return trip had a positive but non-significant impact on path efficiency across categories, with a main effect estimate of 0.01 (95% CI: -0.02, 0.04). Smoothing spline hyperparameters for trial effects suggested that path efficiency trajectories were less stable in Winter Captive shrews (Estimate: 3.35, 95% CI: 0.10, 11.63) compared to

Summer Wild (Estimate: 2.58, 95% CI: 0.06, 9.26) and Winter Wild shrews (Estimate: 1.25, 95% CI: 0.04, 4.66, Figure 4.3). All results are summarized in Table 4.1.

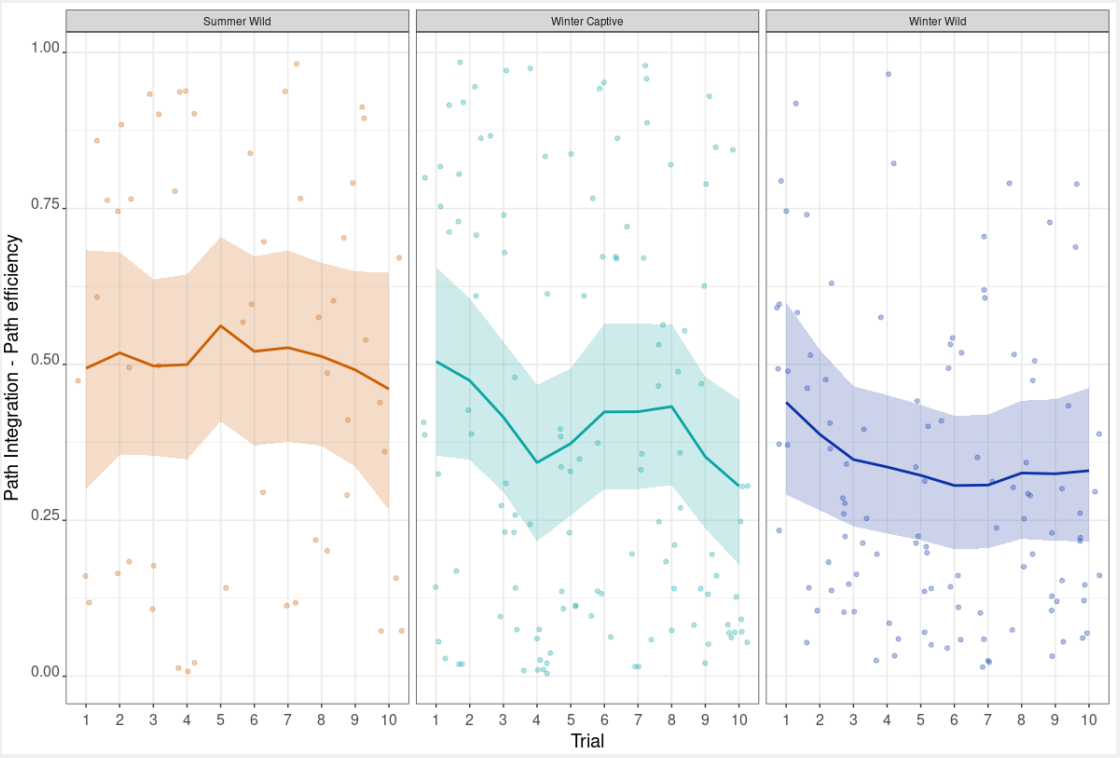

Figure 4.3. Path integration efficiency (Tracked Path Length / Shortest Possible Path) by category. The solid lines show the estimated success rate across trials for three categories: Summer wild (orange), winter captive (light blue) and winter wild (dark blue). Shaded areas indicate the 95% credible intervals (CIs). Jittered points are the observed values recorded in each trial for the respective categories.

Maze Navigation. Path efficiency in the maze was significantly influenced by both the trial number and the shrew category. Winter Captive had a significantly lower performance than Summer Wild, with an estimate of -1.03 (95% CI:-1.93,-0.17), but Winter Wild did not (estimate: -0.35,95% CI: -1.53, 0.84). Smoothing spline estimates for trial number showed that Summer Wild shrews generally improved their efficiency over trials, with estimates increasing from 0.344 (95% CI: 0.175, 0.546) in trial 1 to the highest estimate of 0.716 (95% CI: 0.570, 0.839) in trial 6. In contrast, Winter Captive shrews showed a steady improvement over trials, with estimates starting from 0.337 (95% CI: 0.197, 0.503) in trial 1 and reaching the highest estimate of 0.833 (95% CI: 0.720, 0.916) in trial 10. Winter Wild shrews also displayed an increasing trend, with estimates from 0.363 (95% CI: 0.206, 0.543) in trial 1 to the highest estimate of 0.703 (95% CI: 0.560, 0.825) in trial 7 (Figure 4.4; Table 4.1). Mean speed within the maze significantly affected path efficiency (Estimate: 0.20, 95% CI: 0.12, 0.29), indicating that faster speeds generally led to better performance. However, the interaction effects

suggested differential impacts of speed based on category: speed had a slight positive effect in Winter Captive shrews on efficiency (Estimate: 0.02, 95% CI: -0.09, 0.12), and a small negative effect in Winter Wild shrews (Estimate: -0.05, 95% CI: -0.16, 0.06).

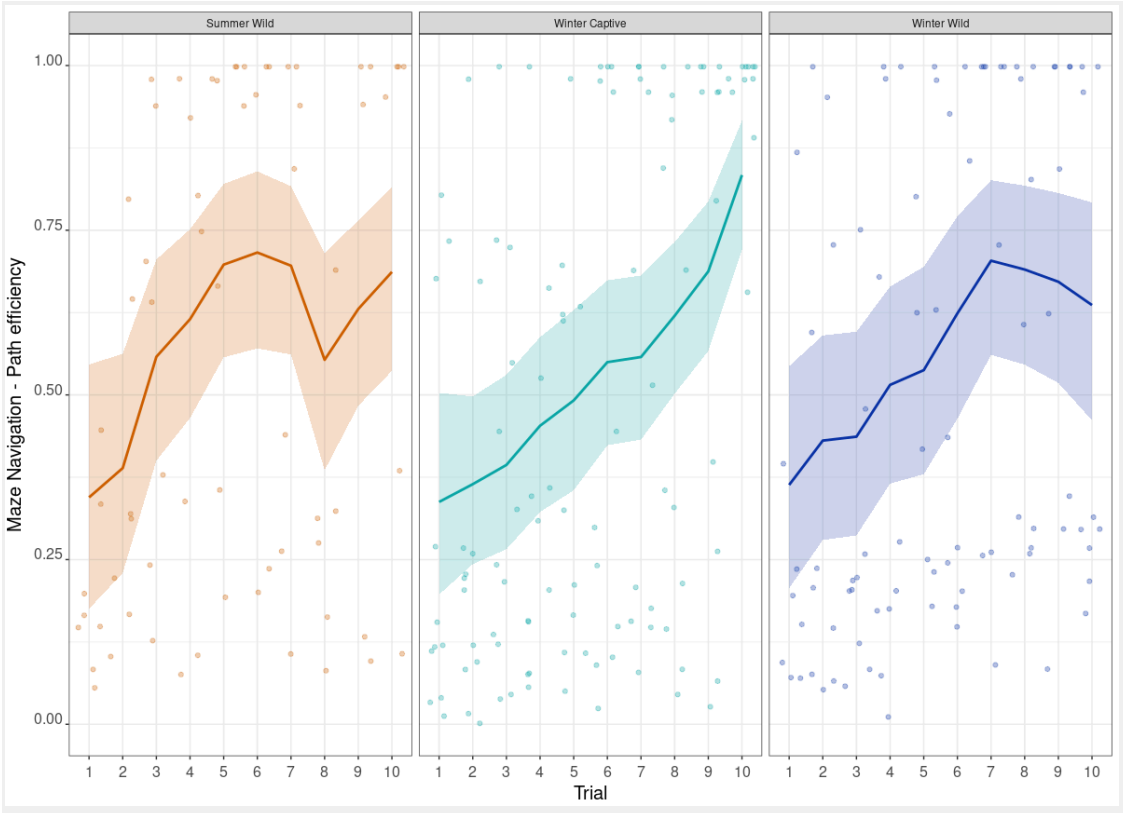

Figure 4.4. Maze navigation path efficiency (Tracked Path Length / Shortest Possible Path) by category. The solid lines show the estimated success rate across trials for three categories: Summer wild (orange), winter captive (light blue) and winter wild (dark blue). Shaded areas indicate the 95% credible intervals (CIs). Jittered points are the observed values recorded in each trial for the respective categories.

Table 4.1. Regression coefficients from the Bayesian models investigating the effect of mean speed on path efficiency in the three experiments.

Associative Learning	Category	Mean Speed	l-95% CI	u-95% CI
	Summer wild	-0.02	-0.06	0.01
	Winter wild	0.02	-0.02	0.07
	Winter captive	0.05	0.01	0.09
Path Integration	Summer wild	0.01	-0.02	0.04
	Winter wild	0.05	0.02	0.09
	Winter captive	0.01	-0.03	0.06
Spatial Learning	Summer wild	0.20	0.12	0.29
	Winter wild	-0.05	-0.16	0.06
	Winter captive	0.02	-0.09	0.12

The analysis of deviations from the designated path in the maze showed that, in Summer Wild shrews, there was a significant decrease in the number of deviations as trials progressed (Estimate: -0.07 per trial, 95% CI: -0.13, -0.02), suggesting an improvement in navigational accuracy over time. Winter Captive shrews started with higher deviation counts than Summer Wild (Estimate: +0.94, 95% CI: 0.53, 1.35), and similarly, Winter Wild shrews also showed increased initial deviations (Estimate: +0.53, 95% CI: 0.12, 0.95) compared to the baseline group. For Winter Captive shrews, there was a notable decrease in the number of deviations with each additional trial (Estimate: -0.12 per trial, 95% CI: -0.20, -0.04), showing a steeper improvement in navigational skills compared to Summer Wild. Conversely, Winter Wild shrews showed a smaller, non-significant reduction in deviations over trials (Estimate: -0.06 per trial, 95% CI: -0.14, 0.02), suggesting a more gradual improvement.

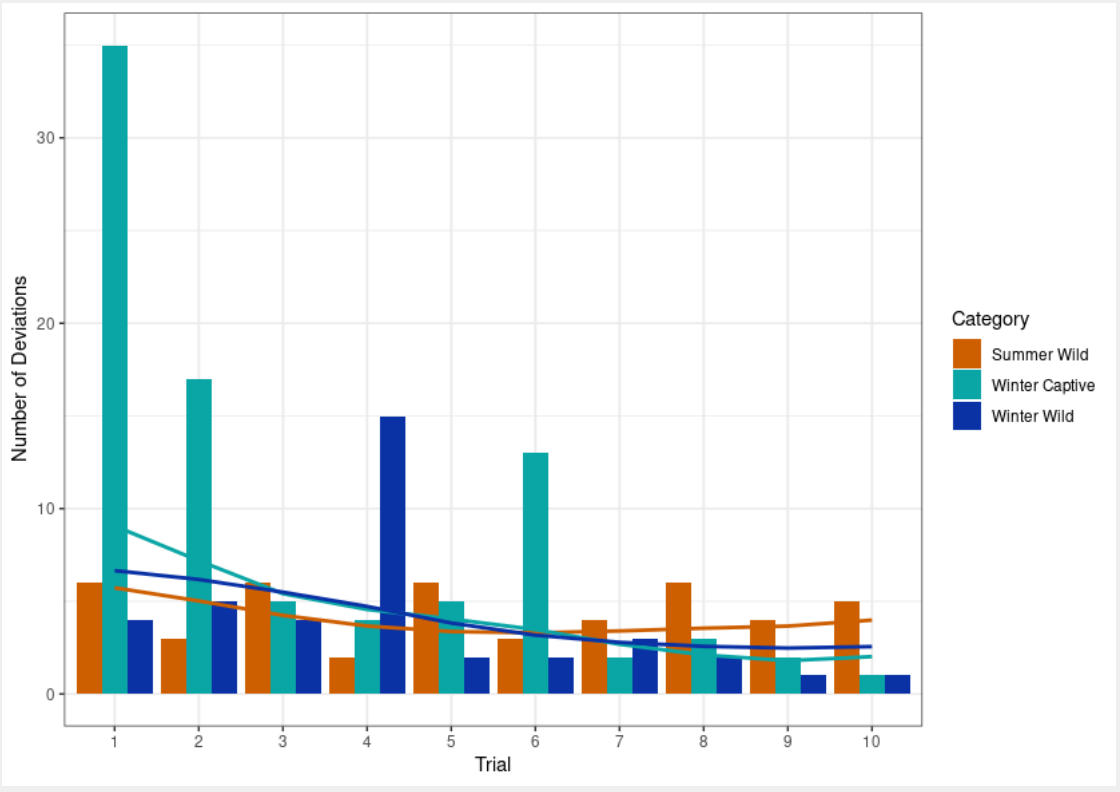

Figure 5. Bar Chart showing the total count of deviations from the correct path in the maze navigation task, grouped by category (Summer Wild, Winter Wild, or Winter Captive) and trial. The smooth lines represent the Smoothing Spline hyperparameter from the Bayesian model for each category.

Discussion

Our investigation into the cognitive capabilities of common shrews reveals significant differences between spatial and associative learning, and demonstrate the essential role these skills play in their survival. Maze navigation, which directly tested spatial learning abilities, was the most proficient skill, with shrews showing the highest performance estimates (between 0.58 and 0.74) and moderate improvements over trials. In the visual cue task, where shrews were expected to form an association between the visual cue and the food location, performance was notably weaker, particularly among captive shrews during winter, with the highest performance ranging from 0.40 in winter captive to 0.57 in summer wild. This result might indicate a reduced reliability for visual associations, and possible subordination to spatial skills in the shrews' cognitive hierarchy, likely due to the variable and transient nature of environmental cues. We investigated path integration performance by quantifying the path efficiency from the food location back to the entrance of the arena. This task showcases the shrews' efficiency in using recent navigational memories to safely return

to starting points, a behavior that might reduce exposure to predators and energy expenditure. The estimates for this task were neither as high as in the maze navigation nor as low as associative learning, placing it at an intermediate level of cognitive demand within our study's scope. Interestingly, this task showed a decrease in performance over trial for the winter population (30% decrease for winter captive, 39% decrease for winter wild). Collectively, these findings showed how different cognitive processes are prioritized and shaped by ecological demands.

Seasonal variations in the cognitive performance of shrews are intricately linked to Dehnel's phenomenon, which entails marked reductions in brain size during winter. Specifically, a previous study using MRI in this population has quantified that both the neocortex and hippocampus—key brain regions involved in cognitive processing—experience a seasonal shrinkage of approximately 7% to 9% (Baldoni et al., in press). The neocortex is crucial for higher-order functions such as sensory perception and associative learning, making it vital for adapting behaviors based on changing environmental cues (Lodato & Arlotta, 2015). Meanwhile, the hippocampus is central to spatial navigation and memory formation, fundamental for exploring and adapting to new or altered environments (Sato & Yamaguchi 2005). The pronounced changes in these regions profoundly affect how shrews handle cognitive tasks across seasons. During summer, when the hippocampus is at its full volume, shrews exhibit enhanced spatial learning capabilities. This enhanced hippocampal function supports efficient spatial navigation, enabling shrews to optimize resource collection and management when environmental resources are plentiful. Conversely, the reduction in hippocampal and neocortical volumes during winter might theoretically impair cognitive abilities. However, our observations suggest a surprising degree of resilience. Spatial learning abilities show some decline but maintain high performance, implying that essential navigation functions are kept to a functional degree even with physiological constraints. On the other hand, associative learning, which relies significantly on the neocortex, appears more adversely affected during winter. The decline in neocortical volume, combined with the reduced reliability and availability of environmental cues in winter, might lead to a more significant drop in associative learning efficiency. While shrews can partly compensate for the reduced cognitive capacities in spatial tasks, associative learning might be more vulnerable to seasonal brain size reductions. The path integration task adds another level of complexity: studies in humans suggest that path integration is mediated by both the prefrontal cortex and hippocampus (Arnold et al., 2014). Our results showed that shrew performance in this task was suboptimal even under the best conditions (i.e. summer), suggesting that factors other than brain region shrinkage may influence cognitive outcomes.

The observed differences in performance between spatial and associative learning tasks may be deeply influenced by the shrews' sensory ecology. Shrews are primarily tactile hunters, relying heavily on vibrissal touch and auditory cues rather than visual signals to interact with their environment (Catania et al. 2008). This reliance on tactile and other non-visual sensory information could explain why this associative learning task, which relied on a visual cue, showed less improvement compared to the spatial tasks. Spatial navigation tasks may be more aligned with the shrews' natural strengths, thus enabling better performance even when visual cues are minimal or unreliable. This sensory preference aligns with the observed cognitive adaptations and emphasizes that the impact of cognitive function is not solely dependent on brain size variation but also varies significantly depending on the ecological context and the sensory modalities primarily used by the species.

Our broader investigation into the cognitive capabilities of common shrews across all tasks reveals distinctive patterns with a shared ecological strategy, possibly driven by the shrews' metabolic demands. In the path integration task, shrews consistently demonstrated suboptimal performance, with a notable decrease over trials, possibly indicating intrinsic challenges in the shrews' ability to integrate complex navigational information. However, the low performance could instead reflect an ecological strategy: shrews need to eat every few hours to sustain their high metabolic rate (Churchfield, 1989), and are driven to continuously explore their environment for food resources. This necessity might lead them to prioritize exploration over efficiency in path integration tasks, potentially increasing their chances of discovering new food locations. Similarly, the associative and spatial learning tasks exhibited a non-classical learning curve with an initial peak in performance and then a drop as the trial progressed. This peak suggests that shrews show initial engagement with the task, followed by a decline in performance once the task becomes familiar and no longer mimics the complexity of their natural, unpredictable environment. This drop likely reflects a shift to exploration over repetitive task execution, aligning with their ecological need for the constant need to locate scattered food resources. Together, these patterns highlight how shrews' cognitive strategies are tuned to prioritize continual exploration, which, while sometimes reducing task-specific efficiency, is adaptively aligned with their survival requirements in dynamic and resource-variable habitats.

Consistent with findings from previous research (Baldoni et al., in press), the comparative analysis of winter captive and winter wild populations showed a lower path efficiency and slower improvement in the associative learning task of captive individuals compared to wild ones. This differential performance aligns with the hypothesis that captivity may impose additional stressors reducing motivational states,

which in turn can affect cognitive functions negatively. Captive conditions lack the environmental complexity and associated challenges, while the enhanced performance in winter wild individuals underscores their adaptation to natural winter hardships, which might stimulate cognitive functions necessary for survival, such as efficient foraging and navigation under resource-scarce conditions. Interestingly, we did not observe this differential performance based on captivity status in the spatial learning task. This could suggest that spatial learning mechanisms are more robust to the effects of captivity, possibly due to their fundamental role in basic survival functions, which remain important even in less complex environments. Another possibility is that the maze used in this experiment for assessing spatial learning was too simple, potentially failing to sufficiently challenge the shrews to reveal any subtle differences in performance between captive and wild individuals.

Our study advances our understanding of cognitive plasticity and shows how these adaptations are directly linked to ecological pressures. In common shrews, the seasonal shrinkage of brain size is intricately tied to their survival strategies. The ability to adjust brain size dynamically allows shrews to optimize their cognitive strategies to meet the specific demands of each season. For instance, despite a reduction in brain size during winter, shrews maintain robust spatial learning abilities, which are essential for navigating environments with scarce resources. This ability to modulate cognitive functions in response to environmental challenges demonstrates the adaptive significance of brain plasticity, ensuring that the shrews are not just physically but cognitively prepared to handle seasonal changes. These findings deepen our comprehension of how animals adapt their cognitive processes to align with ecological pressures, pointing to cognitive flexibility as essential for survival..

General Discussion

The central aim of my dissertation is to explore the dynamic interplay between brain plasticity, cognitive functions, and the impacts of both natural environmental changes and artificial conditions on the common shrew, *Sorex araneus*. Through a series of detailed experimental studies, my research deepens our understanding of how seasonal variations and captivity conditions affect brain morphology and function. By leveraging MRI techniques and behavioral assays, my research uncovered adaptive mechanisms behind brain size fluctuations and their cognitive consequences.

The development of the first high-resolution brain atlases for the common shrew (Chapter 1) represents an advancement in our ability to study neurological structures across different stages and environmental conditions. These atlases, derived from histological sections and Magnetic Resonance Imaging (MRI), serve as essential tools for fundamental and applied neuroscience research. Creating these atlases will facilitate identifying changes in brain structures as they undergo significant seasonal size fluctuations, providing a framework to correlate these structural changes with functional outcomes.

With the use of diffusion-weighted MRI (DW-MRI) imaging, I found that brain size reduction in common shrews is marked by significant microstructural changes from summer to winter (Chapter 2). These results reveal a notable decrease in intracellular water volume fraction from summer to winter and an increase in extracellular water volume across most brain regions. Importantly, our cell population analyses indicate no reduction in the number of cells, suggesting that the observed changes result from a decrease in cell size. This adaptation likely leads to reduced energy requirements for cellular processes: smaller cells typically exhibit lower metabolic demands (Giarmarco et al., 2020), an adaptation during winter when metabolic efficiency becomes essential due to limited resources.

Despite an overall reduction in brain volume during winter, cognitive testing indicates that common shrews maintain a certain level of functionality, particularly in tasks involving spatial navigation (Chapter 4). However, the operational speed of these cognitive functions is compromised: in tasks involving associative learning with visual (Chapter 4) and olfactory cues (Chapter 3), performance declines were more pronounced in winter shrews, especially in later trials. This slowdown in cognitive processes suggests a potential trade-off: maintaining broader cognitive functions might come at the cost of reduced processing speed under energy-limited conditions.

Furthermore, the differential prioritization of cognitive abilities could stem from their association with varying ecological functions. Spatial learning may be prioritized during winter despite reductions in hippocampal volume, possibly because navigating the environment remains a critical survival skill when resources are scarce. In contrast, associative learning appears more susceptible to the impacts of seasonal brain size reduction, potentially due to its lesser immediate relevance in the winter survival strategy. Both the hippocampus and neocortex show similar shrinking magnitude (see Appendix to Chapter 3), but different patterns in diffusion metrics (Chapter 2). The hippocampus variation in endogenous water from summer to winter aligns with the general trend seen in most other brain regions while the neocortex exhibits an opposite pattern, with an increase in intracellular water volume fraction and a decrease in extracellular water volume fraction.

The neocortex's increase in intracellular water volume fraction could be indicative of a compensatory mechanism to maintain synaptic efficacy within a reduced volume, thereby preserving the capability for higher-order processing to some extent. However, this compensation might come at the cost of speed, contributing to the observed slowdown in cognitive processes, particularly in associative learning tasks. This slowdown in associative learning performance during winter might suggest that while essential cognitive functions are retained, their efficiency is diminished to conserve energy. The adaptation of the neocortex in shrews is particularly noteworthy given its smaller size relative to brain size when compared to other mammals (Catania et al., 1999). This suggests that the role of the neocortex in shrews is adapted to their specific ecological needs, which shift seasonally. During winter, with a reduced need for complex processing, energy conservation becomes paramount, and thus, the brain might adapt by reducing neocortex functionality.

The absence of significant differences in brain volume between wild shrews and those maintained in semi-natural captive conditions offers an interesting paradox. While their brain were anatomically similar, these groups exhibited marked behavioral divergences, suggesting that even subtle variations in environmental conditions can profoundly affect cognitive functions. For example, captive shrews demonstrated overall low motivation in cognitive tasks and high activity levels compared to their wild counterparts. Excluding brain size variation, these behavioral differences are likely produced by the reduced complexity and variability of the captive environment, which fails to stimulate the shrews' cognitive and sensory systems as robustly as their natural habitats.

The observed cognitive discrepancies illustrate how environmental stressors, such as confinement and lack of sensory stimulation, can influence neural functionality and cognitive performance. This observation has implications for the methodology of behavioral neuroscience. It raises the question of the validity of data obtained from animals in unnatural settings and whether these conditions might fundamentally alter the neurobehavioral traits being studied. For example, studies on spatial learning and memory in rodents have shown that animals kept in enriched environments perform better on cognitive tasks than those in barren cages, indicating that reduced environmental stimuli can impair natural cognitive abilities (Leger et al., 2015; Simpson & Kelly, 2011). This contrast between captive and wild conditions suggests a need for careful consideration in the design of experiments and the interpretation of neurobehavioral data, as captive settings may inadvertently modify the natural behaviors intended to be studied.

To further advance our understanding of the neural dynamics associated with brain plasticity in response to environmental changes, future studies could adopt Functional Magnetic Resonance Imaging (fMRI) (Hamaide et al., 2016). fMRI can be used to establish baseline activity patterns of brain regions during seasonal transitions. Resting-state fMRI, a specific application of the technique, is particularly suitable for studying animals like the common shrew, as it measures the brain's spontaneous activity and the functional connectivity between various brain regions in a resting or neutral state. Comparing connectivity patterns across seasons allows researchers to examine how seasonal brain size reduction impacts network integration and synchronization. This approach might help understanding the underlying neural adaptations to environmental pressures in more detail.

Within this framework, future research should focus on exploring the long-term evolutionary implications of these observed microstructural adaptations in the hippocampus and neocortex, particularly in relation to reproductive success and generational resilience. This focus could clarify the evolutionary strategies that help small mammals endure seasonal extremes. Additionally, behavioral adaptations to different climates, habitats, and resource levels may be influenced by neural changes, offering a potential explanation for how mammals respond to shifting ecological conditions. For instance, the intensity of seasonal changes varies geographically, being more pronounced in northern and eastern populations. Correspondingly, some brain regions exhibit more significant seasonal shrinkage in northern populations compared to southern ones (Lázaro, Dechmann, et al., 2017; Yaskin, 2011). This approach would not only focus on the mechanisms behind cognitive and physiological adaptations but

also illustrate how shrews and other small mammals might adapt to the pressures of climate change.

Dehnel's phenomenon, viewed within a broader comparative and evolutionary framework, illustrates the adaptive strategies that different species use to manage environmental challenges. This dissertation focuses on the common shrew, *Sorex araneus*, as a model for studying the dramatic, reversible brain size changes tied to seasonal adaptations. Studying other species with similar phenomena offers further perspectives on the evolutionary pressures shaping these unique responses. For instance, the European mole (*Talpa europaea*) shows a similar pattern to the common shrew, with a reduction in skull size by 11% in winter, whereas the Spanish mole (*Talpa occidentalis*) does not exhibit any change (Nováková et al., 2022). This variation can be explained by the different environmental challenges faced by each species. The Iberian mole experiences extremely harsh conditions in the summer, with high temperatures and dry conditions in its habitat, whereas the European mole contends with more severe conditions during the winter. The observation that the Iberian mole does not reduce its skull size supports the hypothesis that winter conditions play a crucial role in the evolution and occurrence of Dehnel's phenomenon. In the case of the common shrew, reducing brain size during the winter could decrease metabolic demands, conserving energy for survival functions such as thermoregulation and foraging efficiency. This trait might have evolved as a crucial strategy for survival in environments with pronounced seasonal fluctuations, aligning metabolic costs with environmental resource availability.

The findings from my dissertation also speak to the field of neuroscience, allowing for a deeper understanding of how brain plasticity functions as a mechanism for adapting to environmental challenges. The ability of shrews to adjust their brain structures in response to seasonal changes offers a model for exploring potential interventions in human health, such as strategies to enhance brain plasticity in response to stress or neurodegenerative diseases. In animals, brain plasticity is not only crucial for adapting to new experiences but also for recovery following brain injuries. For example, following a stroke, humans can recover lost functions through the reorganization of neural pathways (Nudo, 2013). While Dehnel's phenomenon represents an adaptive and reversible modification of brain structure in response to environmental stress, it contrasts strongly with the irreversible changes observed in human neurodegenerative diseases, such as Alzheimer's disease. Diffusion metrics, often used in human studies to assess brain health, indicate white matter degeneration and loss of structural integrity in neurodegenerative conditions like Alzheimer's disease and multiple sclerosis. A striking difference in my results is that while diffusion metrics

show an altered pattern in the shrew brain from summer to winter, they also show remarkable stability. In contrast, human neurodegenerative diseases exhibit both changes in individual metrics and a breakdown in their relationships, reflecting a loss of structural and functional integrity (Rovaris et al., 2005). Interestingly, cognitive tests assessing spatial navigation and path integration in humans have successfully detected early signs of Alzheimer's disease (Newton et al., 2024). The entorhinal cortex, a region highly involved in path integration, is the first cortical region to exhibit neurodegeneration in Alzheimer's disease. Path integration impairments have been shown to predict both hereditary and physiological Alzheimer's disease risk, with no corresponding multi-risk impairment in episodic memory or other spatial behaviors (Newton et al., 2024). These results are strikingly similar to what we found in the common shrew (Chapter 4), with overall lower path integration performance in winter compared to summer. My results suggest a robust fundamental structure that adapts to environmental stressors without compromising the interactions between different brain components. Despite differences, the mechanisms behind the shrew's brain adaptation may be valuable for applied research on human conditions, especially in relation to aging and disease.

This dissertation advances our understanding of brain plasticity and cognitive functions in the common shrew, though it's important to recognize certain limitations. One major limitation is the resolution constraints inherent in diffusion-weighted MRI (DW-MRI) imaging, which, while effective for observing microstructural changes, may lack the precision necessary for cellular-level details. A previous study investigating seasonal differences in soma size, dendrite length and volume, and spine number and density observed a summer to winter decline in neuronal soma size in the caudoputamen and in the somatosensory and anterior cingulate cortices, as well as a reduction in basal dendritic volume in the anterior cingulate cortex (Lázaro et al., 2018). However, these changes alone were not sufficient to account for the total winter volumetric decline, and the study was limited to three brain regions. This limitation is significant because these microscopic changes can have profound implications for neural function and cognitive processes. For instance, changes in synaptic density and dendritic structure are important processes involved in synaptic plasticity, which is linked to learning and memory (Caroni et al., 2012). Without the ability to observe these finer details, our understanding of how brain plasticity operates at the most fundamental level remains incomplete. Future research could benefit from combining DW-MRI with higher resolution techniques, such as electron microscopy or advanced light microscopy, to provide a more comprehensive picture of the cellular and subcellular changes occurring in the brain.

In addition to the resolution constraints of imaging techniques, another significant limitation is the environment in which the behavioral testing of wild shrews was conducted. Although the wild shrews were brought into captivity for controlled observations and experiments, this change of environment could have affected their natural behaviors and cognitive functions. Testing wild shrews in a captive environment, even temporarily, can introduce stress and alter their natural responses. The lack of familiar environmental cues, changes in diet, and the presence of unfamiliar objects and settings could influence their performance in cognitive and behavioral assays. These factors might lead to results that do not accurately reflect the shrews' natural adaptive behaviors. To address this, future studies should consider conducting behavioral testing in the wild. Field-based assays allow observation of shrews in their natural habitats, providing more ecologically valid data. While field-based studies pose challenges, such as controlling environmental variables, the benefits of obtaining more accurate and representative data on natural behaviors outweigh these challenges.

In conclusion, the adaptive modifications observed in the shrew's brain throughout seasonal transitions provide a compelling example of natural neuroplasticity. My research significantly advances our understanding of how the common shrew brain navigates environmental challenges through complex structural and functional changes. This dissertation focuses on mechanisms behind seasonal brain plasticity, contributing to neuroethology and applied fields such as conservation biology and research on neurodegenerative diseases. Moreover, this study creates opportunities for investigations into human brain disorders and explore how environmental and behavioral interventions might influence brain health and disease. . The discoveries here suggest promising directions for harnessing natural brain plasticity mechanisms in human therapeutic strategies.

References

Agaronyan, A., Syed, R., Kim, R., Hsu, C.-H., Love, S. A., Hooker, J. M., Reid, A. E., Wang, P. C., Ishibashi, N., Kang, Y., & Tu, T.-W. (2022). A Baboon Brain Atlas for Magnetic Resonance Imaging and Positron Emission Tomography Image Analysis. *Frontiers in Neuroanatomy*, *15*, 778769. https://doi.org/10.3389/fnana.2021.778769

Anastasopoulos, C., Reisert, M., & Kellner, E. (2017). “Nora Imaging”: A Web-Based Platform for Medical Imaging. *Neuropediatrics*, *48*(S 1), P26. https://doi.org/10.1055/s-0037-1602977

Anderson, M. L. (2016). Neural reuse in the organization and development of the brain. *Developmental Medicine & Child Neurology*, *58*(S4), 3–6. https://doi.org/10.1111/dmcn.13039

Araki, H., Cooper, B., & Blouin, M. S. (2007). Genetic Effects of Captive Breeding Cause a Rapid, Cumulative Fitness Decline in the Wild. *Science*, *318*(5847), 100–103. https://doi.org/10.1126/science.1145621

Arnatkevičiūtė, A., Fulcher, B. D., & Fornito, A. (2019). A practical guide to linking brain-wide gene expression and neuroimaging data. *NeuroImage*, *189*, 353–367. https://doi.org/10.1016/j.neuroimage.2019.01.011

Arnold, A. E. F., Burles, F., Bray, S., Levy, R. M., & Iaria, G. (2014). Differential neural network configuration during human path integration. *Frontiers in Human Neuroscience*, 8, 263.

Ashburner, J., & Friston, K. J. (2000). Voxel-Based Morphometry—The Methods. *NeuroImage*, *11*(6), 805–821. https://doi.org/10.1006/nimg.2000.0582

Assaf, Y., & Pasternak, O. (2008). Diffusion Tensor Imaging (DTI)-based White Matter Mapping in Brain Research: A Review. *Journal of Molecular Neuroscience*, *34*(1), 51–61. https://doi.org/10.1007/s12031-007-0029-0

Avants, B. B., Tustison, N. J., Song, G., Cook, P. A., Klein, A., & Gee, J. C. (2011). A reproducible evaluation of ANTs similarity metric performance in brain image registration. *NeuroImage*, *54*(3), 2033–2044. https://doi.org/10.1016/j.neuroimage.2010.09.025

Baldoni, C., Thomas, W. R., von Elverfeldt, D., Reisert, M., Làzaro, J., Muturi, M., Dávalos, L. M., Nieland, J. D., & Dechmann, D. K. N. (2023). Histological and MRI brain atlas of the common shrew, *Sorex araneus*, with brain region-specific gene expression profiles. *Frontiers in Neuroanatomy*, *17*. https://www.frontiersin.org/articles/10.3389/fnana.2023.1168523

Bartkowska, K., Djavadian, R. L., Taylor, J. R. E., & Turlejski, K. (2008). Generation recruitment and death of brain cells throughout the life cycle of Sorex shrews (Lipotyphla). *European Journal of Neuroscience*, *27*(7), 1710–1721. https://doi.org/10.1111/j.1460-9568.2008.06133.x

Barton, R. A. (1998). Visual specialization and brain evolution in primates. *Proceedings of the Royal Society B: Biological Sciences*, *265*(1409), 1933–1937.

Barton, R. A. (2007). Evolutionary specialization in mammalian cortical structure. *Journal of Evolutionary Biology*, *20*(4), 1504–1511.

https://doi.org/10.1111/j.1420-9101.2007.01330.x

Bedoya Duque, M. A., Thomas, W. R., Dechmann, D. K. N., Nieland, J., Baldoni, C., Von Elverfeldt, D., Muturi, M., Corthals, A., & Dávalos, L. M. (2023). *Large captivity effect based on gene expression comparisons between captive and wild shrew brains* [Preprint]. Genetics. https://doi.org/10.1101/2023.10.02.560583

Benjamini, Y., & Hochberg, Y. (1995). Controlling the False Discovery Rate: A Practical and Powerful Approach to Multiple Testing. *Journal of the Royal Statistical Society: Series B (Methodological)*, *57*(1), 289–300. https://doi.org/10.1111/j.2517-6161.1995.tb02031.x

Benson-Amram, S., Dantzer, B., Stricker, G., Swanson, E. M., & Holekamp, K. E. (2016). Brain size predicts problem-solving ability in mammalian carnivores. *Proceedings of the National Academy of Sciences*, *113*(9), 2532–2537. https://doi.org/10.1073/pnas.1505913113

Berthold, P. & Querner, U. (1988). Was Zugunruhe wirklich ist – eine quantitative Bestimmung mit Hilfe von Video-aufnahmen bei Infrarotlichtbeleuchtung. — *J. Ornithol.* 129:372-375.

Bouton, M. E., Todd, T. P., Miles, O. W., León, S. P., & Epstein, L. H. (2013). Within- and between-session variety effects in a food-seeking habituation paradigm. *Appetite*, *66*, 10–19. https://doi.org/10.1016/j.appet.2013.01.025

Bray, N. L., Pimentel, H., Melsted, P., & Pachter, L. (2016). Near-optimal probabilistic RNA-seq quantification. *Nature Biotechnology*, *34*(5), 525–527. https://doi.org/10.1038/nbt.3519

Budde, M. D., Kim, J. H., Liang, H.-F., Schmidt, R. E., Russell, J. H., Cross, A. H., & Song, S.-K. (2007). Toward accurate diagnosis of white matter pathology using diffusion tensor imaging. *Magnetic Resonance in Medicine*, *57*(4), 688–695. https://doi.org/10.1002/mrm.21200

Bullmore, E., & Sporns, O. (2012). The economy of brain network organization. *Nature Reviews Neuroscience*, *13*(5), 336–349. https://doi.org/10.1038/nrn3214

Burke, D., Cieplucha, C., Cass, J., Russell, F., & Fry, G. (2002). Win-shift and win-stay learning in the short-beaked echidna (Tachyglossus aculeatus). *Animal Cognition*, *5*(2), 79–84. https://doi.org/10.1007/s10071-002-0131-1

Bürkner P. (2021). "Bayesian Item Response Modeling in R with brms and Stan." *Journal of Statistical Software*, 100(5), 1–54. doi:10.18637/jss.v100.i05.

Calisi, R. M., & Bentley, G. E. (2009). Lab and field experiments: Are they the same animal? *Hormones and Behavior*, *56*(1), 1–10. https://doi.org/10.1016/j.yhbeh.2009.02.010

Caroni, P., Donato, F., & Muller, D. (2012). Structural plasticity upon learning: Regulation and functions. *Nature Reviews Neuroscience*, *13*(7), 478–490. https://doi.org/10.1038/nrn3258

Catania, K. C., Lyon, D. C., Mock, O. B., & Kaas, J. H. (1999). Cortical organization in shrews: Evidence from five species. *The Journal of Comparative Neurology*, *410*(1), 55–72. https://doi.org/10.1002/(SICI)1096-9861(19990719)410:10.CO;2-2

Catania, K. C., Hare, J. F., & Campbell, K. L. (2008). Water shrews detect movement,

shape, and smell to find prey underwater. *Proceedings of the National Academy of Science*s, 105(2), 571-576.

Cauchoix, M., Hermer, E., Chaine, A. S., & Morand-Ferron, J. (2017). Cognition in the field: Comparison of reversal learning performance in captive and wild passerines. *Scientific Reports*, *7*(1), 12945. https://doi.org/10.1038/s41598-017-13179-5

Cercignani, M., Inglese, M., Pagani, E., & Filippi, M. (2001). *Mean Diffusivity and Fractional Anisotropy Histograms of Patients with Multiple Sclerosis*.

Changizi, M. A. (2003). Relationship between Number of Muscles, Behavioral Repertoire Size, and Encephalization in Mammals. *Journal of Theoretical Biology*, *220*(2), 157–168. https://doi.org/10.1006/jtbi.2003.3125

Chen, J. L., & Schlaug, G. (2013). Resting State Interhemispheric Motor Connectivity and White Matter Integrity Correlate with Motor Impairment in Chronic Stroke. *Frontiers in Neurology*, *4*. https://doi.org/10.3389/fneur.2013.00178

Chen, S., Zhou, Y., Chen, Y., & Gu, J. (2018). fastp: An ultra-fast all-in-one FASTQ preprocessor. *Bioinformatics*, *34*(17), i884–i890. *https://doi.org/10.1093/bioinformatics/bty560*

Churchfield, J. S. (1979). Studies on the ecology & behaviour of British shrews. Ph.D. thesis. London: Queen Mary University of London.

Churchfield, S. (1981). Water and fat contents of British shrews and their role in the seasonal changes in body weight. *Journal of Zoology*, 194(2), 165-173.

Churchfield, S. (1982). The influence of temperature on the activity and food

consumption of the common shrew. *Acta Theriologica*, *27*, 295–304. https://doi.org/10.4098/AT.arch.82-26

Clubb, R., & Mason, G. (2003). Captivity effects on wide-ranging carnivores. *Nature*, *425*(6957), 473–474. https://doi.org/10.1038/425473a

Collett, T. S., Robert, T., Frasnelli, E., Philippides, A., & Hempel de Ibarra, N. (2023). How bumblebees coordinate path integration and body orientation at the start of their first learning flight. Journal of Experimental Biology, 226(8), jeb245271.

Coppola, G., Di Renzo, A., Tinelli, E., Petolicchio, B., Di Lorenzo, C., Parisi, V., Serrao, M., Calistri, V., Tardioli, S., Cartocci, G., Caramia, F., Di Piero, V., & Pierelli, F. (2020). Patients with chronic migraine without history of medication overuse are characterized by a peculiar white matter fiber bundle profile. *The Journal of Headache and Pain*, *21*(1), 92. https://doi.org/10.1186/s10194-020-01159-6

Cotter, D., Mackay, D., Landau, S., Kerwin, R., & Everall, I. (2001). Reduced glial cell density and neuronal size in the anterior cingulate cortex in major depressive disorder. *Archives of general psychiatry*, 58(6), 545-553.

Crates, R., Stojanovic, D., & Heinsohn, R. (2023). The phenotypic costs of captivity. *Biological Reviews*, *98*(2), 434–449. https://doi.org/10.1111/brv.12913

D'Angelo, E., & Casali, S. (2013). Seeking a unified framework for cerebellar function and dysfunction: From circuit operations to cognition. *Frontiers in Neural Circuits*, *6*. https://doi.org/10.3389/fncir.2012.00116

Dehnel, A. (1949). Studies of the genus Sorex L. Ann. Univ. Mariae Curie-Sklodowska Lublin-Polonia IV, 18–104.

Dickens, M. J., Delehanty, D. J., & Romero, L. M. (2009). Stress and translocation: Alterations in the stress physiology of translocated birds. *Proceedings of the Royal Society B: Biological Sciences*, *276*(1664), 2051–2056. https://doi.org/10.1098/rspb.2008.1778

Dollas, A., Oelschläger, H. H. A., Begall, S., Burda, H., & Malkemper, E. P. (2019). Brain atlas of the African mole-rat Fukomys anselli. *Journal of Comparative Neurology*, *527*(11), 1885–1900. https://doi.org/10.1002/cne.24647

DuRant, S., Love, A. C., Belin, B., Tamayo-Sanchez, D., Santos Pacheco, M., Dickens, M. J., & Calisi, R. M. (2020). Captivity alters neuroendocrine regulators of stress and reproduction in the hypothalamus in response to acute stress. *General and Comparative Endocrinology*, *295*, 113519. https://doi.org/10.1016/j.ygcen.2020.113519

Fagan, W. F., Lewis, M. A., Auger-Méthé, M., Avgar, T., Benhamou, S., Breed, G., ... & Mueller, T. (2013). Spatial memory and animal movement. *Ecology letters*, 16(10), 1316-1329.

Fischer, C. P., Wright-Lichter, J., & Romero, L. M. (2018). Chronic stress and the introduction to captivity: How wild house sparrows (Passer domesticus) adjust to laboratory conditions. *General and Comparative Endocrinology*, *259*, 85–92. https://doi.org/10.1016/j.ygcen.2017.11.007

Frankham, R. (2008). Genetic adaptation to captivity in species conservation programs. *Molecular Ecology*, *17*(1), 325–333. https://doi.org/10.1111/j.1365-294X.2007.03399.x

Freas, C. A., Bingman, K., LaDage, L. D., & Pravosudov, V. V. (2013). Untangling elevation-related differences in the hippocampus in food-caching mountain chickadees: the effect of a uniform captive environment. *Brain, Behavior and Evolution*, 82(3), 199-209.

Garamszegi, L. Z., Eens, M., Erritzøe, J., & Møller, A. P. (2005). Sexually size dimorphic brains and song complexity in passerine birds. *Behavioral Ecology*, *16*(2), 335–345. https://doi.org/10.1093/beheco/arh167

Gaser, C., & Schlaug, G. (2003). Brain Structures Differ between Musicians and Non-Musicians. *The Journal of Neuroscience*, *23*(27), 9240–9245. https://doi.org/10.1523/JNEUROSCI.23-27-09240.2003

Giarmarco, M. M., Brock, D. C., Robbings, B. M., Cleghorn, W. M., Tsantilas, K. A., Kuch, K. C., Ge, W., Rutter, K. M., Parker, E. D., Hurley, J. B., & Brockerhoff, S. E. (2020). Daily mitochondrial dynamics in cone photoreceptors. *Proceedings of the National Academy of Sciences*, *117*(46), 28816–28827. https://doi.org/10.1073/pnas.2007827117

Goldschmidt, D., Manoonpong, P., & Dasgupta, S. (2017). A neurocomputational model of goal-directed navigation in insect-inspired artificial agents. *Frontiers in neurorobotics*, 11, 20.

Hamaide, J., De Groof, G., & Van Der Linden, A. (2016). Neuroplasticity and MRI: A perfect match. *NeuroImage*, *131*, 13–28. https://doi.org/10.1016/j.neuroimage.2015.08.005

Hamet, P., & Tremblay, J. (2005). Genetics and genomics of depression. *Metabolism*,

54(5, Supplement), 10–15. https://doi.org/10.1016/j.metabol.2005.01.006

Healy, S. D., & Rowe, C. (2007). A critique of comparative studies of brain size. *Proceedings of the Royal Society B: Biological Sciences*, *274*(1609), 453–464. https://doi.org/10.1098/rspb.2006.3748

Healy, S. D., & Jozet-Alves, C. (2010). Spatial memory. *Encyclopedia of Animal Behavior*, MD Breed and J. Moore, Eds, 304-307.

Hess, A., Hinz, R., Keliris, G. A., & Boehm-Sturm, P. (2018). On the Usage of Brain Atlases in Neuroimaging Research. *Molecular Imaging and Biology*, *20*(5), 742–749. https://doi.org/10.1007/s11307-018-1259-y

Holtmaat, A., & Svoboda, K. (2009). Experience-dependent structural synaptic plasticity in the mammalian brain. *Nature Reviews Neuroscience*, *10*(9), 647–658. https://doi.org/10.1038/nrn2699

Huang, L., DeVries, G. J., & Bittman, E. L. (1998). Photoperiod regulates neuronal bromodeoxyuridine labeling in the brain of a seasonally breeding mammal. *Journal of neurobiology*, 36(3), 410-420.

Hyvärinen, H. (1969). On the seasonal changes in the skeleton of the common shrew (Sorex araneus L.) and their physiological background (Doctoral dissertation, Tekijä).

Jaggard, J., Lloyd, E., Yuiska, A., Patch, A., Fily, Y., Kowalko, J., Appelbaum, L., Duboue, E., & Keene, A. (2020). Cavefish brain atlases reveal functional and anatomical convergence across independently evolved populations. *SCIENCE ADVANCES*, *6*(38). https://doi.org/10.1126/sciadv.aba3126

Jerison, H. (1974). On the Meaning of Brain Size: Evolution of the Brain and Intelligence. *Science*, *184*(4137), 677–679. https://doi.org/10.1126/science.184.4137.677

Jones, C. M., Papanicolaou, A., Mironidis, G. K., Vontas, J., Yang, Y., Lim, K. S., Oakeshott, J. G., Bass, C., & Chapman, J. W. (2015). Genomewide transcriptional signatures of migratory flight activity in a globally invasive insect pest. *Molecular Ecology*, *24*(19), 4901–4911. https://doi.org/10.1111/mec.13362

Jule, K. R., Leaver, L. A., & Lea, S. E. G. (2008). The effects of captive experience on reintroduction survival in carnivores: A review and analysis. *Biological Conservation*, *141*(2), 355–363. https://doi.org/10.1016/j.biocon.2007.11.007

Kandel, E. R., Markram, H., Matthews, P. M., Yuste, R., & Koch, C. (2013). Neuroscience thinks big (and collaboratively). *Nature Reviews Neuroscience*, *14*(9), 659–664. https://doi.org/10.1038/nrn3578

Keicher, L., O'Mara, M. T., Voigt, C. C., & Dechmann, D. K. N. (2017). Stable carbon isotopes in breath reveal fast incorporation rates and seasonally variable but rapid fat turnover in the common shrew (*Sorex araneus*). *Journal of Experimental Biology*, jeb.159947. https://doi.org/10.1242/jeb.159947

Kellner, E., Dhital, B., Kiselev, V. G., & Reisert, M. (2016). Gibbs-ringing artifact removal based on local subvoxel-shifts: Gibbs-Ringing Artifact Removal. *Magnetic Resonance in Medicine*, *76*(5), 1574–1581. https://doi.org/10.1002/mrm.26054

Kellner, E., Reisert, M., Rau, A., Hosp, J., Demerath, T., Weiller, C., & Urbach, H. (2022). Clinical feasibility of diffusion microstructure imaging (DMI) in acute ischemic stroke. *NeuroImage: Clinical*, *36*, 103189.

https://doi.org/10.1016/j.nicl.2022.103189

Kempermann, G. (2012). New neurons for "survival of the fittest." *Nature Reviews Neuroscience*, *13*(10), 727–736. https://doi.org/10.1038/nrn3319

Kenyon, K. H., Strik, M., Noffs, G., Morgan, A., Kolbe, S., Harding, I. H., Vogel, A. P., Boonstra, F. M. C., & Van Der Walt, A. (2024). Volumetric and diffusion MRI abnormalities associated with dysarthria in multiple sclerosis. *Brain Communications*, *6*(3), fcae177. https://doi.org/10.1093/braincomms/fcae177

Kolb, B., & Gibb, R. (2014). Searching for the principles of brain plasticity and behavior. *Cortex*, *58*, 251–260. https://doi.org/10.1016/j.cortex.2013.11.012

Kuriyama, N., Yamada, K., Sakai, K., Tokuda, T., Akazawa, K., Tomii, Y., Tamura, A., Kondo, M., Watanabe, I., Ozaki, E., Matsui, D., Nakagawa, M., Mizuno, T., & Watanabe, Y. (2015). Ventricular Temperatures in Idiopathic Normal Pressure Hydrocephalus (iNPH) Measured with DWI-based MR Thermometry. *Magnetic Resonance in Medical Sciences*, *14*(4), 305–312. https://doi.org/10.2463/mrms.2014-0076

La Manno, G., Siletti, K., Furlan, A., Gyllborg, D., Vinsland, E., Mossi Albiach, A., Mattsson Langseth, C., Khven, I., Lederer, A. R., Dratva, L. M., Johnsson, A., Nilsson, M., Lönnerberg, P., & Linnarsson, S. (2021). Molecular architecture of the developing mouse brain. *Nature*, *596*(7870), 92–96. https://doi.org/10.1038/s41586-021-03775-x

Lambert, K., Eisch, A. J., Galea, L. A. M., Kempermann, G., & Merzenich, M. (2019). Optimizing brain performance: Identifying mechanisms of adaptive neurobiological plasticity. *Neuroscience & Biobehavioral Reviews*, *105*, 60–71.

https://doi.org/10.1016/j.neubiorev.2019.06.033

LaPoint, S., Gallery, P., Wikelski, M., & Kays, R. (2013). Animal behavior, cost-based corridor models, and real corridors. *Landscape Ecology*, *28*(8), 1615–1630. https://doi.org/10.1007/s10980-013-9910-0

LaPoint, S., Keicher, L., Wikelski, M., Zub, K., & Dechmann, D. K. N. (2016). *Growth overshoot and seasonal size changes in the skulls of two weasel species* (Version 1, p. 188318 bytes) [Dataset]. Dryad. https://doi.org/10.5061/DRYAD.G57G1

Larson, G., & Burger, J. (2013). A population genetics view of animal domestication. *Trends in Genetics*, *29*(4), 197–205. https://doi.org/10.1016/j.tig.2013.01.003

Laughlin, S. (2001). Energy as a constraint on the coding and processing of sensory information. *Current Opinion in Neurobiology*, *11*(4), 475–480. https://doi.org/10.1016/S0959-4388(00)00237-3

Lázaro, J., & Dechmann, D. K. N. (2021). Dehnel's phenomenon. *Current Biology*, *31*(10), R463–R465. https://doi.org/10.1016/j.cub.2021.04.006

Lázaro, J., Dechmann, D. K. N., LaPoint, S., Wikelski, M., & Hertel, M. (2017). Profound reversible seasonal changes of individual skull size in a mammal. *Current Biology*, *27*(20), R1106–R1107. https://doi.org/10.1016/j.cub.2017.08.055

Lázaro, J., Hertel, M., LaPoint, S., Wikelski, M., Stiehler, M., & Dechmann, D. K. N. (2017). Cognitive skills of common shrews (*Sorex araneus*) vary with seasonal changes in skull size and brain mass. *Journal of Experimental Biology*, jeb.166595. https://doi.org/10.1242/jeb.166595

Lázaro, J., Hertel, M., Muturi, M., & Dechmann, D. K. N. (2019). Seasonal reversible size changes in the braincase and mass of common shrews are flexibly modified by environmental conditions. *Scientific Reports*, *9*(1), 2489. https://doi.org/10.1038/s41598-019-38884-1

Lázaro, J., Hertel, M., Sherwood, C. C., Muturi, M., & Dechmann, D. K. N. (2018). Profound seasonal changes in brain size and architecture in the common shrew. *Brain Structure and Function*, *223*(6), 2823–2840. https://doi.org/10.1007/s00429-018-1666-5

Lázaro, J., Nováková, L., Hertel, M., Taylor, J. R. E., Muturi, M., Zub, K., & Dechmann, D. K. N. (2021). Geographic patterns in seasonal changes of body mass, skull, and brain size of common shrews. *Ecology and Evolution*, *11*(6), 2431–2448. https://doi.org/10.1002/ece3.7238

Lefebvre, L., Reader, S. M., & Sol, D. (2004). Brains, Innovations and Evolution in Birds and Primates. *Brain, Behavior and Evolution*, *63*(4), 233–246. https://doi.org/10.1159/000076784

Leger, M., Paizanis, E., Dzahini, K., Quiedeville, A., Bouet, V., Cassel, J.-C., Freret, T., Schumann-Bard, P., & Boulouard, M. (2015). Environmental Enrichment Duration Differentially Affects Behavior and Neuroplasticity in Adult Mice. *Cerebral Cortex*, *25*(11), 4048–4061. https://doi.org/10.1093/cercor/bhu119

Lesch, R., Kitchener, A. C., Hantke, G., Kotrschal, K., & Fitch, W. T. (2022). Cranial volume and palate length of cats, *Felis* spp., under domestication, hybridization and in wild populations. *Royal Society Open Science*, *9*(1), 210477.

https://doi.org/10.1098/rsos.210477

Levy-Gigi, E., Szabó, C., Kelemen, O., & Kéri, S. (2013). Association Among Clinical Response, Hippocampal Volume, and FKBP5 Gene Expression in Individuals with Posttraumatic Stress Disorder Receiving Cognitive Behavioral Therapy. *Biological Psychiatry*, *74*(11), 793–800. https://doi.org/10.1016/j.biopsych.2013.05.017

Lewis, S., Dyvorne, H., Cui, Y., & Taouli, B. (2014). Diffusion-Weighted Imaging of the Liver. *Magnetic Resonance Imaging Clinics of North America*, *22*(3), 373–395. https://doi.org/10.1016/j.mric.2014.04.009

Li, S., Wang, C., Wang, W., Dong, H., Hou, P., & Tang, Y. (2008). Chronic mild stress impairs cognition in mice: From brain homeostasis to behavior. *Life Sciences*, *82*(17–18), 934–942. https://doi.org/10.1016/j.lfs.2008.02.010

Lodato, S., & Arlotta, P. (2015). Generating neuronal diversity in the mammalian cerebral cortex. *Annual review of cell and developmental biology*, 31(1), 699-720.

Love, A. C., Lovern, M. B., & DuRant, S. E. (2017). Captivity influences immune responses, stress endocrinology, and organ size in house sparrows (Passer domesticus). *General and Comparative Endocrinology*, *252*, 18–26. https://doi.org/10.1016/j.ygcen.2017.07.014

Love, M. I., Huber, W., & Anders, S. (2014). Moderated estimation of fold change and dispersion for RNA-seq data with DESeq2. *Genome Biology*, *15*(12), 550. https://doi.org/10.1186/s13059-014-0550-8

Lu, Q., Mouri, A., Yang, Y., Kunisawa, K., Teshigawara, T., Hirakawa, M., Mori, Y., Yamamoto, Y., Libo, Z., Nabeshima, T., & Saito, K. (2019). Chronic unpredictable mild stress-induced behavioral changes are coupled with dopaminergic hyperfunction and serotonergic hypofunction in mouse models of depression. *Behavioural Brain Research*, *372*, 112053. https://doi.org/10.1016/j.bbr.2019.112053

Maguire, E. A., Gadian, D. G., Johnsrude, I. S., Good, C. D., Ashburner, J., Frackowiak, R. S. J., & Frith, C. D. (2000). Navigation-related structural change in the hippocampi of taxi drivers. *Proceedings of the National Academy of Sciences*, *97*(8), 4398–4403. https://doi.org/10.1073/pnas.070039597

Mallory, C. S., Hardcastle, K., Campbell, M. G., Attinger, A., Low, I. I. C., Raymond, J. L., & Giocomo, L. M. (2021). Mouse entorhinal cortex encodes a diverse repertoire of self-motion signals. *Nature Communications*, *12*(1), Article 1. https://doi.org/10.1038/s41467-021-20936-8

Marino, L., Rose, N. A., Visser, I. N., Rally, H., Ferdowsian, H., & Slootsky, V. (2020). The harmful effects of captivity and chronic stress on the well-being of orcas (Orcinus orca). *Journal of Veterinary Behavior*, *35*, 69–82. https://doi.org/10.1016/j.jveb.2019.05.005

Mateos-Aparicio, P., & Rodríguez-Moreno, A. (2019). The Impact of Studying Brain Plasticity. *Frontiers in Cellular Neuroscience*, *13*, 66. https://doi.org/10.3389/fncel.2019.00066

Mazza, V., Eccard, J. A., Zaccaroni, M., Jacob, J., & Dammhahn, M. (2018). The fast and

the flexible: Cognitive style drives individual variation in cognition in a small mammal. *Animal Behaviour*, *137*, 119–132. https://doi.org/10.1016/j.anbehav.2018.01.011

McLean, D. J., & Skowron Volponi, M. A. (2018). trajr: an R package for characterisation of animal trajectories. *Ethology*, 124(6), 440-448.

McNamara, J. M., & Buchanan, K. L. (2005). Stress, resource allocation, and mortality. *Behavioral Ecology*, *16*(6), 1008–1017. https://doi.org/10.1093/beheco/ari087

Mezhzherin, V. A. (1964). Dehnel's phenomenon and its possible explanation. *Acta Theriol*ogica 8, 95–114.

Moirano, J. M., Bezgin, G. Y., Ahlers, E. O., Kötter, R., & Converse, A. K. (2019). Rhesus Macaque Brain Atlas Regions Aligned to an MRI Template. *Neuroinformatics*, *17*(2), 295–306. https://doi.org/10.1007/s12021-018-9400-2

Morales, M. H., & Sánchez, E. J. (1996). Changes in Vitellogenin Expression during Captivity-Induced Stress in a Tropical Anole. *General and Comparative Endocrinology*, *103*(2), 209–219. https://doi.org/10.1006/gcen.1996.0112

Morgan, K., & Tromborg, C. (2006). Sources of stress in captivity. Appl Anim Behav Sci. *Applied Animal Behaviour Science - APPL ANIM BEHAV SCI*, *102*. https://doi.org/10.1016/j.applanim.2006.05.032

Neukomm, L. J., & Freeman, M. R. (2014). Diverse cellular and molecular modes of axon degeneration. *Trends in Cell Biology*, *24*(9), 515–523. https://doi.org/10.1016/j.tcb.2014.04.003

Newman, J. D., Kenkel, W. M., Aronoff, E. C., Bock, N. A., Zametkin, M. R., & Silva, A. C.

(2009). A combined histological and MRI brain atlas of the common marmoset monkey, Callithrix jacchus. *Brain Research Reviews*, *62*(1), 1–18. https://doi.org/10.1016/j.brainresrev.2009.09.001

Newton, C., Pope, M., Rua, C., Henson, R., Ji, Z., Burgess, N., ... & PREVENT Dementia Research Programme. (2024). Entorhinal-based path integration selectively predicts midlife risk of Alzheimer's disease. Alzheimer's & Dementia, 20(4), 2779-2793.

Nováková, L., Lázaro, J., Muturi, M., Dullin, C., & Dechmann, D. K. N. (2022). Winter conditions, not resource availability alone, may drive reversible seasonal skull size changes in moles. *Royal Society Open Science*, *9*(9), 220652. https://doi.org/10.1098/rsos.220652

Nudo, R. J. (2013). Recovery after brain injury: Mechanisms and principles. *Frontiers in Human Neuroscience*, *7*. https://doi.org/10.3389/fnhum.2013.00887

Oberman, L., & Pascual-Leone, A. (2013). Changes in plasticity across the lifespan: cause of disease and target for intervention. *Progress in brain research*, 207, 91-120.

Ochocińska, D., & Taylor, J. (2005). Living at the Physiological Limits: Field and Maximum Metabolic Rates of the Common Shrew (Sorex araneus). *Physiological and Biochemical Zoology : PBZ*, *78*, 808–818. https://doi.org/10.1086/431190

OpenAI. (2024). ChatGPT [Large language model]. https://chat.openai.com/chat

Ortiz, C., Navarro, J. F., Jurek, A., Märtin, A., Lundeberg, J., & Meletis, K. (2020). Molecular

atlas of the adult mouse brain. *SCIENCE ADVANCES*, *6*(26). https://doi.org/10.1126/sciadv.abb3446

Page, R. A., von Merten, S., & Siemers, B. M. (2012). Associative memory or algorithmic search: A comparative study on learning strategies of bats and shrews. *Animal Cognition*, *15*(4), 495–504. https://doi.org/10.1007/s10071-012-0474-1

Panenka, W. J., Lange, R. T., Bouix, S., Shewchuk, J. R., Heran, M. K. S., Brubacher, J. R., Eckbo, R., Shenton, M. E., & Iverson, G. L. (2015). Neuropsychological Outcome and Diffusion Tensor Imaging in Complicated versus Uncomplicated Mild Traumatic Brain Injury. *PLOS ONE*, *10*(4), e0122746. https://doi.org/10.1371/journal.pone.0122746

Paxinos, G., and Franklin, K. B. (2019). Paxinos and Franklin's the mouse brain in stereotaxic coordinates. Academic press.

Pebesma, E., & Bivand, R. (2023). Spatial data science: With applications in R. *Chapman and Hall/CRC*.

Pohle, A.-K., Zalewski, A., Muturi, M., Dullin, C., Farková, L., Keicher, L., & Dechmann, D. K. N. (2023). Domestication effect of reduced brain size is reverted when mink become feral. *Royal Society Open Science*, *10*(7), 230463. https://doi.org/10.1098/rsos.230463

Pontes, A. C., Mobley, R. B., Ofria, C., Adami, C., & Dyer, F. C. (2020). The evolutionary origin of associative learning. *The American Naturalist*, 195(1), E1-E19.

Pucek, Z. (1963). Seasonal Changes in the Braincase of Some Representatives of the Genus Sorex from the Palearctic. *Journal of Mammalogy*, *44*(4), 523.

https://doi.org/10.2307/1377135

Pucek, M. (1965). Water contents and seasonal changes of the brain-weight in shrews. *Acta Theriologica*, *10*, 353–367. https://doi.org/10.4098/AT.arch.65-30

Pucek, Z. (1970). Seasonal and age change in shrews as an adaptive process. *Symp. Zool. Soc. Lond*. 26, 189–207.

R Core Team (2021). R: A language and environment for statistical computing. R Foundation for Statistical Computing, Vienna, Austria. URL https://www.R-project.org/.

Radtke-Schuller, S., Schuller, G., Angenstein, F., Grosser, O. S., Goldschmidt, J., & Budinger, E. (2016). Brain atlas of the Mongolian gerbil (Meriones unguiculatus) in CT/MRI-aided stereotaxic coordinates. *Brain Structure and Function*, *221*(S1), 1–272. https://doi.org/10.1007/s00429-016-1259-0

Raichle, M. E., MacLeod, A. M., Snyder, A. Z., Powers, W. J., Gusnard, D. A., & Shulman, G. L. (2001). A default mode of brain function. *Proceedings of the National Academy of Sciences*, *98*(2), 676–682. https://doi.org/10.1073/pnas.98.2.676

Reader, S. M., & Laland, K. N. (2002). Social intelligence, innovation, and enhanced brain size in primates. *Proceedings of the National Academy of Sciences*, *99*(7), 4436–4441. https://doi.org/10.1073/pnas.062041299

Resende, L. D. S., Neto, G. L. E., Carvalho, P. G. D., Landau-Remy, G., Ramos-Júnior, V. D. A., Andriolo, A., & Genaro, G. (2014). Time Budget and Activity Patterns of Oncilla Cats (*Leopardus tigrinus*) in Captivity. *Journal of Applied Animal Welfare Science*, *17*(1), 73–81.

https://doi.org/10.1080/10888705.2014.856253

Reveley, C., Ye, F. Q., Mars, R. B., Matrov, D., Chudasama, Y., & Leopold, D. A. (2022). Diffusion MRI anisotropy in the cerebral cortex is determined by unmyelinated tissue features. *Nature Communications*, *13*(1), 6702. https://doi.org/10.1038/s41467-022-34328-z

Rochais, C., Hotte, H., & Pillay, N. (2021). Seasonal variation in reversal learning reveals greater female cognitive flexibility in African striped mice. *Scientific Reports*, 11(1), 20061.

Rovaris, M., Gass, A., Bammer, R., Hickman, S. J., Ciccarelli, O., Miller, D. H., & Filippi, M. (2005). Diffusion MRI in multiple sclerosis. *Neurology*, *65*(10), 1526–1532. https://doi.org/10.1212/01.wnl.0000184471.83948.e0

Rymer, T., Pillay, N., & Schradin, C. (2013). Extinction or Survival? Behavioral Flexibility in Response to Environmental Change in the African Striped Mouse Rhabdomys. *Sustainability*, *5*(1), 163–186. https://doi.org/10.3390/su5010163

Salvanes, A. G. V., Moberg, O., Ebbesson, L. O. E., Nilsen, T. O., Jensen, K. H., & Braithwaite, V. A. (2013). Environmental enrichment promotes neural plasticity and cognitive ability in fish. *Proceedings of the Royal Society B: Biological Sciences*, *280*(1767), 20131331. https://doi.org/10.1098/rspb.2013.1331

Sato, N., & Yamaguchi, Y. (2005). Online formation of a hierarchical cognitive map for object–place association by theta phase coding. Hippocampus, 15(7), 963-978.

Schaeffer, P. J., O'Mara, M. T., Breiholz, J., Keicher, L., Lázaro, J., Muturi, M., & Dechmann, D. K. N. (2020). Metabolic rate in common shrews is unaffected by temperature,

leading to lower energetic costs through seasonal size reduction. *Royal Society Open Science*, *7*(4), 191989. https://doi.org/10.1098/rsos.191989

Schmidt, E., Mykytczuk, N., & Schulte-Hostedde, A. I. (2019). Effects of the captive and wild environment on diversity of the gut microbiome of deer mice (Peromyscus maniculatus). *The ISME Journal*, *13*(5), Article 5. https://doi.org/10.1038/s41396-019-0345-8

Seeber, P. A., Morrison, T., Ortega, A., East, M. L., Greenwood, A. D., & Czirják, G. Á. (2020). Immune differences in captive and free-ranging zebras (Equus zebra and E. quagga). *Mammalian Biology*, *100*(2), 155–164. https://doi.org/10.1007/s42991-020-00006-0

Shettleworth, S. J. (2009). Cognition, evolution, and behavior. *Oxford university press*.

Sih, A., Bell, A. M., Johnson, J. C., & Ziemba, R. E. (2004). Behavioral syndromes: an integrative overview. *The quarterly review of biology*, 79(3), 241-277.

Simpson, J., & Kelly, J. P. (2011). The impact of environmental enrichment in laboratory rats—Behavioural and neurochemical aspects. *Behavioural Brain Research*, *222*(1), 246–264. https://doi.org/10.1016/j.bbr.2011.04.002

Smaers, J. B., Rothman, R. S., Hudson, D. R., Balanoff, A. M., Beatty, B., Dechmann, D. K. N., De Vries, D., Dunn, J. C., Fleagle, J. G., Gilbert, C. C., Goswami, A., Iwaniuk, A. N., Jungers, W. L., Kerney, M., Ksepka, D. T., Manger, P. R., Mongle, C. S., Rohlf, F. J., Smith, N. A., … Safi, K. (2021). The evolution of mammalian brain size. *Science Advances*, *7*(18), eabe2101. https://doi.org/10.1126/sciadv.abe2101

Smithson, M., & Verkuilen, J. (2006). A better lemon squeezer? Maximum-likelihood

regression with beta-distributed dependent variables. *Psychological methods*, 11(1), 54.

Sol, D., Lefebvre, L., & Rodríguez-Teijeiro, J. D. (2005). Brain size, innovative propensity and migratory behaviour in temperate Palaearctic birds. *Proceedings of the Royal Society B: Biological Sciences*, *272*(1571), 1433–1441. https://doi.org/10.1098/rspb.2005.3099

Strekalova, T., Spanagel, R., Dolgov, O., & Bartsch, D. (2005). Stress-induced hyperlocomotion as a confounding factor in anxiety and depression models in mice. *Behavioural Pharmacology*, *16*(3), 171.

Sun, X., He, G., Qing, H., Zhou, W., Dobie, F., Cai, F., Staufenbiel, M., Huang, L. E., & Song, W. (2006). Hypoxia facilitates Alzheimer's disease pathogenesis by up-regulating *BACE1* gene expression. *Proceedings of the National Academy of Sciences*, *103*(49), 18727–18732. https://doi.org/10.1073/pnas.0606298103

Sunkin, S. M., Ng, L., Lau, C., Dolbeare, T., Gilbert, T. L., Thompson, C. L., Hawrylycz, M., & Dang, C. (2013). Allen Brain Atlas: An integrated spatio-temporal portal for exploring the central nervous system. *Nucleic Acids Research*, *41*(D1), D996–D1008. https://doi.org/10.1093/nar/gks1042

The MathWorks Inc. (2022). Optimization Toolbox version: 9.4 (R2022b), Natick, Massachusetts: The MathWorks Inc. https://www.mathworks.com

Todd, E. V., Black, M. A., & Gemmell, N. J. (2016). The power and promise of RNA-seq in ecology and evolution. *Molecular Ecology*, *25*(6), 1224–1241. https://doi.org/10.1111/mec.13526

Trouard, T. P., Harkins, K. D., Divijak, J. L., Gillies, R. J., & Galons, J. (2008). Ischemia-induced changes of intracellular water diffusion in rat glioma cell cultures. *Magnetic Resonance in Medicine*, *60*(2), 258–264. https://doi.org/10.1002/mrm.21616

Ullmann, J. F. P., Janke, A. L., Reutens, D., & Watson, C. (2015). Development of MRI-based atlases of non-human brains: Development of MRI brain atlases. *Journal of Comparative Neurology*, *523*(3), 391–405. https://doi.org/10.1002/cne.23678

Van Dongen, P. A. M. (1998). Brain size in vertebrates. *The central nervous system of vertebrates*, 3, 2099-2134.

Van Rossum, G., & Drake, F. L. (2009). Introduction to python 3: python documentation manual part 1. *CreateSpace*.

Veraart, J., Novikov, D. S., Christiaens, D., Ades-aron, B., Sijbers, J., & Fieremans, E. (2016). Denoising of diffusion MRI using random matrix theory. *NeuroImage*, *142*, 394–406. https://doi.org/10.1016/j.neuroimage.2016.08.016

Vollmayr, B., & Henn, F. A. (2003). Stress models of depression. *Clinical Neuroscience Research*, *3*(4), 245–251. https://doi.org/10.1016/S1566-2772(03)00086-0

Vorhees, C. V., & Williams, M. T. (2014). Assessing spatial learning and memory in rodents. *ILAR journal*, 55(2), 310-332.

Walter, T., & Couzin, I. D. (2021). TRex, a fast multi-animal tracking system with markerless identification, and 2D estimation of posture and visual fields. *Elife*, 10, e64000.

Wang, J. T., Medress, Z. A., & Barres, B. A. (2012). Axon degeneration: Molecular mechanisms of a self-destruction pathway. *Journal of Cell Biology*, *196*(1), 7–18. https://doi.org/10.1083/jcb.201108111

Wang, X., Xu, J., Wang, Q., Ding, D., Wu, L., Li, Y., Wu, C., & Meng, H. (2021). Chronic stress induced depressive-like behaviors in a classical murine model of Parkinson's disease. *Behavioural Brain Research*, *399*, 112816. https://doi.org/10.1016/j.bbr.2020.112816

Washington, S. D., Hamaide, J., Jeurissen, B., van Steenkiste, G., Huysmans, T., Sijbers, J., Deleye, S., Kanwal, J. S., De Groof, G., Liang, S., Van Audekerke, J., Wenstrup, J. J., Van der Linden, A., Radtke-Schuller, S., & Verhoye, M. (2018). A Three-dimensional Digital Neurological Atlas of the Mustached Bat (Pteronotus parnellii). *NeuroImage*, *183*, 300–313. https://doi.org/10.1016/j.neuroimage.2018.08.013

Webber, E. S., Chambers, N. E., Kostek, J. A., Mankin, D. E., & Cromwell, H. C. (2015). Relative reward effects on operant behavior: Incentive contrast, induction and variety effects. *Behavioural Processes*, *116*, 87–99. https://doi.org/10.1016/j.beproc.2015.05.003

West, M. J. (2001). Design based stereological methods for estimating the total number of objects in histological material. *Folia Morphol.*, *60*(1).

West, M. J., Slomianka, L., & Gundersen, H. J. G. (1991). Unbiased stereological estimation of the total number of neurons in the subdivisions of the rat hippocampus using the optical fractionator. *The Anatomical Record*, *231*(4),

482–497. https://doi.org/10.1002/ar.1092310411

Wickham, H., Averick, M., Bryan, J., Chang, W., McGowan, L. D. A., François, R., ... & Yutani, H. (2019). Welcome to the Tidyverse. *Journal of open source software*, 4(43), 1686.

Wójcik, J. M., Polly, P. D., Wójcik, A. M., & Sikorski, M. D. (2007). Epigenetic variation of the common shrew, Sorex araneus, in different habitats. *Russian Journal of Theriology*. Русский териологический журнал, 6(1), 43-49.

Wu, Y., Wang, X., Mo, X., Li, J., Yuan, J., Zheng, J., Feng, Y., & Tang, M. (2011). Expression of Laminin β1 and Integrin α2 in the Anterior Temporal Neocortex Tissue of Patients With Intractable Epilepsy. *International Journal of Neuroscience*, *121*(6), 323–328. https://doi.org/10.3109/00207454.2011.558224

Yamamoto, S., Shigeyoshi, Y., Ishida, Y., Fukuyama, T., Yamaguchi, S., Yagita, K., Moriya, T., Shibata, S., Takashima, N., & Okamura, H. (2001). Expression of the Per1 gene in the hamster: Brain atlas and circadian characteristics in the suprachiasmatic nucleus. *Journal of Comparative Neurology*, *430*(4), 518–532. https://doi.org/10.1002/1096-9861(20010219)430:4

Yaskin, V. A. (1994). Variation in brain morphology of the common shrew. In *Advances in the Biology of Shrews* (ed. Merrit, J. F., Kirkland, G. L. and Rose, R. K.), pp. 155–161. Pittsburgh: Carnegie Museum of Natural History, special publication.

Yaskin, V. A. (2011). Seasonal changes in hippocampus size and spatial behavior in mammals and birds. *Biology Bulletin Reviews*, *1*(3), 279–288. https://doi.org/10.1134/S2079086411030108

Yohe, L. R., Davies, K. T. J., Simmons, N. B., Sears, K. E., Dumont, E. R., Rossiter, S. J., & Dávalos, L. M. (2020). Evaluating the performance of targeted sequence capture, RNA-Seq, and degenerate-primer PCR cloning for sequencing the largest mammalian multigene family. *Molecular Ecology Resources*, *20*(1), 140–153. https://doi.org/10.1111/1755-0998.13093

Yoshimura, T. (2010). Neuroendocrine mechanism of seasonal reproduction in birds and mammals. *Animal Science Journal*, 81(4), 403-410.

Zannas, A. S., Wiechmann, T., Gassen, N. C., & Binder, E. B. (2016). Gene–Stress–Epigenetic Regulation of FKBP5: Clinical and Translational Implications. *Neuropsychopharmacology*, *41*(1), Article 1. https://doi.org/10.1038/npp.2015.235

Zebunke, M., Puppe, B., & Langbein, J. (2013). Effects of cognitive enrichment on behavioural and physiological reactions of pigs. *Physiology & Behavior*, *118*, 70–79. https://doi.org/10.1016/j.physbeh.2013.05.005

Zeder, M. A. (2012). Pathways to Animal Domestication. In P. Gepts, T. R. Famula, R. L. Bettinger, S. B. Brush, A. B. Damania, P. E. McGuire, & C. O. Qualset (Eds.), *Biodiversity in Agriculture* (1st ed., pp. 227–259). Cambridge University Press. https://doi.org/10.1017/CBO9781139019514.013

Zhang, K., & Sejnowski, T. J. (2000). A universal scaling law between gray matter and white matter of cerebral cortex. *Proceedings of the National Academy of Sciences*, *97*(10), 5621–5626. https://doi.org/10.1073/pnas.090504197

Zhang, Y., & Burock, M. A. (2020). Diffusion Tensor Imaging in Parkinson's Disease and

Parkinsonian Syndrome: A Systematic Review. *Frontiers in Neurology*, *11*, 531993. https://doi.org/10.3389/fneur.2020.531993

Zhou, F.-L., McHugh, D. J., Li, Z., Gough, J. E., Williams, G. R., & Parker, G. J. M. (2021). Coaxial electrospun biomimetic copolymer fibres for application in diffusion magnetic resonance imaging. *Bioinspiration & Biomimetics*, *16*(4), 046016. https://doi.org/10.1088/1748-3190/abedcf

Zhou, L., Li, X., & Su, B. (2022). Spatial Regulation Control of Oxygen Metabolic Consumption in Mouse Brain. *Advanced Science*, *9*(34), 2204468. https://doi.org/10.1002/advs.202204468

Acknowledgments

As I sit down to write these acknowledgments, I'm struck by how many people I need to thank and how clueless I am about where to start. I never thought saying thank you could be so challenging, but here goes my best attempt at it. If I overlook anyone, please know that your help has meant the world to me, even if my memory fails me now.

To my boss Dina, your support has been unparalleled. Thank you for your understanding when I needed time to focus on this project and for pushing me beyond my limits. Your mentorship has made all the difference, and I am deeply appreciative of everything you've done for me.

To the members of my advisory committee, Dino, Liliana, Pizza, and Dominik, your collective wisdom has been invaluable. Dino, thank you for convincing Dina I was the best person for this job; without you, I would not be here. Pizza, thank you for pushing me to think deeper and to aim higher. Liliana, your critical feedback helped shape this work into its best form. Dominik, my time in Freiburg was the best, and you made it better.

To the two incredible technicians who got me through this like a beacon in the night, Marion and Ivan. Marion, you taught me everything I needed to know in those crucial first two years (including how to make a cappuccino with Hafermilch). Ivan, you saw me through to the completion of this work, providing support and much-needed comic relief. I couldn't have done this without you both.

To all the amazing students who helped me with the shrews: Angela, Milena, Ellen, and Anka. Your curiosity and eagerness to learn have been a constant source of inspiration. Thank you for challenging me with your questions and for reminding me why I love this field.

To two of my most dedicated students, Marina and Costa, who started as "slaves," then became interns, and eventually rose to the ranks of research assistants. I still don’t know why you kept coming back, but I’m profoundly grateful that you did. Your unwavering support, tireless work ethic, and boundless enthusiasm were instrumental in bringing this project to completion. Without you, I would not be here today—maybe a

few months later, but certainly not with the same level of success and sanity (yes Marina, I said sanity!).

A special nod to my peers at the IMPRS— camaraderie and shared misery were the glue that held us all together. Together, we navigated the labyrinth of academia, and I couldn't have asked for a better crew.

To my phenomenal lab team, you turned every day into a blend of scientific wonder and hilarious moments. From the celebratory cakes for every published paper to our debates on the best place to eat, working with you was always great. Your creative problem-solving and energy made even the toughest challenges fun. Whether it was late-night experiments or early morning meetings, your dedication and enthusiasm were inspiring. Thank you for being the backbone of this project.

To my incredible friends, Kavitha, Maud, Jana, and Mari, who doubled as proofreaders, brunch companions, and party animals. You saw me through the best times and most of the worst (including two broken knees, one bout of COVID, an ear infection, and a broken toe). Your unwavering support, infectious laughter, and never-ending encouragement kept me going. You turned every obstacle into a memorable story. You were the glue that held my sanity together and always a source of writing motivation.

Alla mia mamonzi e babonzolo, e Mari e Richi. Anche se non avete la piú pallida idea di cosa ho fatto negli ultimi quattro anni, mi siete tutti veniti a trovare in quel di Costanza e siete sempre stati piú interessati al fatto che fossi contenta. Grazie di tutto.

To my husband Jan, you are my voice of reason and caffeine-supplier. Thank you for putting up with my late nights, my research rants, and my Spezi-fueled insanity. Your support has kept me grounded through the toughest times. You listened to my shrew theories, offered me a shoulder to lean on, and brought me booze when I needed it most. Your love and patience are the true heroes of this story, and I am incredibly grateful to have you by my side every step of the way.

And last, thanks to my study animals, without whom this research would have been impossible. You tolerated my intrusions with grace and taught me more than any textbook ever could. I owe you a heartfelt thank you for your unwitting participation:

Mashrewsalem, Isaac Shrewton, Marie Shrewrie, Shrewlock Holmes, Shrewpillon, Stephen Shrewking, Copernishrews, Captain Shrewk, Malshrewficent, Shrewa Lipa, Shrewsain Bolt, Shrewella Devil, Shrewdy Mercury, Picashrew,
And all the other anonymous heroes.

Author Contributions

Chapter 1

CB, DD, MM, and JL captured the shrews and extracted the brains. CB, JL, and MM prepared the histological sections and the histology atlas. WT performed the gene expression analyses, LD supervised. MM, MR, DE, and CB designed the 3D atlas. CB, WT, DE, DD, LD, and JN wrote the manuscript. CB and WT prepared the figures. All authors discussed the results and contributed to the final version of the manuscript.

Chapter 2

CB captured the shrews for the MRI scans. BS and JL captured and sampled the shrews for the cell count. BS collected cell count data. CB performed all statistical analyses and prepared figures. CB, BS, MR, DvE, DKND wrote the first manuscript draft. LD and WRT gave input on the first draft and helped finalize the manuscript. All authors discussed the results and contributed to the final version of the manuscript.

Chapter 3

CB, DKND, LMD, and JN designed the study. CB, KR, MF, IL, MM captured the shrews. CB, KR, MF designed the associative learning task and performed cognitive experiments. KR and MF coded videos. CB, DvE and MR performed MRI data acquisition and validation. KSL and MHMM designed the computerized running wheel system and analyzed data. CB conducted statistical analyses and prepared figures. CB, DKND, DvE, MR, KR, MF and WRT wrote the manuscript. All authors discussed the results and contributed to the final version of the manuscript.

Chapter 4

CB, MF, KR captured the shrews, designed the experiments and performed all cognitive experiments. MF tracked all videos. EN preprocessed the associative learning and path integration data. CB preprocessed the spatial learning data, performed all statistical analyses and prepared figures. CB, MF, DKND wrote the manuscript. All authors discussed the results and contributed to the final version of the manuscript.

Appendices

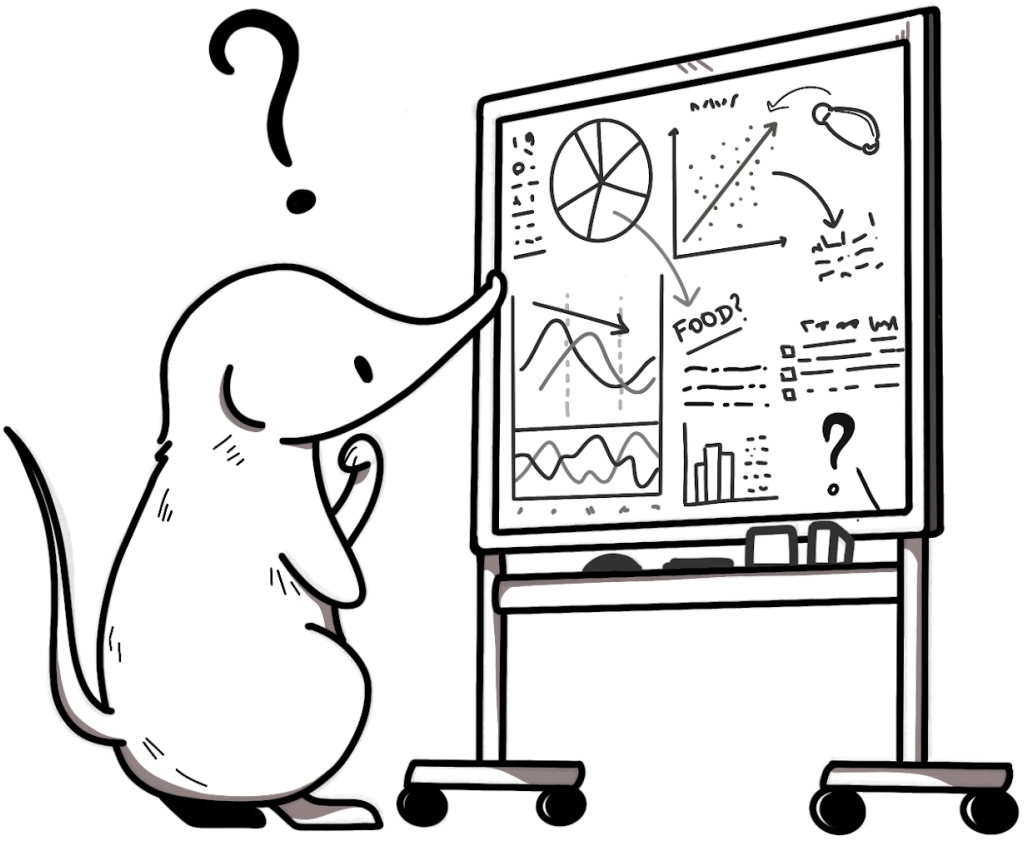

Appendix to Chapter 1

Table A1.1. List of brain structures identified in histological sections and MRI, with corresponding abbreviations. In the MRI atlas, Piriform and entorhinal areas are grouped together.

	Histology	MRI	Gene Expression
Cerebrum:			
CTX	cerebral cortex	X	X
MOB	main olfactory bulb	X	X
mi	mitral layer		
gr	granule layer		
opl	outer plexiform layer		
ipl	inner plexiform layer		
gl	glomerular layer		
onl	olfactory nerve layer of main olfactory bulb		
AON	Anterior olfactory nucleus		
OT	olfactory tubercle	X	
pir	piriform area	X	
aco	anterior commissure, olfactory limb		
iso	isocortex		
HIP	hippocampal region	X	X

CA1	CA1 field	
CA2	CA2 field	
CA3	CA3 field	
sr	stratum radiatum	
so	stratum oriens	
sp	pyramidal layer	
slm	stratum lacunosum-moleculare	
DG	dentate gyrus	
mo	dentate gyrus, molecular layer	
FA	fasciola cinerea	
Retrohippocampal region:		
ent	entorhinal area	X
SUBd	Subiculum, dentral part	
SUBv	Subiculum, ventral part	
Cerebral Nuclei:		
STR	Striatum	
ACB	Nucleus accumbens	X
CP	caudoputamen	X

LS	Lateral septal nucleus		
sAMY	Striatum- like amygdalar nuclei	X	
PAL	pallidum		
Brain stem:			
HY	hypothalamus	X	X
TH	thalamus	X	X
MB	midbrain	X	
P	pons	X	
MY	medulla	X	
CBX	cerebellum	X	
PFL	paraflocculus		
Fi	fiber tracts:		
cc	corpus callosum		
VL	lateral ventricle		
V3	third ventricle		
AQ	cerebral aqueduct		
aco	anterior commissure, olfactory limb		
act	anterior commissure, temporal limb		

Cpd	cerebral peduncle
sg	granule cell layer
po	polymorph layer
SUBd	Subiculum, dentral part
SUBv	Subiculum, ventral part

Appendix to Chapter 2

Table A2.1. Estimates from Bayesian hierarchical models assessing the impact of season on tissue diffusion metrics across 13 brain regions.

Intracellular water volume fraction		**Estimate**	**Est. Error**	**Lower CI**	**Upper CI**
	Amygdala	-0.074	0.064	-0.212	0.041
	AON	-0.037	0.062	-0.171	0.076
	Caudoputamen	0.038	0.061	-0.078	0.166
	Cerebellum	0.078	0.065	-0.037	0.216
	Hippocampus	0.016	0.06	-0.101	0.138
	Midbrain	0.071	0.065	-0.046	0.208
	Nucleus accumbens	-0.036	0.061	-0.166	0.081
	Neocortex	0.118	0.073	-0.008	0.274
	Olfactory Bulb	-0.035	0.062	-0.165	0.082
	Olfactory Tubercle	-0.084	0.069	-0.23	0.037
	Piriform and Enthorinal cortices	-0.063	0.064	-0.199	0.049
	Pons and Medulla	-0.003	0.061	-0.128	0.12
	Thalamus	-0.004	0.059	-0.123	0.116
Extracellular water volume fraction		**Estimate**	**Est. Error**	**Lower CI**	**Upper CI**

Season interaction	**Amygdala**	0.092	0.104	-0.093	0.312
	AON	0.067	0.101	-0.12	0.28
	Caudoputamen	-0.036	0.097	-0.236	0.148
	Cerebellum	-0.167	0.116	-0.412	0.03
	Hippocampus	-0.05	0.098	-0.259	0.138
	Midbrain	-0.077	0.106	-0.3	0.115
	Nucleus accumbens	0.094	0.104	-0.09	0.314
	Neocortex	-0.184	0.117	-0.43	0.014
	Olfactory Bulb	0.038	0.099	-0.152	0.243
	Olfactory Tubercle	0.145	0.12	-0.064	0.402
	Piriform and Enthorinal cortices	0.05	0.098	-0.135	0.252
	Pons and Medulla	0.021	0.104	-0.184	0.235
	Thalamus	0.052	0.098	-0.134	0.235
Mean Diffusivity (MD)		**Estimate**	**Est. Error**	**Lower CI**	**Upper CI**
Season interaction	**Amygdala**	0.092	0.049	-0.001	0.194
	AON	-0.006	0.048	-0.104	0.088
	Caudoputamen	-0.07	0.049	-0.168	0.025
	Cerebellum	-0.035	0.049	-0.135	0.062

	Hippocampus	-0.016	0.049	-0.112	0.082
	Midbrain	-0.092	0.05	-0.193	0.005
	Nucleus accumbens	-0.009	0.049	-0.107	0.087
	Neocortex	-0.074	0.049	-0.173	0.018
	Olfactory Bulb	0.031	0.049	-0.066	0.127
	Olfactory Tubercle	0.179	0.055	0.077	0.291
	Piriform and Enthorinal cortices	0.074	0.049	-0.021	0.176
	Pons and Medulla	-0.004	0.049	-0.099	0.093
	Thalamus	-0.072	0.049	-0.177	0.019
Fractional Anisotropy (FA)		**Estimate**	**Est. Error**	**Lower CI**	**Upper CI**
Season interaction	**Amygdala**	0.016	0.038	-0.059	0.092
	AON	-0.047	0.038	-0.125	0.024
	Caudoputamen	-0.011	0.038	-0.088	0.063
	Cerebellum	0.049	0.038	-0.021	0.126
	Hippocampus	-0.019	0.037	-0.095	0.054
	Midbrain	0.034	0.037	-0.034	0.111
	Nucleus accumbens	0.025	0.038	-0.049	0.1
	Neocortex	0.08	0.041	0.004	0.165

	Olfactory Bulb	-0.009	0.037	-0.082	0.064
	Olfactory Tubercle	-0.06	0.04	-0.143	0.013
	Piriform and Enthorinal cortices	0.042	0.039	-0.032	0.124
	Pons and Medulla	-0.024	0.036	-0.099	0.047
	Thalamus	-0.081	0.04	-0.166	-0.007
Axial Diffusivity (aD)		**Estimate**	**Est. Error**	**Lower CI**	**Upper CI**
Season interaction	**Amygdala**	0.104	0.055	0.003	0.219
	AON	-0.014	0.053	-0.119	0.092
	Caudoputamen	-0.081	0.053	-0.188	0.024
	Cerebellum	-0.032	0.053	-0.14	0.072
	Hippocampus	-0.022	0.053	-0.127	0.079
	Midbrain	-0.095	0.054	-0.205	0.008
	Nucleus accumbens	-0.003	0.052	-0.107	0.1
	Neocortex	-0.06	0.053	-0.168	0.042
	Olfactory Bulb	0.037	0.053	-0.066	0.141
	Olfactory Tubercle	0.189	0.058	0.079	0.307
	Piriform and Enthorinal cortices	0.091	0.054	0.079	0.202
	Pons and Medulla	-0.007	0.052	-0.109	0.096

	Thalamus	-0.097	0.054	-0.207	0.005
Radial Diffusivity (rD)		**Estimate**	**Est. Error**	**Lower CI**	**Upper CI**
Season interaction	**Amygdala**	0.076	0.046	-0.011	0.17
	AON	0.015	0.045	-0.072	0.106
	Caudoputamen	-0.048	0.045	-0.137	0.041
	Cerebellum	-0.043	0.046	-0.138	0.045
	Hippocampus	0.002	0.045	-0.087	0.092
	Midbrain	-0.087	0.047	-0.182	0.001
	Nucleus accumbens	-0.019	0.046	-0.11	0.067
	Neocortex	-0.106	0.047	-0.204	-0.018
	Olfactory Bulb	0.023	0.046	-0.067	0.116
	Olfactory Tubercle	0.168	0.052	0.066	0.273
	Piriform and Enthorinal cortices	0.045	0.045	-0.043	0.136
	Pons and Medulla	0.004	0.046	-0.087	0.095
	Thalamus	-0.02	0.046	-0.112	0.07
Cerebrospinal fluid volume fraction (CSF)		**Estimate**	**Est. Error**	**Lower CI**	**Upper CI**
Season interaction	**Amygdala**	0.039	0.096	-0.146	0.235
	AON	-0.113	0.103	-0.326	0.077

Caudoputamen	-0.005	0.099	-0.201	0.188
Cerebellum	0.248	0.097	0.065	0.445
Hippocampus	0.149	0.101	-0.038	0.357
Midbrain	-0.008	0.092	-0.19	0.177
Nucleus accumbens	-0.143	0.105	-0.364	0.054
Neocortex	0.096	0.098	-0.087	0.295
Olfactory Bulb	-0.027	0.094	-0.216	0.155
Olfactory Tubercle	-0.008	0.091	-0.191	0.168
Piriform and Enthorinal cortices	-0.019	0.092	-0.198	0.16
Pons and Medulla	-0.013	0.088	-0.185	0.162
Thalamus	-0.214	0.106	-0.438	-0.028

Table A2.2. Regression coefficients from the model predicting intracellular water volume fraction using interactions between extracellular water volume fraction (Extra) and CerebroSpinal Fluid (CSF) by seasons (summer and winter). Coefficients represent the changes in the log odds of the response variable(Intracellular water volume fraction) due to one-unit changes in predictors.

	Estimate	**Est. Error**	**Lower CI**	**Upper CI**
Intercept	1.58	0.06	1.46	1.69
Extra - summer	-2.93	0.11	-3.15	-2.71
Extra - winter	-2.69	0.07	-2.84	-2.55
CSF - summer	-0.58	0.25	-1.07	-0.10
CSF - winter	-0.65	0.20	-1.03	-0.25

Table A2.3. Regression coefficients from the model predicting Fractional Anisotropy (FA) fraction using interactions between Radial Diffusivity (rD) and Axial Diffusivity (aD) by seasons (summer and winter). Coefficients represent the changes in the log odds of the response variable due to one-unit changes in predictors.

	Estimate	Est. Error	Lower CI	Upper CI
Intercept	-0.79	0.05	-0.89	-0.69
Intercept - winter	-0.11	0.07	-0.24	0.02
rD - summer	-8.28	0.32	-8.90	-7.67
rD - winter	-7.40	0.27	-7.93	-6.86
aD - summer	5.04	0.21	4.63	5.46
aD - winter	4.71	0.22	4.26	5.13

Table A2.4. Multilevel model estimates of the impact of various brain tissue changes on overall brain volume, using a Gaussian family with identity links for both mean and standard deviation. Predictors include changes in intracellular water (change-intra), extracellular water (change_extra), cerebrospinal fluid (change-csf), fractional anisotropy (change-fa), mean diffusivity (change_md), axial diffusivity (change-ad), and radial diffusivity (change-rd).

	Estimate	Est. Error	Lower CI	Upper CI
Change - Intra	-0.12	0.32	-1.99	1.67
Change - Extra	0.21	0.81	-1.40	1.75
Change - csf	0.01	0.96	-1.90	1.90
Change - fa	0.00	0.96	-1.90	1.90
Change - md	0.25	0.99	-1.70	2.20
Change - ad	0.32	0.93	-1.51	2.09
Change - rd	0.18	0.97	-1.70	2.06

Appendix to Chapter 3

Odor preference testing and exposure trials

In the exposure trials, we removed the one-way doors thereby allowing the shrews the possibility to reverse their choice during each exposure trial, as their entry and exit were no longer restricted. Each shrew performed six trials, during which it was able to inspect both boxes and locate the reward exclusively in the correct box. We recorded the first box the shrew entered. The exposure trials allowed the shrews to become familiar with the setup and reward and allowed us to determine whether shrews preferred or avoided specific odors. The predefined criterion for odor preference or avoidance was if a shrew first entered the same box during five consecutive trials, and in this case the odor in question would have been replaced. However, none of the shrews strongly preferred or avoided any of the presented odors. Test trials were conducted the following day and consisted of ten trials. During test trials, boxes were equipped with one-way doors, ensuring that once a decision was made and the shrew entered a box, it could not reverse its choice, concluding the trial.

Video coding

We recorded the associative learning trials individually with an AXIS P3344 Network Camera. We coded behaviors using Solomon Coder (video coding software, beta 19.08.02). The coding resolution was set to 0,2 sec/frame to achieve higher accuracy in the coding process. Once the experimenter opened the connection from the homecage to the Y-maze, the test officially started. We recorded the time from the start of the experiment until the shrew entered the Y-maze as 'latency', measured in minutes. The coding started once the shrews had entered the Y-maze for the first time (decision tube). The total time spent in the maze was coded as “test_time” in seconds. Additionally, we coded the following behaviors: (1) location: position of the shrew between homecage, decision tube, decision box, correct tube, incorrect tube; (2) sitting: no movement for more than 3 seconds; (3) change of direction: complete body turn followed by movement in the opposite direction or walking backward; (4) choice: Correct = 1, Incorrect = 0. The coding stopped as soon as the shrew, i.e., its entire body minus the tail, entered one of the two boxes. Out of the 280 videos initially considered, we successfully coded 256. The remaining 24 videos were corrupted and, consequently, could not be analyzed.

Associative Learning Task – Alternative hypotheses checking

1. *Effect on success by other variables.*

We performed a Generalised Linear Model to check if other variables could influence the success. For this purpose, we used the variables: change of direction, test time, latency and sitting. Only sitting was found to be negatively correlated with success in winter wild populations.

Table A3.1. Estimates from the Generalised Linear Model with lower and upper 95% credible interval on the effect of change of direction, test time, latency and sitting to success. Results are summarised in the three categories: Summer wild, Winter wild, and Winter captive.

COD	**Category**	**Success Estimate**	**l-95% CI**	**u-95% CI**
	Summer wild	0.02	-0.13	0.19
	Winter wild	0.03	-0.13	0.19
	Winter captive	-0.04	-0.25	0.16
Test Time	**Category**	**Success Estimate**	**l-95% CI**	**u-95% CI**
	Summer wild	-0.00	-0.01	0.01
	Winter wild	-0.00	-0.01	0.00
	Winter captive	0.00	-0.00	0.01
Latency	**Category**	**Success Estimate**	**l-95% CI**	**u-95% CI**
	Summer wild	0.00	-0.00	0.00
	Winter wild	0.00	-0.00	0.00
	Winter captive	-0.00	-0.00	0.00
Sitting	**Category**	**Success Estimate**	**l-95% CI**	**u-95% CI**
	Summer wild	0.05	-0.00	0.12
	Winter wild	-1.11	-3.34	0.44
	Winter captive	-0.00	-0.01	0.01

Table A3.2. Results from generalized additive models (GAMs) with estimates and lower and upper 95% credible interval, comparing the effect of trial number on success in each category: Summer wild, Winter wild, and Winter captive. Bold values highlight first and last trial, and the peak in performance for the two wild categories (Trial 1, 6, 8, 10).

Associative Learning Success per Trial	Category	Trial	Success Estimate	l-95% CI	u-95% CI
	Summer wild	**1**	**0.504**	**0.263**	**0.745**
		2	0.423	0.236	0.617
		3	0.420	0.221	0.621
		4	0.610	0.409	0.785
		5	0.833	0.677	0.953
		6	**0.894**	**0.758**	**0.983**
		7	0.812	0.651	0.928
		8	**0.654**	**0.446**	**0.823**
		9	0.499	0.301	0.703
		10	**0.235**	**0.070**	**0.462**
	Category	**Trial**	**Success Estimate**	**l-95% CI**	**u-95% CI**
	Winter wild	**1**	**0.376**	**0.139**	**0.654**
		2	0.416	0.212	0.633
		3	0.473	0.281	0.684
		4	0.475	0.271	0.676
		5	0.450	0.200	0.663
		6	**0.533**	**0.289**	**0.732**

	7	0.685	0.479	0.893
	8	**0.725**	**0.505**	**0.926**
	9	0.638	0.425	0.837
	10	**0.470**	**0.165**	**0.767**

Category	**Trial**	**Success Estimate**	**l-95% CI**	**u-95% CI**
Winter Captive	**1**	**0.376**	**0.139**	**0.654**
	2	0.416	0.212	0.633
	3	0.473	0.281	0.684
	4	0.475	0.271	0.676
	5	0.450	0.200	0.663
	6	**0.533**	**0.289**	**0.732**
	7	0.685	0.479	0.893
	8	**0.725**	**0.505**	**0.926**
	9	0.638	0.425	0.837
	10	**0.470**	**0.165**	**0.767**

Table A3.3. Results from the hurdle negative binomial model of the latency data, with lower and upper 95% credible interval. The table is separated into estimates from the count part of the model (log scale) and estimates from the hurdle part (logit scale).

Latency -Count Part Log Scale	**Category**	**Estimate**	**l-95% CI**	**u-95% CI**	
	Summer wild	2.51	1.99	2.95	exp(2.51) = 12.28
	Winter wild	-0.43	-1.00	0.15	exp(-0.43) = 0.65
	Winter captive	0.12	-0.55	0.79	exp(0.12) = 1.13
Latency - Hurdle Part Logit Scale	*Summer wild*	-2.09	-2.67	-1.58	exp(-2.09)) = 0.11
	Winter wild	-2.57	-4.90	-0.75	exp(-4.66)) = 0.009
	Winter captive	1.65	0.96	2.38	exp(-0.44)) = 0.39

Table A3.4. Results from the Bayesian mixed-effects regression model of the running wheel data, with estimates by hour and category, with lower and upper 95% credible interval.

Run Distance per Hour	**Category**	**Hour**	**Estimate**	**l-95% CI**	**u-95% CI**
	Summer wild	0	2.88	2.82	2.93
		2	2.99	2.92	3.05
		4	2.7	2.65	2.76
		6 (sunrise)	**1.69**	**1.60**	**1.78**
		8	0.58	0.43	0.73
		12	0.98	0.77	1.16
		14	-0.18	-0.36	0.00
		17	-0.22	-0.39	-0.06
		20 (sunset)	**2.23**	**2.15**	**2.30**

	22	2.72	2.67	2.78
Winter Wild	0	2.84	2.81	2.88
	2	2.94	2.90	2.97
	4	2.89	2.85	2.93
	6	2.62	2.57	2.67
	8 (sunrise)	**2.73**	**2.67**	**2.79**
	12	1.11	1.03	1.19
	14	1.63	1.56	1.69
	17 (sunset)	**2.7**	**2.65**	**2.75**
	20	3.00	2.97	3.03
	22	2.86	2.83	2.89
Winter Captive	0	0.59	0.54	0.64
	2	0.57	0.51	0.63
	4	0.34	0.28	0.40
	6	0.32	0.25	0.38
	8 (sunrise)	**0.18**	**0.10**	**0.26**
	12	-0.64	-0.92	-0.37
	14	-0.66	-0.87	-0.48
	17 (sunset)	**0.58**	**0.47**	**0.69**
	20	0.23	0.17	0.28

	22	0.17	0.12	0.23

2. *Reinforcement learning hypothesis.*

We investigated whether individuals merely remembered the rewarded side (left or right) and subsequently based their decisions on that position, rather than associating the reward with a specific odor. Under this side association hypothesis, a successful trial would prompt the individual to choose the same side in the sequent trial, while an unsuccessful attempt would lead them to switch sides. We coded side and success for all trials (left & unsuccess = 1; right & unsuccess = 2; right & success = 3; left & success = 4) and checked if they would switch sides based on success and unsuccess in consecutive trials. To evaluate the validity of this side-based reinforced learning, we conducted a Bayes Factor Analysis for Goodness-of-Fit to assess statistical significance. Among the three categories (summer wild - winter wild - winter captive), the Bayes Factor was approximately 0.08, indicating that the null hypothesis of independence is more likely.

Brain region size change

We evaluated changes in brain region sizes between the three categories (Summer wild, Winter wild, Winter Captive) using the same model used to quantify the overall brain volume. The brain regions modeled included neocortex, hippocampus, olfactory bulb, nucleus accumbens, olfactory tubercle, amygdala, caudoputamen, cerebellum, midbrain, piriform and entorhinal cortex, thalamus, pons and medulla.

Table A3.5. Estimates from Bayesian linear regression model of brain region size change, with lower and upper 95% credible interval.

	Category	**Estimate (µl)**	**l-95% CI**	**u-95% CI**
Neocortex	*Summer wild*	29.39	28.25	30.56
	Winter wild	26.57	24.00	29.13
	Winter captive	27.39	24.9	29.72
Hippocampus	*Summer wild*	19.03	18.41	19.70
	Winter wild	17.67	16.14	19.24
	Winter captive	17.41	16.04	18.76
Olfactory bulb	*Summer wild*	19.95	19.21	20.72
	Winter wild	18.27	16.48	20.08
	Winter captive	18.47	16.83	20.08

Nucleus accumbens	*Summer wild*	2.12	2.02	2.23
	Winter wild	2.12	1.86	2.38
	Winter captive	1.97	1.72	2.21
Olfactory tubercle	*Summer wild*	3.43	3.25	3.62
	Winter wild	3.23	2.77	3.7
	Winter captive	3.20	2.75	3.6
Amygdala	*Summer wild*	3.21	3.03	3.40
	Winter wild	3.1	2.63	3.56
	Winter captive	3.01	2.55	3.46
Caudoputamen	*Summer wild*	5.62	5.35	5.90
	Winter wild	5.36	4.69	6.05
	Winter captive	5.6	5.04	6.13
Cerebellum	*Summer wild*	26.46	25.34	27.62
	Winter wild	23.5	20.97	26.05
	Winter captive	24.13	21.67	26.5
Midbrain	*Summer wild*	8.37	7.93	8.86
	Winter wild	7.94	6.77	9.11
	Winter captive	8.23	7.05	9.39
Piriform and Entorhinal cortex	*Summer wild*	15.16	14.65	15.69
	Winter wild	14.04	12.68	15.21
	Winter captive	14.16	13.05	15.23
Thalamus	*Summer wild*	5.36	5.11	5.62
	Winter wild	5.09	4.45	5.74
	Winter captive	5.35	4.74	5.9
Pons and Medulla	*Summer wild*	26.41	25.15	27.69
	Winter wild	24.8	21.97	27.6
	Winter captive	24.1	21.41	26.82

Appendix to Chapter 4

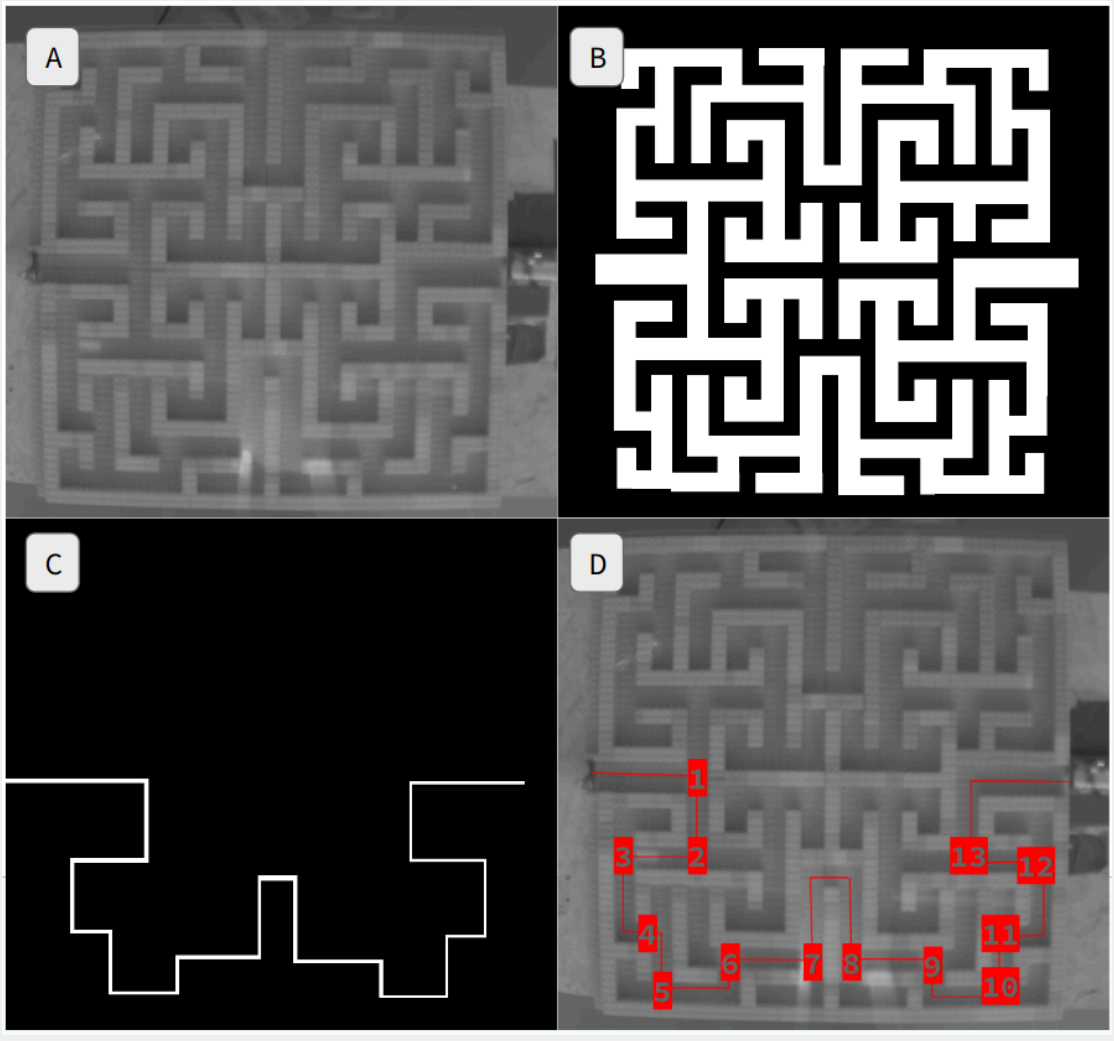

Figure A4.1. Maze Navigation Analysis and Key Components. Panel A: average image derived from a tracked video of the maze. Panel B: binary mask used to isolate the maze structure from the background, enhancing analytical precision. Panel C: binary image of the correct path through the maze, which serves as a reference for identifying decision points along the route. Panel D: Map of decision points within the maze, numbered sequentially from the entrance to the exit where navigation choices occur; decision points are determined based on the correct path from Panel C.

Table A4.1. Results from generalized additive models (GAMs) of the associative learning, path integration, and spatial learning models, with estimates and lower and upper 95% credible interval. The estimates represent the effect of trial number on success in each category: Summer wild, Winter wild, and Winter captive.

Associative Learning (from entrance to food)	**Category**	**Trial**	**Estimate**	**l-95% CI**	**u-95% CI**
	Summer wild	1	0.348	0.180	0.539
		2	0.355	0.214	0.510
		3	0.390	0.242	0.550
		4	0.451	0.296	0.603
		5	0.495	0.350	0.652
		6	0.537	0.379	0.717
		7	0.574	0.422	0.736
		8	0.530	0.375	0.687
		9	0.528	0.355	0.689
		10	0.560	0.560	0.744
	Category	Trial	Estimate	l-95% CI	u-95% CI
	Winter wild	1	0.381	0.216	0.543
		2	0.426	0.284	0.568
		3	0.493	0.353	0.650
		4	0.525	0.379	0.706
		5	0.523	0.384	0.664
		6	0.510	0.375	0.644
		7	0.491	0.348	0.628
		8	0.520	0.372	0.658
		9	0.510	0.360	0.662
		10	0.506	0.346	0.667

	Category	Trial	Estimate	l-95% CI	u-95% CI
	Winter captive	1	0.315	0.191	0.453
		2	0.337	0.225	0.464
		3	0.357	0.244	0.484
		4	0.370	0.256	0.496
		5	0.382	0.271	0.502
		6	0.391	0.275	0.516
		7	0.394	0.275	0.520
		8	0.408	0.287	0.541
		9	0.405	0.279	0.536
		10	0.408	0.263	0.561
Path Integration (from food to entrance)	**Category**	**Trial**	**Estimate**	**l-95% CI**	**u-95% CI**
	Summer wild	1	0.492	0.299	0.686
		2	0.517	0.355	0.680
		3	0.497	0.354	0.637
		4	0.498	0.346	0.645
		5	0.561	0.407	0.709
		6	0.520	0.371	0.673
		7	0.527	0.377	0.683
		8	0.513	0.369	0.662
		9	0.491	0.335	0.649
		10	0.462	0.268	0.647
	Category	**Trial**	**Estimate**	**l-95% CI**	**u-95% CI**
	Winter wild	1	0.504	0.356	0.653
		2	0.474	0.347	0.606
		3	0.416	0.296	0.538

		4	0.344	0.219	0.467
		5	0.374	0.259	0.493
		6	0.423	0.301	0.564
		7	0.425	0.302	0.565
		8	0.434	0.309	0.566
		9	0.353	0.239	0.479
		10	0.305	0.182	0.443
	Category	**Trial**	**Estimate**	**l-95% CI**	**u-95% CI**
	Winter captive	1	0.440	0.293	0.601
		2	0.388	0.268	0.523
		3	0.347	0.241	0.464
		4	0.335	0.226	0.450
		5	0.322	0.218	0.434
		6	0.306	0.203	0.418
		7	0.307	0.206	0.419
		8	0.326	0.221	0.441
		9	0.325	0.217	0.443
		10	0.330	0.216	0.460
Spatial Learning	**Category**	**Trial**	**Estimate**	**l-95% CI**	**u-95% CI**
	Summer wild	1	0.344	0.175	0.546
		2	0.338	0.230	0.562
		3	0.557	0.400	0.705
		4	0.614	0.464	0.751
		5	0.697	0.556	0.820
		6	0.716	0.570	0.839
		7	0.696	0.561	0.816
		8	0.553	0.385	0.715

	9	0.630	0.483	0.764
	10	0.686	0.536	0.815
Category	**Trial**	**Estimate**	**l-95% CI**	**u-95% CI**
Winter wild	1	0.363	0.206	0.543
	2	0.430	0.279	0.590
	3	0.436	0.286	0.595
	4	0.515	0.365	0.664
	5	0.537	0.379	0.694
	6	0.623	0.463	0.771
	7	0.703	0.560	0.825
	8	0.690	0.546	0.817
	9	0.671	0.518	0.806
	10	0.636	0.461	0.792
Category	**Trial**	**Estimate**	**l-95% CI**	**u-95% CI**
Winter captive	1	0.337	0.197	0.503
	2	0.364	0.243	0.497
	3	0.393	0.265	0.530
	4	0.453	0.322	0.587
	5	0.491	0.355	0.628
	6	0.549	0.423	0.673
	7	0.557	0.432	0.681
	8	0.620	0.501	0.731
	9	0.687	0.566	0.793
	10	0.833	0.720	0.916